REINFORCING BAR CONNECTION OF HOLLOW-CORE SLABS TO STEEL BEAMS AND MASONRY WALL SUPPORTS

by

Susana Hernández Brito

A Thesis submitted to the Faculty of Graduate Studies of

The University of Manitoba

In partial fulfillment of the requirements of the degree of

MASTER OF SCIENCE

Department of Civil Engineering

University of Manitoba

Winnipeg, Manitoba, Canada

September 2021

ABSTRACT

The bearing connections of hollow-core slab (HCS) floors require the use of steel reinforcement to prevent slab displacements under lateral loads. Inadequate connection detailing could result in compromising the structural integrity of buildings that utilizes HCS floors. Traditionally, size 10M steel bars have been implemented in several regions in Canada as connections of HCS floors to supporting members. However, North American design codes and guidelines do not offer sufficient provisions to predict the capacity of these connections, and the literature has not yet addressed their behaviour. Hence, this thesis presents the test results of twenty full-scale reinforcing bar connections of HCS to steel beam and masonry wall supports under in-plane forces to investigate their modes of failure and carrying load capacities. The connections were constructed using 203-mm thick HCS, cut to 1,220-mm square segments. Eleven HCS specimens were supported on steel beam, while nine specimens were supported on masonry walls. Test parameters included the type of HCS bearing (end or side bearing), in-plane load direction (pulling or pushing against the support) and orientation (parallel or normal to the axis of the support). Test results revealed that the connection detailing used in HCS floors over steel beams is adequate to ensure the structural integrity of HCS floors as it satisfies code requirements under tension (pulling) forces. Reducing the free length of the connection bar and decreasing the bar bends resulted in greater stiffness and ductility, yet the bars had relatively lower strength under compression. On the other hand, the connection bars in specimens supported on masonry did not meet the specified strength under tension for buildings more than three floors. The specimens suffered bar pull-out, excessive slab displacements and loss of bearing before attaining the peak load. Bonding the connection bar to the masonry wall prevented the bar pull-out but did not provide the required strength in tension.

ACKNOWLEDGMENTS

I wish to express my sincere appreciation and gratitude to my supervisor Dr. Ehab El-Salakawy, P.Eng., FCSCE, Professor of Structural Engineering in the Department of Civil Engineering at the University of Manitoba, for his kind guidance and continuous support throughout this research program. It has been an honour to work and learn from him.

I would also like to thank my mentor Dr. Karam Mahmoud, P.Eng, Post-Doctoral Fellow, and Mr. Karl Truderung, MSc, P.Eng, for their remarkable suggestions and assistance to the development and implementation of the research project. In addition, the help received from all members of our research group during the construction and testing of the specimens is greatly appreciated.

Special thanks to the technical staff at W. R. McQuade structures laboratory, Dr. Chad Klowak, Mr. Sam Abraha and Mr. Syed Mohit, for the technical assistance during the laboratory work made this research project possible.

The financial support and in-kind contribution provided by the Natural Sciences and Engineering Research Council of Canada (NSERC), the Canadian Precast/Prestressed Concrete Institute (CPCI), the CPCI Technical Committee, Manitoba Masonry Institute, Tower Engineering Group and Armtec Manufacturer are gratefully acknowledged.

Thanks to my friends and colleagues for their care and company at both good and bad times. Last but not least, my deepest and most sincere indebtedness to my family, especially my husband, Alberto, for their immense patience, support, and encouragement.

Susana Hernández Brito, September 2021

Table of Contents

List of Figures

List of Tables

List of Notation

The following symbols are used in this thesis:

A_b = cross-section area of the reinforcing bar

A_{vf}= cross-section area of shear-friction reinforcement

A_c= cross-section area of concrete under shear-friction

ρ_v= ratio of shear-friction reinforcement

C = compression force applied

T = tension force applied

T_e = bond strength

γ = factor obtained in evaluating grout strength

ℓ_e = embedment length

ℓ_n = clear span between supports

f'_c = maximum compressive stress in grout obtained using grout cubes

f_y = yielding strength of steel bars

f_s = tensile stress of the bar

w = lateral load

V_n= in-plane shear strength

F_{tie} = resistance force of the tie

λ= density factor

μ = friction coefficient

α = angle between the shear-friction reinforcement and the shear plane

b_{eff} = breadth of the HCS-beam composite section or required length of concrete infill

P_{RD} = capacity of the connection (composite sections)

List of Abbreviations

General Abbreviations

ACI	American Concrete Institute
ASTM	American Society for Testing and Materials
CPCI	Canadian Precast/Prestressed Concrete Institute
CSA	Canadian Standards Association
HCS	Hollow-core slab
NZS	New Zealand Standards

Specimen Code

Phase I (Steel beam supports)

EB-CN-90	End bearing specimen tested under pushing (compression) in-plane normal force with 90-degree bent connection bar
EB-CN-45	End bearing specimen tested under pushing (compression) in-plane normal force with 45-degree bent connection bar
EB-CN-90R	End bearing specimen tested under pushing (compression) in-plane normal force with 90-degree bent connection bar and reduced unrestrained length
EB-CN-45R	End bearing specimen tested under pushing (compression) in-plane normal force with 45-degree bent connection bar and reduced unrestrained length
EB-TN-90	End bearing specimen tested under pulling (tension) in-plane normal force with 90-degree bent connection bar
EB-TN-45	End bearing specimen tested under pulling in-plane normal force with 45-degree bent connection bar

EB-CP-90 End bearing specimen tested under pushing (compression) in-plane parallel force with 90-degree bent connection bar

SB-CN-90 End bearing specimen tested under pushing (compression) in-plane normal force with 90-degree bent connection bar

SB-TN-90 Side bearing specimen tested under pulling (tension) in-plane normal force with 90-degree bent connection bar

SB-CP-90 Side bearing specimen tested under pushing in-plane parallel (shear) force with 90-degree bent connection bar

SB-TP-90 Side bearing specimen tested under pulling in-plane parallel force (shear) with 90-degree bent connection bar

Phase II (Masonry wall supports)

EB-CN-D End bearing specimen tested under pushing (compression) in-plane normal force with "dry-fit" connection bar

EB-CN-D End bearing specimen tested under pushing (compression) in-plane normal force with adhesive

EB-TN-D End bearing specimen tested under pulling (tension) in-plane normal force with "dry-fit" connection bar

EB-TN-A End bearing specimen tested under pulling (tension) in-plane normal force with adhesive

EB-CP-D End bearing specimen tested under pushing (compression) in-plane parallel force with "dry-fit" connection bar

SB-CN-D End bearing specimen tested under pushing (compression) in-plane normal force with "dry-fit" connection bar

SB-TN-D	Side bearing specimen tested under pulling (tension) in-plane normal force with "dry-fit" connection bar
SB-CP-D	Side bearing specimen tested under pushing in-plane parallel (shear) force with "dry-fit" connection bar
SB-TP-D	Side bearing specimen tested under pulling in-plane parallel force (shear) with 90-degree "dry-fit" connection bar

CHAPTER 1 - INTRODUCTION

1.1 Background

Designers commonly choose precast/prestressed hollow-core slabs (HCS) to cover large spans in multi-storey buildings. The continuous voids or cores running along the loading transfer direction eliminate up to 50% of the concrete volume used to cast solid section slabs of equivalent thickness. This volume reduction results in relatively lighter elements, which allow for longer spans, reducing deflections and section height. These properties coupled with the effect of prestressing result in a structurally efficient cross-section and reduced maintenance structures. Prestressing optimizes the use of high-strength concrete and further reduces deflections. In addition, prestressing results in crack-free members, which eliminates the problem of steel reinforcement corrosion and associated maintenance costs. Therefore, HCS are suitable for many complex projects owing to their relatively high load-carrying capacity and low maintenance (Truderung 2011).

The design of HCS floors as horizontal continuous diaphragms is recognized and regulated in current design codes and standards such as CPCI (CPCI 2017), PCI Manual for the Design of Hollow Core Slabs (PCI 2015), ACI 318-19 (ACI 2019) and CSA A23.3-19 (CSA 2019). When lateral loads (e.g., wind/seismic, movements of the supports or loads during construction) act on HCS floors, in-plane axial and shear forces are generated across the diaphragm, depending on the load path. These in-plane forces are carried by steel reinforcement in boundary elements and transferred to the supports through the HCS bearing connections.

These bearing connections rely on the use of steel reinforcement as links to the supports for transferring the load adequately. Moreover, the steel reinforcement acts as ties to prevent slab displacements caused by the lateral load, ensuring the structural integrity of the floor. Given the

function of these ties, current design codes and standards such as CSA A23.3-19 (CSA 2019) and ACI 318-19 (ACI 2019) refer to this steel reinforcement as "integrity ties". For end-bearing slabs, integrity ties are typically inserted at the shear keys between adjacent HCS on one side and fixed to the supporting member on the other side (Fig. 1.1). For side bearing slabs, the connection bars are inserted in a slot that is cut into the side of the slab as shown in Fig. 1.1.

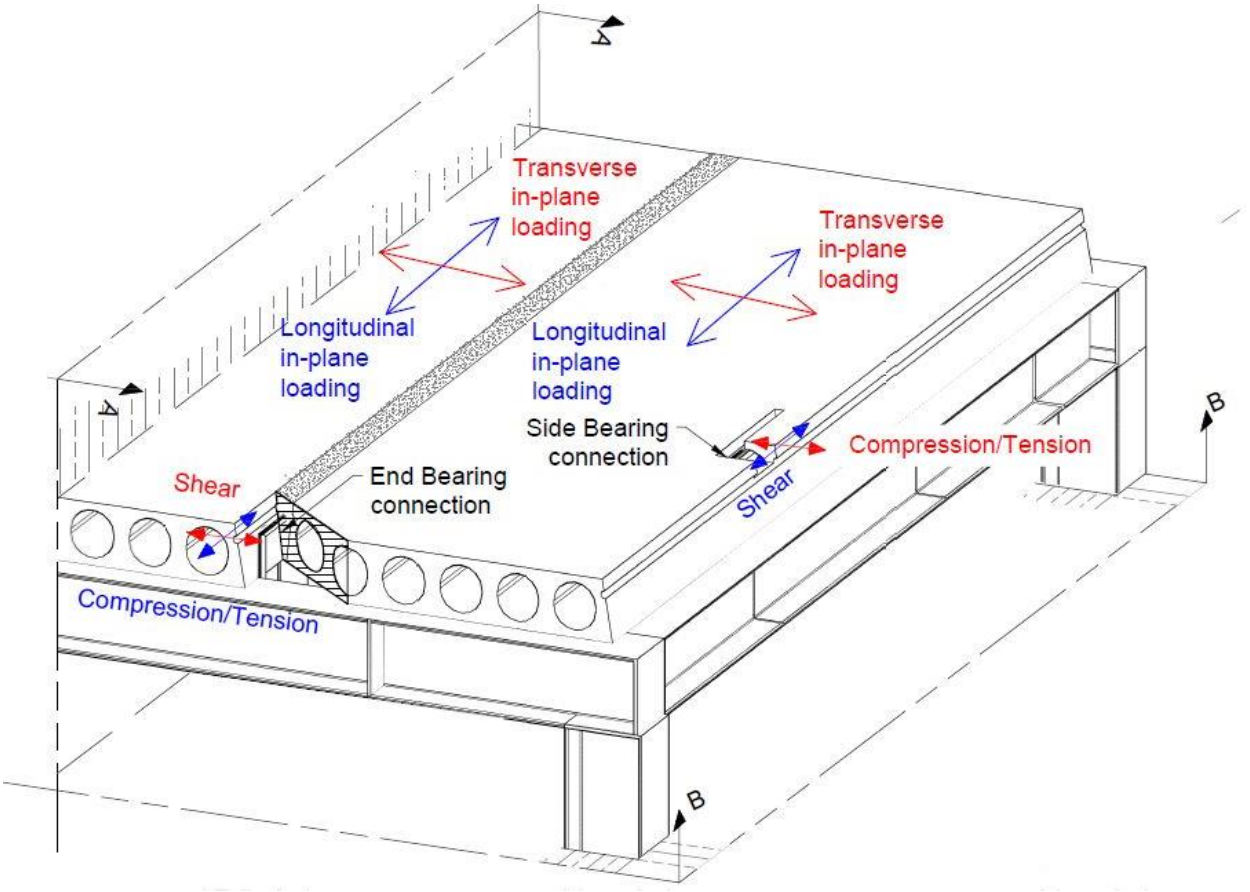

Fig 1.1: Horizontal in-plane forces acting in a HCS floor without topping — location of End- and Side-Bearing connections.

In Canada, there are different types of these bearing connections depends on the geographic location. This study is focusing on the common detailing used for the majority of HCS floors in

Canada (mostly in Ontario and Quebec). These bearing connections do not behave compositely, nor are they monolithic. This connection detailing involves using one 10M, Grade 400W steel bar as connection reinforcement or integrity tie. The connection bar is commonly shaped with 90-degree bends and a bend diameter of 60-mm. Furthermore, a minimum bar development length of 450-mm in the HCS joint is provided. For end bearing HCS, a minimum spacing of one bar diameter is provided between units to minimize grout volume.

The reinforcing bar connection is broadly employed in HCS floors owing to its economy, convenience, and fast installation. For example, the small diameter (size 10M) allows for on-site bending with leftover steel. In addition, minimal grout volume is involved in the assembly of this connection, which results in significant savings. Furthermore, the bearing connection relies on welding or dry fitting to a masonry beam, allowing for early loading of the floor and fast erection of upper-level floors.

Ultimately, this reinforcing rebar serves three primary purposes in HCS bearing connections: a) to ensure lateral bracing for supporting members and tightening the structure in buildings with bearing walls, b) to transfer horizontal loads from HCS to the supporting members, and c) to provide structural integrity to the building by avoiding slab displacements that could result in missing the bearing length, misalignment, or a progressive collapse.

1.2 Problem Statement

Current design standards and codes, such as CSA A23.3-19 (CSA 2019) and ACI 318-19 (ACI 2019), indicate that bearing connections are expected to: a) deform under loading effect, b) ensure sufficient ductility or warning before failure, c) accommodate or allow floor movements without compromising its stability, and d) transfer in-plane stresses from lateral/horizontal loads.

In addition to wind and seismic lateral loads, HCS bearing connections provide stability and bracing to the building against accidental loading during the construction stage. The accidental lateral loads can be caused by bumping with adjacent units during HCS placement, vibrations from the utilization of heavy equipment, etc. In these situations, bearing connections offer additional stiffness to the building while assembling the structure. Also, floor dilation from thermal effects, volume changes and creep, particularly in large rectangular plans, are carried by the steel reinforcement of HCS bearing connections. Improper design or evaluation of steel reinforcement in bearing connections could provoke floor misalignments, loss of bearing, progressive collapse, or structure instability under cited lateral loads.

North American standards and design codes suggest the shear-friction theory to calculate the reinforcement ratio of monolithic bearing connections. However, this theory is not adequate for the reinforcing bar connections. First, the connection contains portions of the reinforcement unrestrained, i.e., not embedded in the grout. The presence of unrestrained bar portions can trigger a local failure compromising the behaviour of the connection. Second, the zone of shear stresses or friction interlock between the supports and the HCS does not contain steel reinforcement. Given the geometry of the connection bar in steel beams and L-bars in masonry supports, the bar is inserted outside the interlock friction zone between the slabs and the supports. Third, the zone of friction-interlock between the HCS and the supporting member is eccentric with respect to the load application.

Additionally, these codes and standards illustrate numerous examples of detailing for HCS bearing connections to supporting structures. Yet, due to lack of experimental data, a design methodology or an expected mode of failure/capacity are not included in the description. As a result, the

reinforcing bar connection and other connection detailing are employed in HCS floors without proper evaluation of its capacity or behaviour. Therefore, this pioneer study aims at investigating the mode of failure and evaluate the capacity of the reinforcing bar connections under different in-plane loading scenarios. Also, the influence of alternative detailing to the geometry of the bar and its unrestrained portion is examined. To date, no code in North America offers design details or methodology for the design of these connection bars (such as bar size, shape, length, spacing, etc.).

1.3 Research Significance

It is estimated that 1.81 million m^2 of HCS are employed annually in flooring across Canada (Personal contact 2021). Most of this amount was utilized in the Eastern Coast, where the reinforcing bar connection detailing, used in this study, is employed. Based on that, it deemed necessary to investigate the behaviour and capacity of these connection bars. The research outcomes of this study provide preliminary information, which serves to elaborate a design methodology and explore connection detailing enhancements in future works.

1.4 Objectives

As mentioned in the previous section, this research was intended to provide information on the capacity and behaviour of the reinforcing bar connection. Thus, the following objectives were planned:

1. Investigate the capacity and mode of failure of the connection bar under different loading scenarios.
2. Examine the capacity and overall behaviour against the limited provisions found in North American codes and previous research recommendations in the field.

3. Understand the differences in the capacity and behaviour between end-bearing and side-bearing connections.
4. Investigate the effect of connection detailing such as the angle of bar bends and the use of adhesive in case of masonry supports.

1.5 Scope

Hollow core slab bearing connection to steel beam and masonry wall supports were considered in this study. These assembled HCS bearing connections were tested under monotonic in-plane axial or shear forces (pull or push against supports) until failure. No gravity load was added to the loading scheme to reduce friction resistance between HCS and supports. The experimental research was limited to the reinforcing bar connection detailing constructed with 10M Grade 400W bars, typically used in the Eastern Coast of Canada. Only 203-mm thick HCSs were employed to construct the connection subassembly. This connection subassembly simulated the construction practice for interior bearing connections in HCS roofs. The grout used in the construction of the HCS joints was of regular strength (20-25 MPa).

1.6 Methodology

The behaviour of the reinforcing bar connection was assessed throughout full-scale testing of twenty connection subassemblies. The experimental work was divided into two phases according to the supporting element: Phase I - steel beams, and Phase II - masonry walls. In the case of masonry supports, a two-course, single wythe, with a typical bond beam on top, was used instead of a full-height wall to simplify the construction procedure. Concrete blocks, measuring 390×190×190 mm, were used to construct the masonry wall. For steel beam supports, a W250×67 mm steel beam was used. HCS square segments, measuring 1,220×1,220×203 mm, were used to

construct the test specimens. Two HCS segments were used for the end-bearing connections, while a single segment was used for the side-bearing one. Both steel and masonry beams were simply supported on two concrete blocks and prestressed to the laboratory strong floor.

Test variables in this research include type of connection (end bearing or side bearing), type of support (steel or masonry), direction of loading (pushing or pulling), orientation of loading (parallel or perpendicular to the connection bar), bend angle of the connection bar (90 or 45 degrees) and the use of adhesive in case of masonry supports. Special attention was paid to measure the maximum load (capacity), displacement and mode of failure for all the specimens. Recommendations for design and future work were proposed.

1.7 Thesis Organization

This thesis consists of six chapters arranged as follows:

Chapter 1 defines the problem, outlines the main objectives, scope, and methodology of this study.

Chapter 2 summarizes the relevant information based on available literature concerning HCS bearing connections. The chapter includes provisions from codes and current construction practices. The general modes of failure of such connections are highlighted.

Chapter 3 explains fundamental details about the experimental program. This chapter covers the design and construction of test specimens, instrumentation, test setup construction and testing procedure.

Chapter 4 discusses the results of Phase I for reinforcing bar connections to steel beams. In this chapter, the behaviour of the reinforcing bar connection is evaluated in terms of mode of failure, cracking patterns, ductility of the connection bar.

Chapter 5 presents the test results of Phase II for reinforcing bar connections to masonry walls. This chapter has a similar organization to Chapter four.

Chapter 6 summarizes the most important conclusions of this research and provides recommendations for future work.

CHAPTER 2 - LITERATURE REVIEW

2.1 Introduction

The construction practice of HCS bearing connections to the supporting members differs widely among practitioners. The lack of experimental evidence and code provisions led to a wide range of connection details, which are based on work experience. These variations range from steel connection bar detailing (such as embedment length, bar diameter, and bend angle) to binding materials (epoxy resin, grout, or concrete). Consequently, these connection details are being employed in HCS bearing connections without properly understanding their behaviour. In addition, the capacity, ductility and mode of failure of the connections built with such connection bars have not been determined yet.

This chapter presents a compilation of information about the HCS bearing connection detailing that is most used in Canada. Connection details are reviewed in terms of behaviour and methods of analysis as well as previous research carried on similar detailing. In addition, practical aspects for construction (such as cost, ease and time of construction, etc.) are examined.

Additionally, a summary of the research conducted on HCS connections under seismic loading is presented. This previous research, particularly the experimental ones, served to design the test setup for this study under monotonic in-plane loading. Even though under seismic loading, the experimental research offered examples of connection detail enhancements with tested capacity and well observed behaviour. Finally, recommendations for construction from international and North American codes are summarized.

.

2.2 Forces in Hollow-Core Slab Bearing Connections

In addition to carrying gravity loads, HCS floors are designed to act as a continuous horizontal diaphragm that distributes and transfers lateral forces to the supporting members. There are two main approaches suggested in the codes to deal with the flow of lateral forces in the floor and determine the stresses acting at the joints. In many situations, the strut-and-tie model, considering multiple alternative load paths, is widely recommended as the most appropriate method to determine the flow and concentration of forces in the HCS floors (CPCI 2017). This global approach is useful in rigid or semi-rigid HCS floor diaphragms with discontinuities, openings, and abrupt changes in the geometry of the floor. In low and moderate seismic design regions, the deep horizontal beam analogy can be employed (CPCI 2017). This approach also depends on the rectangularity of the HCS floor and the location of the lateral force-resisting support members (Fig. 2.1). In this case, the supports of the beam are the shear walls or the structural frames.

In both approaches, boundary elements are provided around the perimeter of the floor or openings. The boundary element consists of grouted steel reinforcement acting as a chord or collectors to resist axial and drag shear stresses across the floors. The steel reinforcement placed normal to the in-plane force, along the end of slabs (illustrated as continuous orange/green lines in Fig. 2.1), carries the compressive and tensile stresses in the floor. This bar reinforcement is called "chords". In Fig. 2.1, the orange and the green arrows represent the flow of compressive and tensile stresses, respectively, in an HCS floor without topping. Also, the CPCI Design Manual (CPCI 2017) refers to the steel reinforcement that prevents joint opening and cracking due to shear as "shear connections". Fig. 2.1 depicts these shear stresses in blue colour and the blue dashed lines represent the location of these shear connections in the floor.

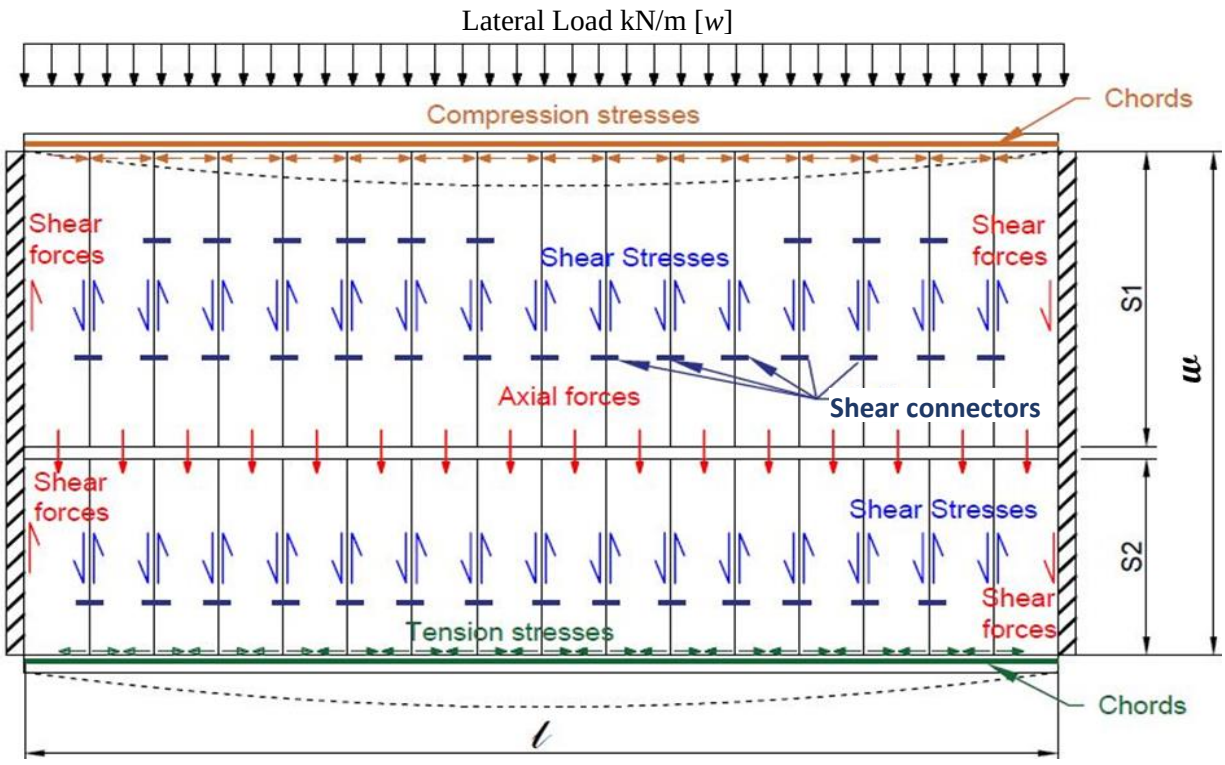

Fig. 2.1: Scheme of un-topped HCS diaphragm floor – Deep horizaontal beam analogy. Reproduced from CPCI (2017)

As described in Chapter 1, bearing connections in un-topped HCS floor transfer the resultant of lateral forces to the supports, brace the structure and avoid slab displacements to preserve the structural integrity of the floor. Fig. 2.1 illustrates in red arrows the resultant forces acting on bearing connections. Given the main function of the steel reinforcement in bearing connections, current North American codes, such as ACI 318-19 (ACI 2019) and CSA A23.3-19 (CSA 2019), define them as "integrity ties". Accordingly, these codes require a minimum strength of 14 and 22 kN per meter length of support in internal integrity ties, for buildings of three-storeys or more with precast bearing walls. Then, the tie spacing depend on the tensile yielding strength of each tie. Additionally, for the case of buildings with one or two-storeys, and structures with supporting

members other than precast bearing walls, the CSA A23.3 (CSA 2019) code suggest providing a factored tensile resistance of 5.0 kN/m or more, while the ACI 318 (ACI 2019) recommends 4.4 kN/m of HCS supported-length. The disparity between the two-specification limits results from the function of the integrity ties. While the higher bound requirements (14 or 22 kN/m) are applied to buildings with precast bearing walls and larger number of floors, which rely on these ties to brace and tighten the structure, the lower bound limits (5.0 and 4.4 kN) are intended for low-rise and frame buildings, where mainly the HCS are required to be tied. However, if the acting in-plane forces acting on the HCS are greater than these limits, then adequate tie spacing shall be provided to maintain the integrity of the floor.

When the horizontal in-plane loads act on the HCS floor, the connection reinforcement is subjected to compression (pushing) at one end of the HCS floor, while the other end is subjected to tension (pulling). In addition, this horizontal load generates shear forces at the edges of side units. Given the nature of horizontal loads in service (wind/seismic), the loading orientation is reversal such that the compression/tension at end bearing connections and shear at the side bearing connections can be alternated. It is to be noted that to date, un-topped HCS diaphragms are not recommended to be used in high and moderate seismicity zones (ACI 2019) unless experimental evidence and analysis demonstrates that the system behaves as an equivalent monolithic structure (Angel et al. 2019; Cleland and Ghosh 2002). Therefore, the sources of the forces applied to the bearing connection remain of low intensity.

In HCS floors with cast-in-place concrete toppings, the diaphragm action includes the contribution of the topping. The presence of concrete topping also allows for designing a continuous and monolithic connection that behaves compositely. This type of connection has been broadly covered in experimental research (Jensen 2006). Their capacity and modes of failure under seismic loads

have been addressed with supporting structures constructed with steel (Lam 2002) and concrete members (Mejia-McMaster and Park 1994; Herlihy 1999). This type of topped HCS is not covered by the current study. The reinforcing bar connection hereby investigated is proper from un-topped HCS floor diaphragms.

2.3 Current Construction Practice

2.3.1 HCS bearing connections to steel beam supports

This section reviews the information available on connection details and construction practices for the HCS with different support members typically used in Canada.

2.3.1.1 Welded steel "Z-shaped" reinforcing bar

As mentioned in Chapter 1, the construction procedure of the "Z-shaped" reinforcing bar connection is relatively simple and inexpensive. The attachment to the supports consists of welding the shorter end to the beam. This step can be performed in a short time with limited resources, which is convenient to practitioners. Also, the bar is grouted to the joint between adjacent HCS (shear keys or cores). In the side bearing (SB) connections, the core is not grouted completely. Styrospan discs of 3 to 4-inches thickness are inserted in the cores as formwork to restrict the grout to the joint location only. In addition, the 3-day compressive strength of the used grout mixture is recommended to reach 20 MPa with normal/wet curing. Therefore, the construction process of the entire flooring can continue with minimal interruptions.

The construction of this connection consists of four steps (Fig. 2.2). First, the HCS planks are erected on the steel beams while maintaining a minimum bearing length. According to the CPCI 2017, this bearing length should be the larger value of 50-mm and ℓ_n/180, where ℓ_n is the clear spans between supports. Second, the "Z-shaped" bars are inserted at HCS joints providing the

longer bar end fits into the shear keys of the slabs. Third, the bar is welded to the underside of the top flange of the beam. A segment of bar, between the end of the bend and the welding, is left unrestrained/free. This free bar length is not less than 50 mm or twice the diameter of the connection bar. However, the length can also differ according to the work experience. Finally, the joints, and the cores for side connections, are grouted.

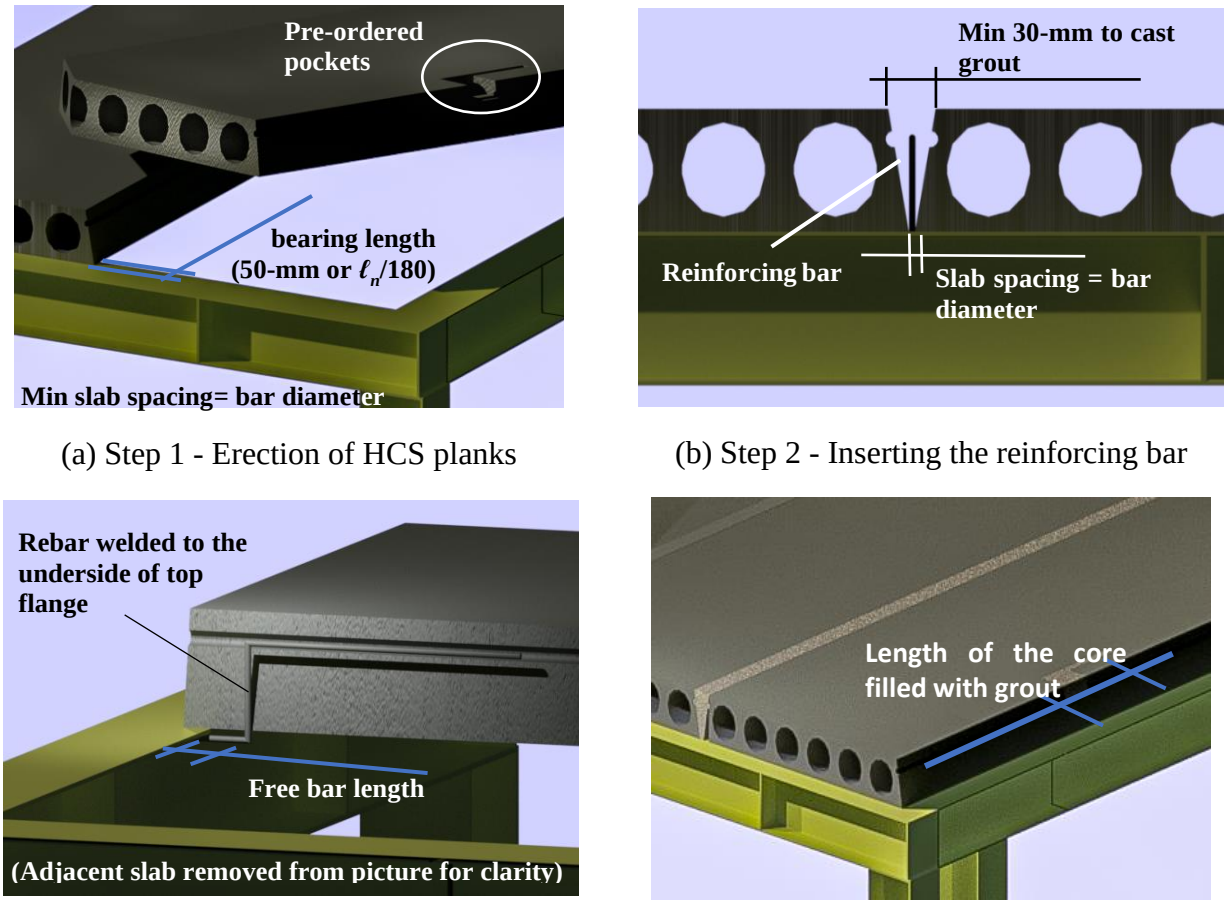

(a) Step 1 - Erection of HCS planks

(b) Step 2 - Inserting the reinforcing bar

(c) Step 3 - Bar welding

(d) Step 4 - Grout placement

Fig. 2.2: Bearing connection construction procedure

Furthermore, the geometry of the connection bar varies from region to region. Whereas some practitioners prefer to use 90-degree bend bars, others employ 45-degree bend bars. Regarding the

angle of bar bends, Minor (1971) found that anchored bars in concrete with 45-degree bends have higher axial capacity compared to bars with 90-degree bends. Minor (1971) carried out an experimental study on the anchorage capacity of bent bars in concrete. His experimental program consisted of pull-out testing of eighty steel bars, with different geometry, embedded in concrete blocks (Fig. 2.3). The anchorage behaviour of these bars was described in terms of bond length, bend angle, bend radios, and bar diameter. The author demonstrated that as the angle of bar bend increases, the stiffness of the anchorage embedded in concrete decreases.

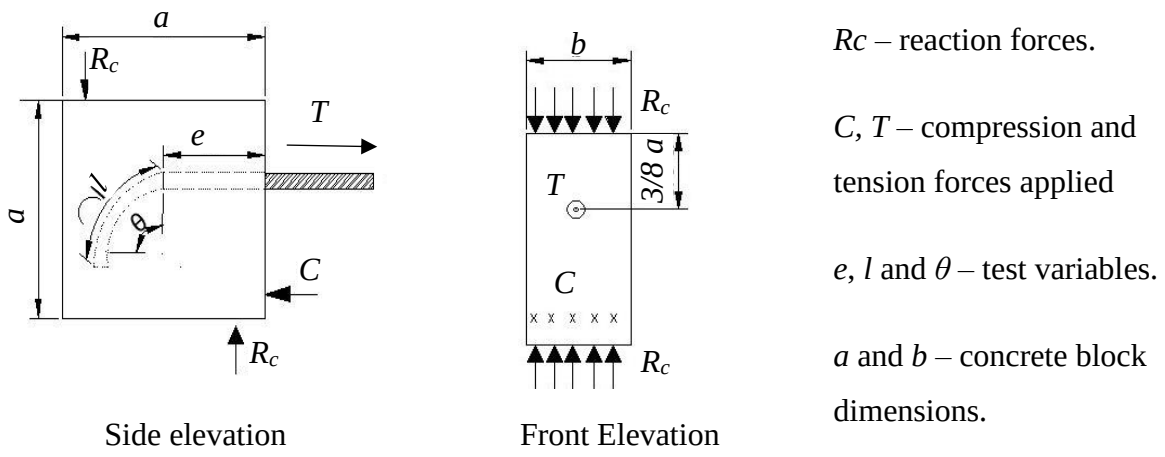

Fig. 2.3 Pull-out test scheme of steel bar embedded in a cuboid concrete block - Reproduced from Minor (1971)

Therefore, anchored bars in concrete with 45-degree bends tend to have more stiffness and slip less than those with 90-degree bends under axial loads. For anchored bent bars in concrete under tension, the bars tend to straighten out and crush the concrete contained within the hook. The connection bar with 45-degree bends had a shape closer to the straight bar and it directly proceeded to yield. However, the 90-degree bend rebar turned into a lower angle bend (approximately 45-degree) then reached its maximum capacity (yielding), causing more damage to the concrete.

However, these outcomes have not yet been proved in grouted bent bars similar to those used in bearing connection of HCS.

The construction practice regarding bar embedment length in grouted joints also varies. While some practitioners provide a conservative bar development length of 600-mm (Fig. 2.4), others recommend embedding the bar for 450-mm in grout after the bends. Bond strength of grouted bars increases proportionally to grout cover, bar size and embedment length. According to Darwin and Zavaregh (1996), the bond strength of grouted bars can be calculated using Equation 2.1.

$$T_e = \gamma \ell_e \sqrt{f'_c} = A_b f_s \tag{2.1}$$

Where:

T_e = bond strength

γ = factor obtained in evaluating grout strength = $\begin{cases} 30 \text{ Strength Class A} \\ 21 \text{ Strength Class B} \\ T_e(ave)/\ell_e\sqrt{f'_c} \end{cases}$

ℓ_e =embedment length = $\begin{cases} 9d_b \text{ for } d_b \geq 16\ mm \text{ or 15M} \\ 15d_b \text{ for } d_b < 16\ mm \end{cases}$

f'_c= grout compressive strength

A_b , f_s = sectional area and tensile stress of the bar

Grout Classes A and B refer to grout categories of economical and highest and lowest compressive strength, respectively. These classes comprise non-shrink grout mixtures for top-cast horizontal bars with a maximum cover of 3 inches (75 mm). Special Strength Class refers to grout used based

on its actual tested performance. The compressive strength of the special strength class may be above or below the compressive strength of grout class B or A.

Assuming the bond strength ($T_e = \phi T_n$) is 40 kN ($A_b \times f_y = 100\ mm^2 \times 400\ MPa$) or 8992-lb and the compressive strength of the grout mixture is 20 MPa (2900 psi), the minimum embedment length is 315-mm. (Equations 2.2 and 2.3). The equations used to calculate the embedment length were formulated based on experimental testing of 15.9-mm diameter steel bars. To date, no pull-out test has been conducted in bar sizes smaller than 15M to test grout bond strength. Therefore, the value of 450-mm of embedment length for 10M bars (135-mm longer than calculations) deems reasonable and still relatively economic. According to Darwin and Zavaregh (1996), "bond strength increases with increasing embedment length, bar size and grout cover. Conversely, the embedment length of 600-mm is overly conservative for the expected capacity of the connection (40 kN).

$$\ell_e = \frac{\phi A_b f_s}{\phi \gamma \sqrt{f'_c}} = \frac{9000}{0.65 \times 21\ \sqrt{2900}} = 12.24 \text{ in.} = 315 \text{ mm} \tag{2.2}$$

$$\ell_e = 15 d_b = 15 \times 11.33 = 170 \text{ mm} \tag{2.3}$$

In addition, Minor (1971) concluded that where a bent bar anchorage is subjected to axial forces (push/pull), most of the stresses and the slip occur at the bend. Therefore, the straight portions carry a small percentage of the applied axial force. Based on that concept, it is also acknowledged that end hooks offer higher bond strength compared to straight bars. Therefore, in the case of bent bars, the bend angle significantly influences to the bond strength.

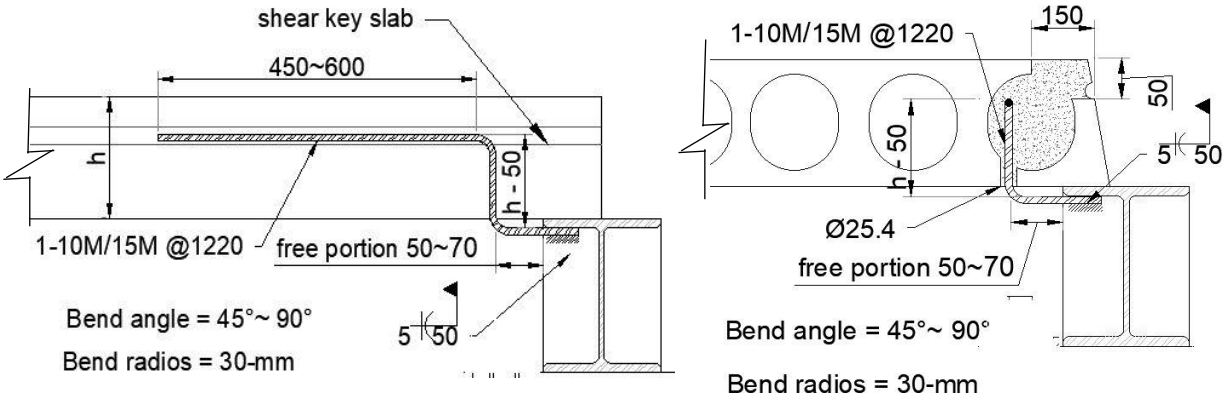

a) End Bearing Connection (section elevation view)

b) Side Bearing Connection (section elevation view)

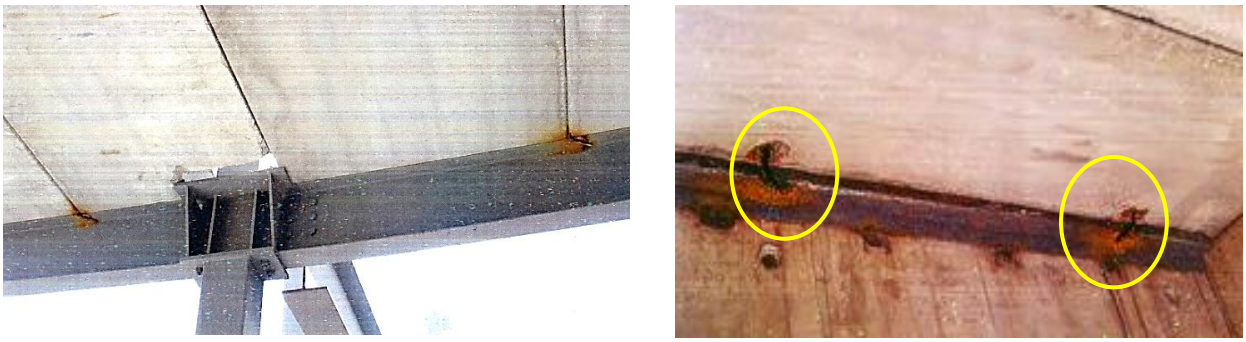

c) End Bearing Connection (bottom view)

d) Side Bearing Connection (bottom view)

Fig. 2.4: Z-rebar connection of HCS to steel beams (Personal Contact 2019).

Moreover, the diameter of the connection bar may differ. Whereas some practitioners use size 10M (11.3-mm diameter) bars, others claim that size 15M (15.9-mm diameter) bars are more appropriate for these connections. The reason is that 10M bars may yield under relatively low levels of lateral load (particularly under compressive stresses), preventing the bar from properly resist lateral loads from wind or earthquakes. Given the nature of HCS bearing connections, the connection detail is limited to accommodate one Z-bar in the shear-keys. Otherwise, the grouted joint would be wider or further modifications would be necessary such as changing the location of the reinforcing bar to the cores of the slabs. Therefore, the 10M connection bar is limited to a

minimum capacity of 40 kN spaced at 1.22-meters, which satisfies code requirements. However, the 15M rebar doubles this value, which results in a stiffer connection with relatively reasonable cost.

2.3.1.2 Mechanical anchors

Composite connections involving steel sections and anchors are typically used to fix the slabs to the supports (Fig. 2.5). At least one of these connections is provided per HCS, resulting in a maximum spacing of 1,220 mm. The steel sections, typically angles, channels or steel plates, are welded to the supporting beam, working as an extension of its flanges. These steel sections have perforations to insert the anchors and connect them to the bottom side of the HCS units.

Depending on the manufacturer specifications, the installation of anchors in HCS may require using epoxy resin to fix the sleeve and bolts to the anchor. Drilling in the webs of the HCS, which includes the prestressing strands, are avoided in all situations as the load-carrying capacity depends on their integrity, and the installation of anchors may cause cracks or concrete spalling. Therefore, technical specifications indicate that the best positioning for connection bars would be at the middle of the HCS flanges, allowing for full embedment length. These connections do not involve concrete or grout placement. As a result, the floor construction proceeds without delays related to curing or casting grout; the construction is relatively clean and less labour intensive than connections with grouted joints.

The main purpose of these systems is to ensure structural integrity and to prevent lateral displacements of the HCS during floor erection and construction work. Therefore, these joints alone have a relatively low axial and shear capacity. For instance, typically, 12.9-mm diameter expansion bolts, with a tensile strength of approximately 8 kN and shear strength of 12.5 kN, are

used in these connections. Fig. 2.5 and b) illustrate two examples of HCS joints with mechanical anchors typically used in buildings (Hilti Manufacturer Brochure 2019).

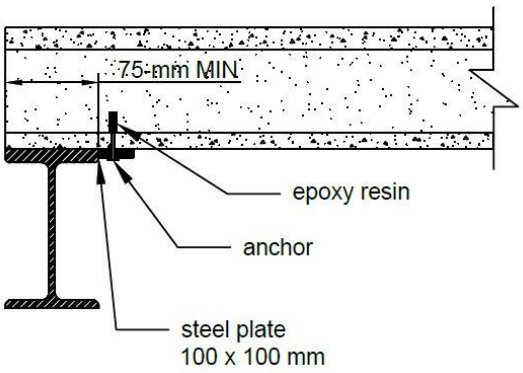

a) Steel plates with anchors and adhesive (section elevation view) - Reproduced from PCI (2015)

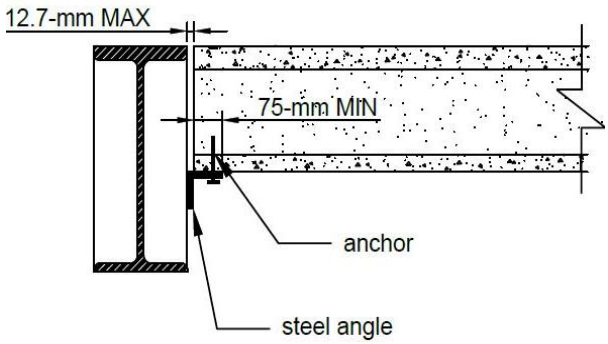

b) Steel angles with anchors (section elevation view) - Reproduced from PCI (2015)

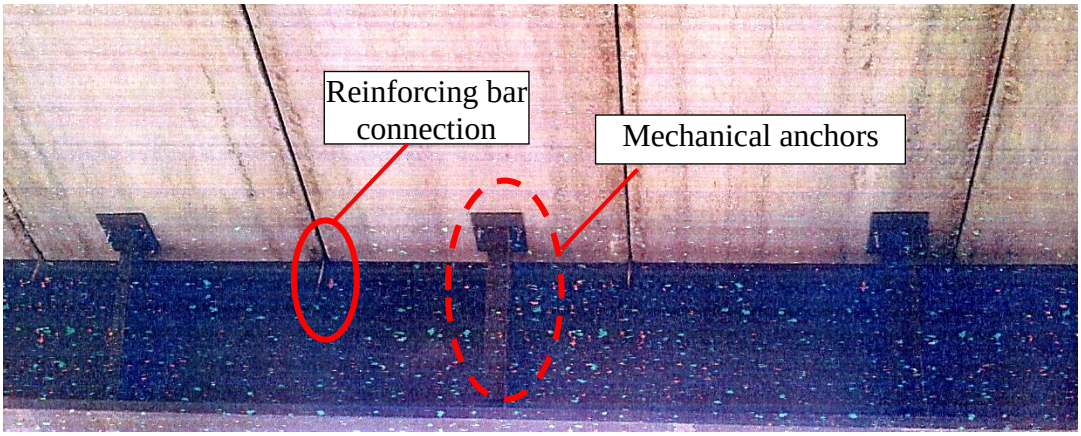

c) Hybrid system using anchors installed through steel pieces combined with reinforcing bar connection welded to supporting beams (Personal Contact 2019).

Fig. 2.5: HCS connections using mechanical anchors and steel pieces welded to steel beams.

The connection described above can be combined with the reinforcing bar connection welded to the beam to form a hybrid system. Fig. 2.5(c) illustrates a system composed of the connection rebar

described in Fig. 2.4 and a steel piece composed of steel plates and channels with anchors to achieve a stiffer fixation of the slabs to the supports.

2.3.1.3 Headed-stud connectors and transverse ties

HCS bearing connections composed of headed-stud connectors and transverse reinforcement/ties are considered typical in Western Canada. However, these bearing connections vary in the location in HCS floors, the shape of the reinforcement and the presence of saw-cut or milled slots/pockets in the HCS.

In these connections, headed studs are welded on the top flange of the steel supporting beams at the specified spacing to match the location of HCS joints or pockets. Ties are conveniently placed and shaped according to the location of the bearing connection in the floor (exterior/edge or interior) and the shape of HCS pockets. The connection bar usually consists of "U-shaped" hooked or straight bars that go around the headed stud. Fig. 2.6 shows schematic drawings of the components of this type of connection, typically used in Manitoba. Fig. 2.6 shows an example of the typical connection detail with "U-shaped" bars as transverse reinforcement.

Depending on the project, the headed-stud connectors can be pre-welded on the beam before shipping to the construction site. Next, HCS are erected on top of the steel beam, steel connection bars are inserted and tied, and finally, the joint is grouted. Typically, slots/pockets are cut on the flanges of the slabs for placement of grout or concrete. These slots are pre-ordered, and the slabs arrive on-site prepared to install the bars and cast the grout. Milled slots can measure anywhere between 300 and 500-mm in length. The grout or concrete, usually employed for this connection, is of regular strength (20-40 MPa).

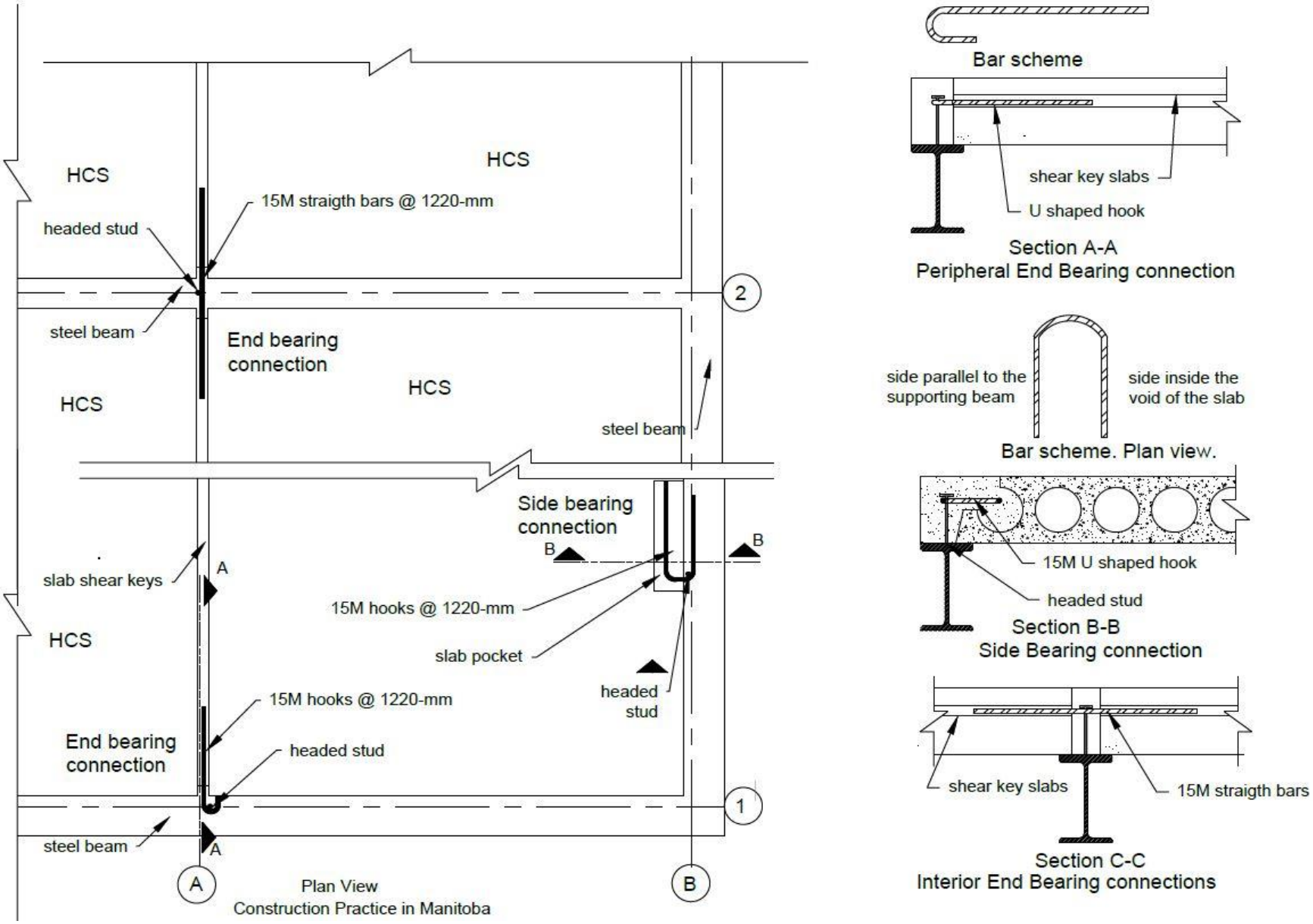

Fig. 2.6: Construction Practice in Manitoba - End and Side bearing connection.

In general, this type of connection requires more planning and design, and it is less economical than other connection details discussed earlier; however, the construction procedure is still relatively simple. Also, this connection detail is suitable for the composite action of the HCS with the supporting beam, which ensures higher in-plane axial and shear capacity as well as two times the stiffness of the isolated steel beam section Research has been conducted on HCS-beam composite sections using this connection detailing to evaluate their performance under lateral forces.

Fig. 2.7 illustrates the components of the bearing connection tested by Lam et al. (1998, 2002, 2007), who conducted an experimental study on HCS connections using headed-stud connectors intercepted by steel ties (Fig. 2.7). These researchers conducted near to 100 push-out tests to evaluate the capacity of HCS bearing connections with headed-stud connectors to lateral forces. The test specimens comprised of headed-stud connectors welded to the steel beam supports, and ties were embedded in the voids of the HCS. Regular strength concrete (25 MPa) was poured into the voids to integrate ties to the HCS. The results of that research demonstrated that HCS bearing connections are suitable to increase flexural capacity, ductility and stiffness due to the composite action. Lam et al. (2007) also observed the best shear performance at those specimens with 16-mm diameter ties combined with 19-mm diameter headed-stud connectors of 100-mm length. Based on this full-scale testing and a parametric study using computational modelling, the following empirical expressions to estimate the breadth (b_{eff}) of the HCS-beam composite section or required length of concrete infill and the capacity (P_{RD}) of the connection was validated.

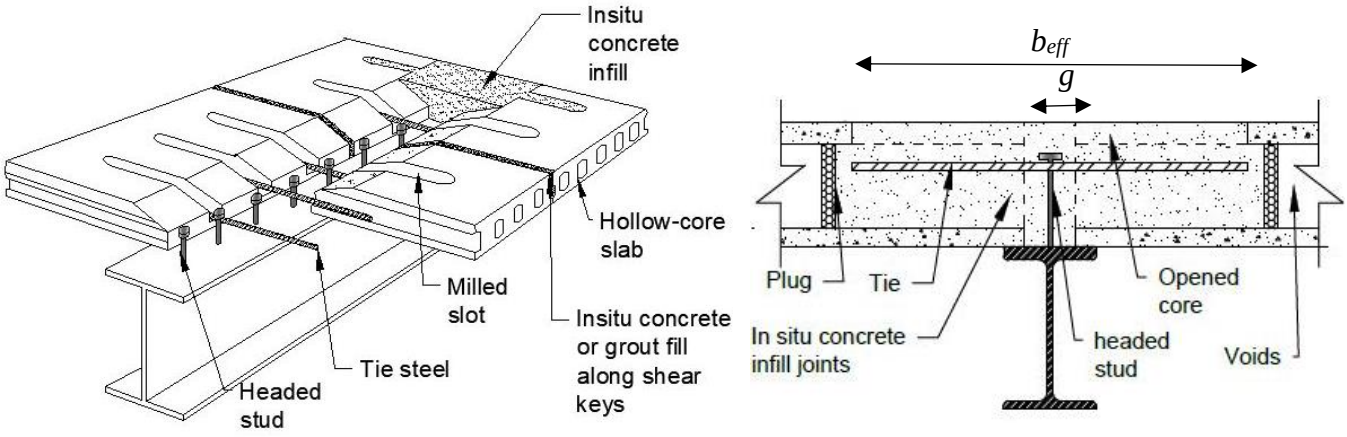

a) Scheme of composite action of HCS-beam. 3D perspective view.

b) 2D scheme of composite action of HCS-beam (side section elevation view)

Fig. 2.7: Composite beams with precast hollow core slabs - Reproduced from Lam et al. (2002)

$$b_{eff} = \left(\frac{25}{f_{cu}}\right)^2 \left(\frac{0.4}{f'_t}\right) 1000 + 300 \tag{2.4}$$

where f_{cu} = compressive concrete cube strength of *in-situ* infills in MPa and $f'_t = \frac{A_s f_y}{A_c}$ (MPa).

$$P_{RD} = 0.29 \propto \beta \varepsilon d^2 \sqrt{f_{ck}} E_c / \gamma_v \tag{2.5}$$

$$P_{RD} = 0.8 f_u \frac{\pi d^2}{4\gamma_v} \tag{2.6}$$

Where:

f_{ck} is the average cylinder strength of the in-situ and precast concrete

E_c is the average modulus of elasticity of the in-situ and precast concrete

f_u is the ultimate tensile strength of the headed stud (450 N/mm^2)

γ_v is the partial safety factor, which is taken as 1.25 at the ultimate limit state

$\propto$ is the factor which considers the height of the stud and is given by 0.2 (h/d +1) < 1.0

β is the factor that considers the in-situ infill gap between the HCS, g_i (gap between consecutive slabs in continuous spans, as shown in Fig. 2.8b)), and is given by 0.5 (g_i/71+1) < 1.0 and g_i > 30-mm

ε is the factor that considers the transverse reinforcement. It is given by 0.5 (ϕ/20 + 1) < 1.0, where ϕ is the transverse reinforcement diameter.

2.3.2 HCS bearing connections to masonry supports

The connection detail of HCS to masonry supports typically involves masonry wall reinforcement and transverse reinforcement or ties to fix the slab to the wall. In case of multi-story buildings with reinforced masonry walls, the continuity of the masonry wall relies on the composite action of lap splice of the wall reinforcement with the next two courses of masonry units in the next level. In non-reinforced masonry walls, this steel reinforcement is still placed to ensure continuity between levels of the wall. In this case, this vertical steel reinforcement can be called dowels or ties. Vertical dowels are embedded at least 150-mm into the bond beam and extended up to the second course of masonry units in the following level. Therefore, these straight bars are 500-mm long at least. Depending on the connection detail, these dowel bars can be monolithically cast with the bond beam or post-installed by drilling and epoxying the bars. Typically, the HCS bearing connection reinforcement or ties are wrapped around the vertical reinforcement of the wall at the level of the slabs. Similar to the connection formed with pre-welded headed-stud connectors and transverse reinforcement, the latter is conveniently shaped as straight bars, "L-shaped bars" or hooks, for internal or peripheral bearing connections.

The material and geometric properties of these components widely differ among practitioners. The CPCI (CPCI 2017) and the PCI (PCI 2015) manuals illustrate a number of HCS bearing connection detail over masonry walls. The following section describes the connection detail more commonly

used in Canada and highlights their advantages and construction procedures. The PCI Manual for the Design of HCS acknowledges the connection detail hereby presented as suitable for transferring shear forces in HCS diaphragm floors. Also, these connection details are relatively simple to assemble and grout.

2.3.2.1 Starter bars and hooks or L-shaped rebar

Figure 2.8 illustrates an HCS bearing connection detail constructed with dowels and hooks or L-shaped as transverse reinforcement. This is the common practice in Manitoba and Western Canada. The construction of this type of connections includes the following steps. First, the bond beam (upper course of the masonry wall supporting the HCS) is grouted with the dowels in place. Then, the HCS are erected, providing for the minimum bearing length. These slabs may have saw-cut slots (End bearing connections) or pockets (side bearing connections) for easy grouting. Also, when tie spacing (transverse reinforcement spacing) is 1,220-mm, the bars can be inserted at the shear key of the slabs to avoid saw-cutting slots in the flanges of the slab (Fig. 2.8). Ties or hooks are then inserted and locked around dowels, and the connection is grouted.

Figure 2.9 depicts a connection detail where HCS bearing ties are not locked around the steel reinforcement (dowels) of the wall. Instead, the reinforcement is anchored into the steel reinforcement of the boundary element (chords). Both the HCS joints and the boundary element can be cast in one operation, making it relatively less labor-intensive and more efficient in terms of construction time. Also, since the location of the tie does not depend on the masonry wall reinforcement, their installation requires less planning and allows for more freedom for its placement. Usually, ties are spaced at 610 mm in end bearing, while in side-bearing connections, the spacing is set to a maximum of three meters.

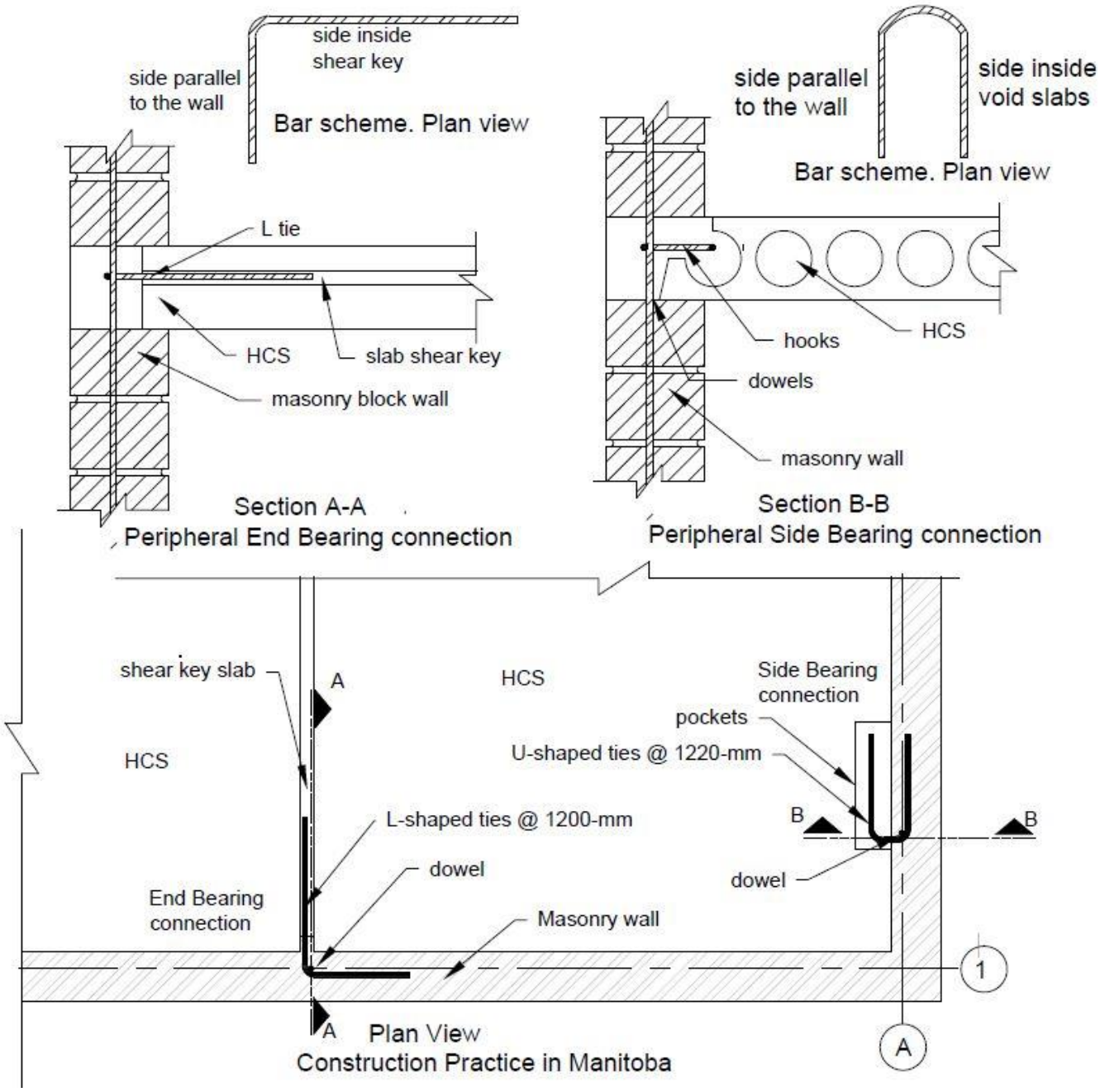

Fig. 2.8: Bearing connections using L-ties and hooks - Construction practice in Manitoba

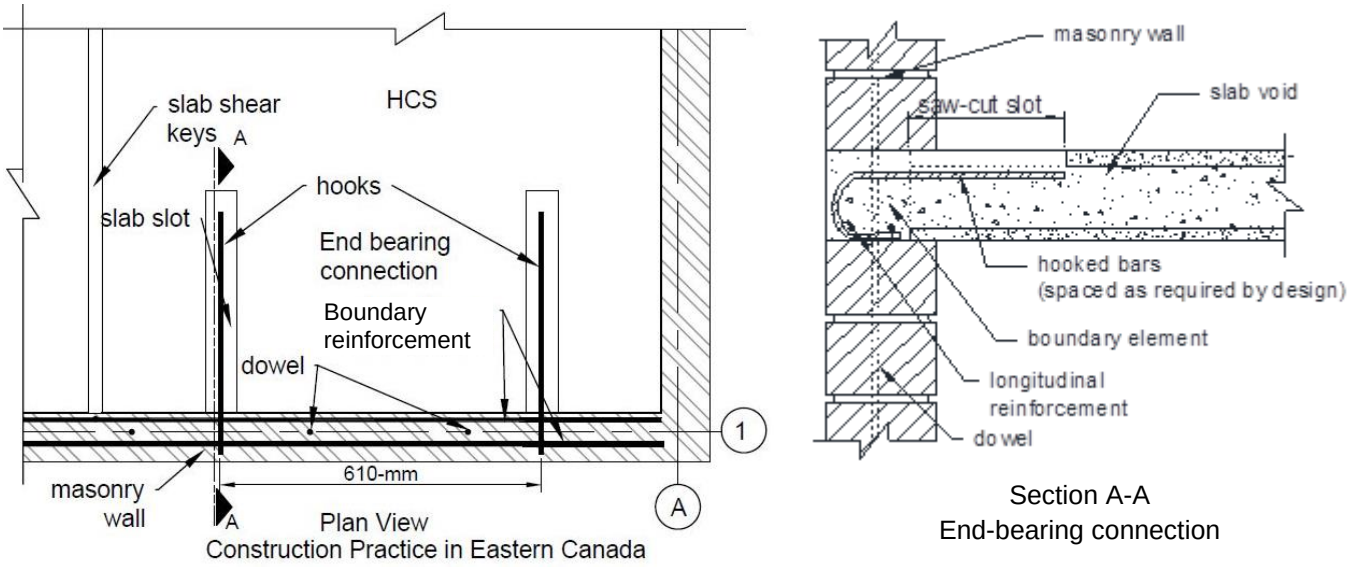

Fig. 2.9: End Bearing Connection using hooks imbedded in bond beams - Reproduced from PCI (2015)

2.3.2.2 L-shaped steel reinforcing bar

The connection detail described in Chapter 1, which consists of a 10M reinforcing bar inserted in the masonry wall and grouted to the HCS, is often employed in building sites on Eastern Canada. This connection detailing is illustrated in Fig. 2.10. Practitioners often choose this detailing for bearing connections because of its simplicity, economy, and relatively fast installation. Typically, the "L-shaped" connection bar is hammered into the bond beam, which results in no work disruptions and relatively early loading of the connection.

Nevertheless, other practitioners are inclined to use adhesive to enhance the bonding to the masonry wall. Also, the use of adhesive eliminates the risk of bar pull-out from the beam. However, including adhesive carries additional costs, and in large projects, it could become unsuitable. According to the manufacturers, the used adhesive (epoxy resin) setting times range from 10 minutes to 2 hours, resulting in minimal or no delays in the construction process. Other

aspects, such as embedment length into masonry (150-mm), bar size (10M or 15M), and embedment into HCS joints (450 ~ 600-mm), remain equal to previously discussed connections.

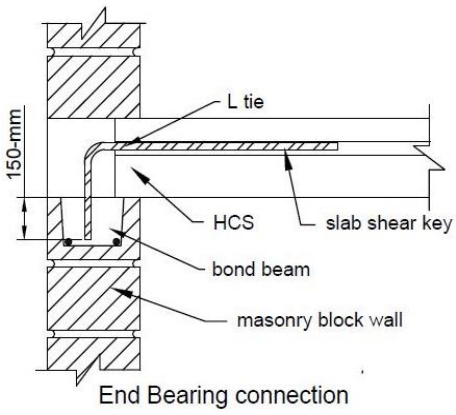

a) L-tie in End Bearing connection

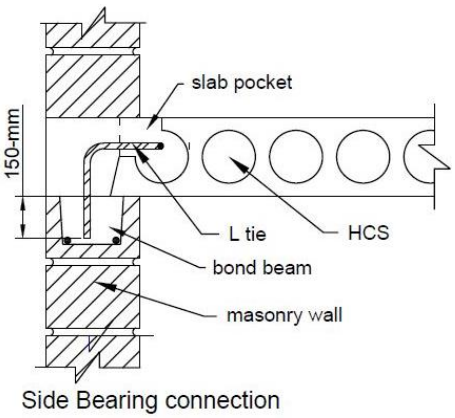

b) L-tie in Side Bearing connection

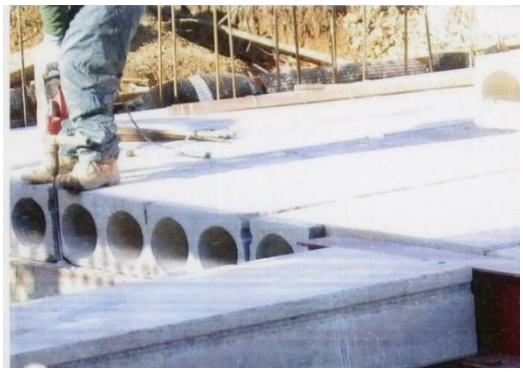

c) Drilling of the bond beam on top of the wall

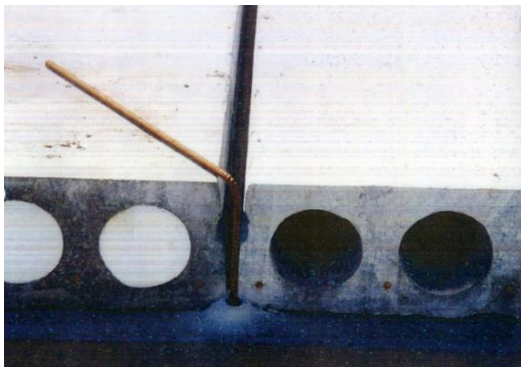

d) Reinforcing bar dry-fit

Fig. 2.10: Construction and connection detailing of "L-shaped" connection bar of HCS floors over masonry (Personal Contact 2019)

The construction process of the L-shaped bar (inserted in the masonry wall) begins with drilling the bond beam 150-mm from the top of the slabs as shown in Fig. 2.10 (c). The hole is thoroughly vacuumed to remove debris from drilling. Next, the hole is filled with the adhesive (epoxy), if applicable, while following the manufacturer guidelines, and the bar is inserted or hammered, as

illustrated in Fig. 2.10 (d). For bar connections without adhesive, hammering the bar is necessary to ensure tight-fitting and minimize bar pull-out. Finally, the HCS joints are grouted.

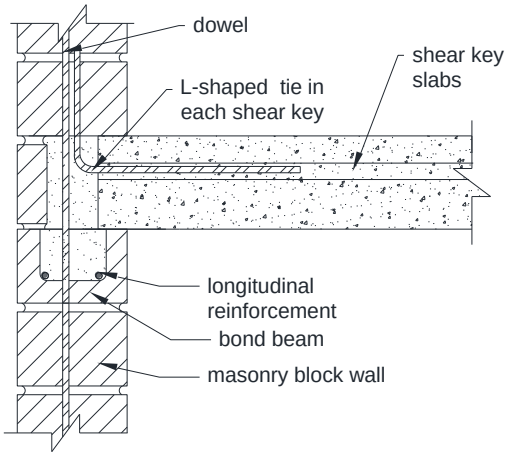

Fig. 2.11: Inverted L-ties in End-Bearing connection - Reproduced from PCI (2015)

Another connection detail variation consists of inverting the position of the reinforcing bar, as shown in Fig. 2.11. Therefore, the construction process differs from what was mentioned above. After placing the slabs on the masonry walls, the L-shaped bar is inserted at the HCS joints, and the connection is grouted, leaving the other end exposed. Later, the next course of masonry units is laid down, inserting these masonry units throughout the steel bar. Placing heavy masonry units throughout the bar is the most outstanding drawback of this connection detail. Compared to the previously introduced connection detail, the construction procedure of this bearing connection is more labor-intensive and requires more grout volume. Finally, the connection is fully assembled after grouting the masonry units on the top level.

2.4 Research Conducted on HCS Bearing Connections to Concrete Beams

Critical incidents during earthquakes in the United States and New Zealand (Northridge 1994; Christchurch 2011) resulted in the collapse of several buildings constructed with HCS floors. An analysis of the causes for these collapses demonstrated that local failures occurred at the HCS bearing connections, which led to a global collapse. These events raised concerns regarding the safety of buildings constructed with HCS, which led to in-depth investigations of continuous HCS connections under seismic loads.

Researchers from the University of Canterbury in New Zealand investigated the seismic response of HCS bearing connections to concrete beams (Mejia-McMaster and Park 1994; Herlihy 1999; Matthews et al. 2001; Lindsay et al. 2004; MacPherson et al. 2005). These investigations were focused on enhancing the connection detail. The connection detail most used in New Zealand up to that date (Fig. 2.12a). This connection detail was expected to offer stability to the slabs and transferring horizontal forces from earthquakes. Other connection details (Fig. 2.12) were proposed and investigated to increase ductility, energy dissipation and capacity of the connection and optimize the seismic response of the connection. The outcome of their investigations resulted in a design methodology in the NZS 3001: 2006 code (Concrete Design Committee P 3101, 2006). Also, this series of experimental research influenced the approach to construct HCS bearing connections in North America. Therefore, further investigations were conducted to verify the applicability of the connection detail employed in New Zealand to deep HCS bearing connections (Corney et al. 2018).

2.4.1 New Zealand connection detail

New Zealand is in the Ring of Fire, one of the zones with higher vulnerability to earthquakes of great intensity. The catastrophe of Northridge, California in 1994 alarmed the international community about the stability of buildings constructed with HCS floors in seismic areas. After a profound analysis of the event, Mejia-McMaster and Park (1994) noted that the HCS floors collapsed after the slabs were displaced and missed their seating length. The progressive collapse was owed to the improper steel detail of a few connections. The improper steel detailing caused slab debonding, bearing loss and diagonal cracks. Later, Matthew (2004) identified the rotation of the HCS over the supporting beam as a mechanism of failure that had not been addressed in previous research. The rotation of the connection caused topping lifting, cracking and ultimately slab debonding. Then, a series of experimental investigations started at the University of Canterbury to optimize the connection details (MacPherson 2005). Finally, Jensen et al. (2006) studied previous results to classify the mechanism of failure of HCS bearing connections. Based on this knowledge, new connection detail was proposed and tested. This connection detail is included in the design code of New Zealand. Fig. 2.12 illustrates the connection details tested to horizontal in-plane loads at the University of Canterbury.

2.4.1.1 Loss of bearing

Using the analysis of the 1994 Northridge events, Mejia-McMaster and Park (1994) designed an experimental program focused on evaluating the existing connection detail and assessing their safety. These researchers included in the program a new connection with enhanced steel details (Fig.2.12 (b) and (c)). The main objective was to evaluate the floor stability after the event of loss of bearing. Post-failure HCS stability would provide sufficient time for the public to evacuate and

save lives. In this case, the steel reinforcement would carry the gravity loads in extreme conditions and maintain the floor stable. A second initial condition was also included in that research. The HCS connection assembly would be subjected to lateral loading that would cause loss of bearing and continue the test after the loss of bearing. This second case examined the influence of the damage accumulated in the bearing connection on the stability of the floor. Gravity loads were taken into account using an equivalent weight of cement bags.

The three connection details tested involved steel ties of f_y = 300 MPa and 16-mm diameter inserted in two voids of the 200-mm thick HCS. Two 750-mm deep cuts were made in the flanges of the slabs at the void locations to insert such ties and ensure full embedment in concrete. Concrete topping of 65-mm thickness was cast on top of the HCS floor. This topping was reinforced with a steel mesh. The three tested connections were essentially different in the shape of ties. The first type of connection had straight bars with hooked ends (Fig. 12 (a)). This connection was integrally cast with the beam section; thus, the straight ties passed through the supporting beam reinforcement. Ties in the second type of connection were shaped as inclined hanger bars or saddle bars without hooks at the end (Fig. 12 (b) and (c)). The last type of connection was a combination of the first two types. In this case, ties were shaped as bent bars with hooks at the ends (Fig. 12c)

Full-scale connection assemblies were constructed and tested under monotonic unidirectional load until failure. The assembly included three continuous spans constructed with 200-mm thick HCS and their bearing connections over concrete beams. These bearing connections were supported on a hinging mechanism attached to a rolling support frame. The force was applied by two parallel hydraulic actuators attached to clamping beams, which formed a single piece with the rolling support frame. These clamping beams distributed the load along the side face of the HCS (Jensen 2006).

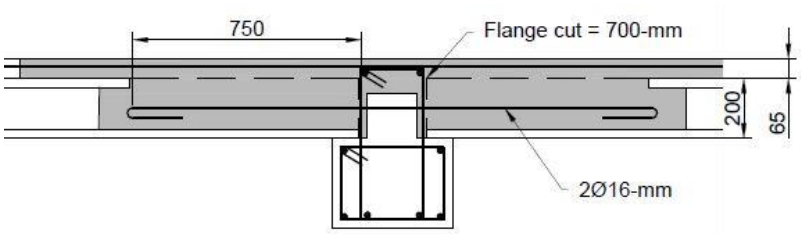

a) Straight tie with end hooks (Mejia-McMaster and Park 1994)

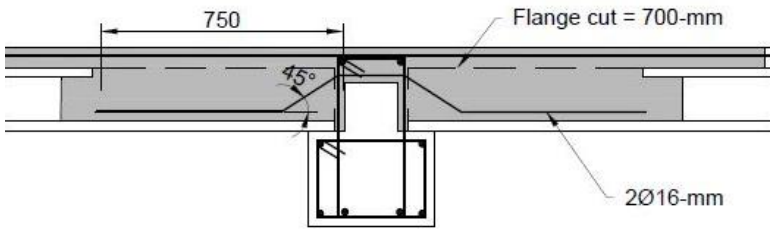

b) Saddle bar ties (Mejia-McMaster and Park 1994)

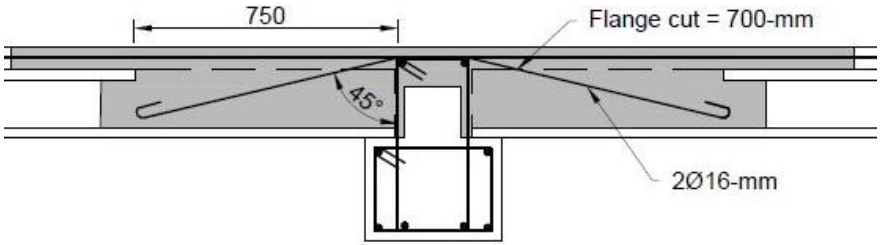

c) Saddle bar ties with end hooks (Mejia-McMaster and Park 1994)

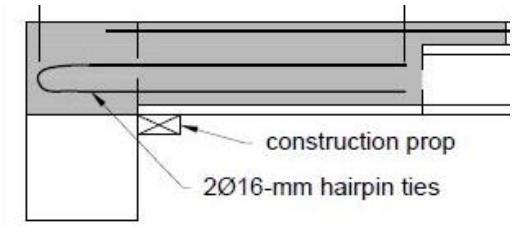

Note: Bull and Matthews (2003) tested closed paper clips ties with identical detailing

d) Hairpin ties. 300-mm series HCS (Herlihy 1999).

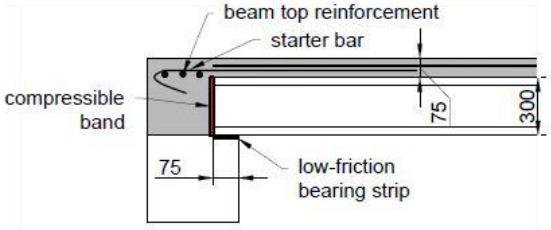

Note: Matthew detailing is identical but with a mortar bed instead of a low friction bearing strip and plugs instead of compressible bands

e) Starter bars with compressible bands (Matthews 2004)

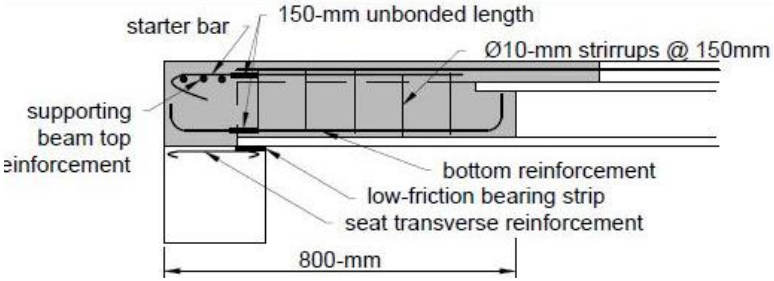

f) Reinforced timber infill (MacPherson 2005)

Fig. 2.12: Evolution of connection detail - Reproduced from (Mejia-McMaster and Park 1994, Herlihy 1999, Matthews 2004, MacPherson 2005)

Test results revealed that ties were able to maintain the slabs suspended after the event of loss of bearing. The capacity of the connection after the loss of bearing can be calculated with the expression found in the shear friction theory. However, the large horizontal displacement of the HCS making the shear friction principles not valid. The best performance was observed for the connection detail Types 1 and 3, in which the ties were shaped with round plain straight bars and ends shaped as hooks. These connections were capable of supporting a vertical shear force of 85 kN after the HCS were pulled 55 mm out of the supports. The tie bars with segment inclined or saddle bars resulted in an undesired behaviour owing to web splitting due to the lack of shear reinforcement in the slabs.

Herlihy (1999) employed a similar setup to test four types of HCS bearing connections to concrete beams. However, the HCS bearing connection sub-assembly included a single span of an HCS floor. At one end, the HCS units were tied to a hinging mechanism supported on a rolling support frame. The other end consisted of the bearing connection cast integrally with the supporting beam. The concrete beam was tied to the laboratory floor. The type of test employed was pull-out testing using two hydraulic actuators attached to clamping beams, which were fastened together to the HCS rolling end.

The two bearing connections tested were taken from the construction practice at that time. The first bearing connection involved 12-mm diameter steel ties, or starter bars, embedded for 600 mm in the concrete topping. The second type of connection consisted of steel reinforcement shaped as hairpin ties inserted at the cores of the slabs and extended for 500 mm into the hollow core (Fig. 12 (d)). The flanges of the slabs were cut to allow for pouring concrete and ensure full reinforcement cover.

The third bearing connection included a straight continuity bar detail integrated with the supporting beam and the concrete topping. In this case, the continuity reinforcement had an "L-shaped", where the shorter end was intertwined with the shear reinforcement of the supporting beam and cast integrally. A fourth connection detail that consisted of inclined or bent steel ties inserted in the cores of the slabs and cast integrally with the beam and the topping was also tested.

The comprehensive program of Herlihy (1999) covered numerous test variables in HCS bearing connections. For instance, Herlihy (1999) tested these connections under different loading schemes (monotonic and cyclic), initial conditions (with initial supporting length equal to zero or fully supported) and with/without gravity load. After the series of sub-assembly testing, Herlihy (1999) drew the following conclusions about the connection detail.

- First, starter bars and their variations do not offer ductility and trigger HCS floor debonding. In the case of testing the connection with the continuity bar detail, the topping slab uplifted, and significant bond degradation occurred.
- On the other hand, hairpin connection detail provided a ductile and controlled response against the monotonic and cyclic loading.
- Also, removing part of the HCS flanges and fully grouting the voids magnified topping bond capacity.
- Finally, the fourth connection detail involving the embedded tie bar detail exhibited an excellent response to the cyclic loading. The latter connection demonstrated sufficient ductility and strength. However, the inclined ties exhibited an onset of buckling, which caused topping concrete spalling and bar popping out of the slabs.
- In agreement with Mejia Mc-Master and Park's (1999) results, Herlihy (1994) also concluded that the reinforcement detail with bent portions resulted in little ductility and

web splitting and forced a slab debonding. Round plain bars also offered great energy dissipation and sufficient capacity. The greatest contribution of Herlihy (1999) was the open hairpin steel detail, which would be later studied in ensuing research.

2.4.1.2 Relative rotation of the floor

After the series of pull-out tests conducted by Mejia-McMaster and Park (1994) and Herlihy (1999) to investigate the loss of bearing, a new failure mechanism was identified: relative rotation of the HCS in relation to the supporting beam. When cyclic loading acts in the frame, torsion occurs in the beam, which is transferred at the slabs through the bearing connections. Matthews (2004) found that this rotation of the HCS connections provokes topping uplifting, diagonal cracking and ultimately, slab debonding. The HCS suffers cycles of elongation/contractions, generating a plastic hinge in its bearing connection. To reach this conclusion, the researcher applied a theory proposed by Lee and Watanabe (2003) that is related to beam-column connections under cyclic loading. Lee and Watanabe (2003) had previously demonstrated that whenever a plastic hinge occurs in a beam-column joint, the beam elongates. In general, this elongation occurs due to for either of these two reasons: (a) the reinforcement yields in tension and concrete cracks, or (b) a flexure- shear truss is formed within the beam. Based on (a), the bearing length can be calculated with the peak rotation of the joint that contributes to beam elongation.

Matthews (2004) disregarded reason (b) and measured the elongation of the slabs, deformation of steel versus drift storey and constructed a "rainflow counting method " based on Lee and Watanabe (2003) work to obtain the maximum rotation and maximum displacement of the slabs.

The rainflow counting method (Lee & Watanabe, 2003) consists of plotting inter-storey drift (x-axis) versus elongation (y-axis) and adding the amplitude of the x components to estimate total

slip. Through experimental testing, Lee and Watanabe (2003) defined four stages on the formation of the plastic hinge until ultimate failure occurs: pre-flexural yielding, post-flexural yielding region, slip region and repeated loading region. Typically, the graphs show a reversal of the direction of the slip (elongation/contraction) at these four points. According to expected patterns, equations can be used to estimate the slip/strain out the rainflow graph.

Using this method and the equations from Lee and Watanabe (2003), Matthew (2004) predicted a slab elongation of 37-mm. From the experimental research, a slab elongation of 35-mm was obtained. Hence, this result validated the equations of Lee and Watanabe (2003) for their use in HCS bearing connections. This method quantified the seating length necessary for the slabs to elongate under cyclic loading without early cracking. Matthew (2004) also demonstrated that providing a seating length of 75-mm would be more appropriate for seismic conditions. A seating length would leave enough room for the slabs to elongate in compression and tension without loss of bearing. Prior to his research, the New Zealand code only demanded 50-mm of seating length in HCS floors. As a contingency measure, Matthew (2004) recommended installing a steel angle in those HCS bearing connections where the seating length was shorter than 75-mm, especially in high-risk seismic zones. The steel angle would catch the HCS in the event of loss of bearing.

The connection detail tested by Matthew (2004), shown in Fig. 2.12 (e), comprised a starter bar, a 75-mm concrete topping with a wire mesh reinforcement and a concrete supporting beam. The HCS was supported on a mortar bed on the concrete beam, and its seating length was 50-mm as specified. The starter bar was extended 600-mm in the concrete topping and tied to the transverse reinforcement of the beam. This connection detail was previously tested by Herlihy (1999) without assessing the effect of relative floor rotation. To induce floor rotation, the supporting concrete frame (beams and columns) was supported on hinges and loaded with two hydraulic actuators at

the ends of the columns. A self-acting steel frame distributed these forces to interior columns. These actuators were fixed to two individual reaction frames. Test results revealed that the frame suffered little damage while the HCS floor diaphragm failed at relatively low values of inter-storey drift (1.9-2.5%). Matthews (2004) also proposed retrofitting techniques for potentially dangerous HCS bearing connections.

Based on the research of Matthew (2004), a new approach to investigate HCS bearing connections continued. This approach focused on modifying the steel detail of HCS connections to reduce slab elongation due to the rotation of the connection. The researchers used the same test setup and assembly after Matthew (2004). Lindsay et al. (2004) continued the investigation by testing connection modifications proposed by Matthew (2004). The connection contained a low friction bearing strip, compressible bans and a 750-mm length timber infill along with the typical starter bars. The purpose of such modifications was to facilitate slab elongation in the expected zone of plastic hinge with the low friction bearing strips. The compressible band was placed at the interface of the HCS with the beam. This band was intended to reduce compression stresses from the slabs pressing the beam down and mitigate the possibility of cracking in both members.

However, these materials did not behave as expected. The compressible band was able to compress 1 mm only, and the bearing pad exhibited excessive friction. Despite the unexpected behaviour, these changes in the connection details resulted in little damage to the HCS and the supporting frame. The new system was able to survive a ± 3.0% of inter-storey drift without loss of bearing. Later, MacPherson et al. (2005) concluded that the concept was innovative, but the materials involved demonstrated poor performance. The second generation of the compressive band and the low-friction strip could have achieved the elastic behaviour predicted.

The HCS bearing connection detail, tested by MacPherson et al. (2005), illustrated in Fig. 2.12 (f), contained four main components: (1) starter bars extended 600-mm into the concrete topping, (2) seat transverse reinforcement in the supporting beam, (3) a low friction bearing strip, and (4) 750-mm concrete infill, which included bottom reinforcement and stirrups. These stirrups were spaced at 150-mm. The bottom reinforcement and starter bars had a 150-mm unbonded length to allow for free elongation without cracking. Additionally, these authors modified the length of the longitudinal bars. For their specimens, the bars extended 900-mm from the peripheral beam towards the HCS. The NZS 3101:1995 code (NZS, 1995) had stated that those bars should be extended to either the largest of 20% of the slab span or the development length (l_d) plus 400-mm. Nevertheless, the authors considered that this distance was unnecessarily long and overly conservative in terms of effective anchorage (T_e). In addition, regarding the concrete infill, the authors carefully implemented plugs (foam cut in circular shapes) for enclosing the concrete while casting because the asymmetrical distribution of flooring masses could alter the rotation of the floor and affect the results.

After these modifications to the connection detail, the HCS exhibited little damage at the end of testing. Instead, the column to beam connection suffered severe damage, and the failure happened due to the collapse of the frame. The HCS connection resisted an inter-storey drift of ±5%. The damage in the HCS units was minimal. This outcome demonstrated that the clause from the code of limiting inter-storey drifts up to 1.2% was no longer needed in designs of buildings with HCS floors. This investigation validated the details of steel reinforcement proposed by Matthew (2004) and Lindsay et al. (2004) and set the standard for the behaviour of HCS bearing connections.

Jensen et. al (2006), Jensen (2006) and Jensen and Bull (2007) analyzed the outcomes of previous research to classify the mechanisms of failure of HCS diaphragm floors over concrete beams and propose retrofitting techniques. The classification consisted of four main mechanisms:

1. *Loss of seating with delamination of topping from the hollow-core units (LOSD)* In this case, the connection fails because the seating length was too short and the ledge of support below the hollow-core is spalled, or the HCS webs fractured. HCS floor debonding can occur when the starter bar is not long enough.
2. *Loss of seating without delamination of the topping (LOS)* This failure mechanism is similar to the LOSD mechanism. The difference is that the topping does not delaminate from the HCS units. If the steel reinforcement does not overcome the acting stresses (e.g. not sufficient steel reinforcement ratio), the starter bars fail along with the mass of concrete.
3. *Flexural-shear failure (FS).* (Matthews 2004) This mechanism can be identified for HCS snapping. It occurs because the connection has excessive fixity in relation to the hollow-core shear strength. Diagonal shear cracks are the usual cracking pattern in the HCS ends starting at the ledge of support. It grows through the hollow-core webs until it reaches the topping.
4. *Offset flexural shear failure (OFS)* (Liew 2004). The cause of this mechanism is excessive tie reinforcement at the end of the hollow-core unit. The behaviour is like (FS) mechanism, but they differ on the plane of failure. In this case, the cracking pattern appears offset from the origin of the hollow-core unit.

The proposed retrofitting technique were low-invasive and relatively simple. The first technique included installing a steel angle seat, which had clearance to reduce friction or clamping effect. This was previously recommended by Matthews (2004), yet not tested. The second retrofitting

technique consisted of drilling and installing reinforcement plates anchored with steel bolts, or similar, to increase robustness of the connection. Finally, to reduce fixity and rotation, a weakening method was introduced in the third technique: saw-cutting the joint between the slab and the beam face until the reinforcement. These methods were tested individually and combined to assess their performance. The steel angle and the saw-cut weakening prevented loss of bearing until 85-95-mm of slab elongation. However, the connection exhibited approximately 35% of flexural strength reduction. Other combinations exhibited less desirable failure modes.

2.4.1.3 Deep hollow-core slabs bearing connections to concrete beams

Previous studies were limited to shallow HCS bearing connections (slabs of maximum 300-mm thickness). It was acknowledged, in more recent investigations, that deep Hollow-core slabs HCS exhibit different behaviour under shear compared to their counterparts with shallower depth (less than 300 mm). Then, the bearing connection details recommended in the NZS 3101:2006 (Concrete Design Committee P 3101 2006) needed validation for deep HCS. Currently, 400-mm and 500-mm deep HCSs have become common in parking structures, where long spans and clear heights are required.

Corney et al. (2018) performed five full-scale pull-out tests on deep HCS bearing connection sub-assemblies under seismic load. The connections contained the detailing proposed by the New Zealand standard NZS 3101: 2006 (Concrete Design Committee P 3101 2006) shown in Fig. 2.14. Test results confirmed the suitability of the steel detail proposed by the NZS 3101: 2006 code (Concrete Design Committee P 3101 2006). The five specimens survived up to 4.5% of inter-storey drift and slab elongations of 60-mm. Also, the HCS remained stable (suspended) after completely missing the seating length. They also demonstrated that the reduction of flexural

strength at the connection allows for free rotation without damage in the beam or the slabs. Despite the specimens did not exhibit spalling, these authors recommended increasing the seating length to 100 or 150-mm when designing deep HCS connections.

2.5 Provisions for HCS Bearing Connections in International Codes

2.5.1 NZS 3101-06 (Concrete Design Committee P 3101 2006)

The NZS 3101-2006 (Concrete Design Committee P 3101 2006) is a design code with recommendations, design methodology, and specifications for concrete structures in general. The last amendment to this code was released in 2017. This code comprises multiple sections dedicated to the seismic design of HCS floor diaphragms. Fig. 2.13 illustrates the connection detailing recommended by the NZS 3101-2006 (Concrete Design Committee P 3101 2006) . First, the code recommends inserting transverse steel reinforcement or ties in grouted cores or shear keys of HCS to prevent loss of bearing of the units (bottom infill reinforcement as discussed in previous research). The embedment length is larger than 600-mm in seismic resistant HCS diaphragms, and up to two ties are sufficient per slab (tie spacing at 610-mm). The capacity of such ties in tension should be larger to 70 kN per meter of the wall in peripheral connections and 22 kN in internal connections.

Also, concrete topping of at least 65-mm thickness is recommended with wire mesh as reinforcement. Starter bars are necessary to integrate the topping with the supporting beam and ensure the composite/monolithic behaviour. In interior connections, the starter bars overlap. This overlapping shall be the greater of the L_d + 400-mm or $0.2l_n$. The bar diameter employed in the connection detail should be less than one-fifth of the topping thickness, and the steel quality should be Grade 300. Ties and starter bars shaped with these steel bars shall be anchored to the supporting beam Opening the flanges of the slab with saw-cutting or milled methods is suggested for

placement of concrete infill into the cores of the slabs. This could potentially avoid floor debonding. In case of casting a timber infill, stirrups shall be provided spaced at 150-mm or according to calculations of shear transfer. Conservative values of seating lengths (always greater than 75-mm) are also encouraged as long they are practical. HCS bearing connections to concrete beams should be cast in one operation to obtain monolithic connections that behave compositely.

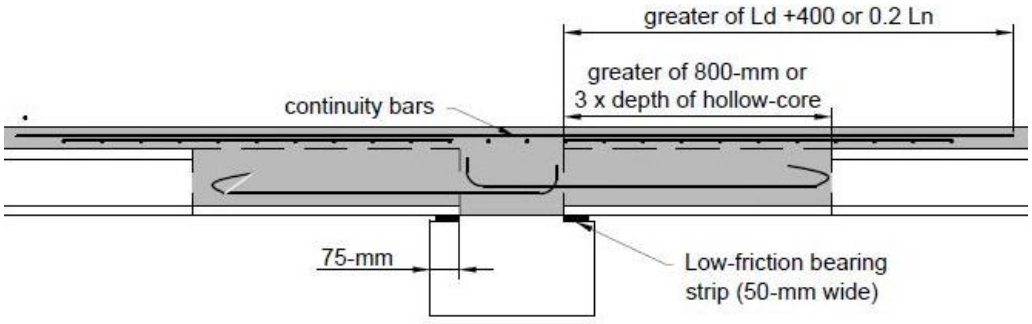

a) Internal bearing connection with ties and continuity bars

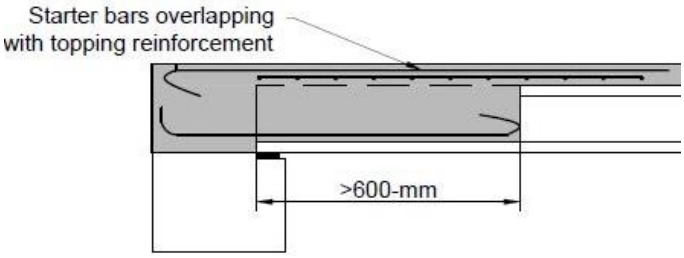

Note: Reinforcement ratio must be calculated according to Comment C18.7, Chapters 13 and 18. Recommended diameter and material is 16-mm Grade 300 or larger. Minimum two ties should be provided per slab.

b) Peripheral bearing connections with ties and starter bars

Fig. 2.13: HCS bearing connections - Reproduced from NZS 3101 (NZS 2006).

In February 2011, an earthquake of magnitude 6.3 on the Richter scale stroke the centre of the city in Christchurch, New Zealand. Despite the short duration of the earthquake, the centre of the city suffered irreparable damage, more than 185 people lost their lives and thousands suffered major injuries (McSaveney, 2017). However, a report (Henry et al. 2014) of the incident pointed out that bearing connections complying with the NZS 3101:2006 (CDC-P 3101, 2006) exhibited minor

damage.. It is understood that the buildings with these connection detail did not collapse thanks to the lateral strength provided by HCS floor diaphragms to the frames and moment resistant walls (Henry et al. 2014). In contrast, those older building without code compliant bearing connection detailing failed due to loss of bearing and beam-slab elongation (Henry et al. 2014). Therefore, the tragic incident offered an opportunity to test the HCS bearing connections.

2.5.2 European Standards. DIN EN.1168: 2008 and EN-1992-1-2004

The European Standards DIN EN.1168:2008 (CEN/TC-229 2010) and EN-1992-1-2004 (CEN/TC 250 2008) complement each other to provide best practices, design and specification criteria for HCS bearing connections. Annexes B and H of DIN EN.1168-2008 (CEN/TC 229 2010) state design principles and concepts to consider while designing such connections. First, for cases of low-risk seismic loading, such as in low-rise buildings, the HCS ties can be calculated using the shear friction theory in monolithic/continuous connections. In contrast, in high-risk seismic regions, this code states that, at least, one of the following should be provided: (a) a concrete topping of at least of 40-mm of thickness, (b) a system of properly designed ties (Fig 2.14), or (c) a system of indented lateral edges (Fig. 2.15).

In HCS floors without concrete topping, the tie system consists of a hairpin tie for intentionally flexible connections or enclosed ties for rigid connections. The flanges of the slabs should be cut to insert the hairpin ties or enclosed ties and grout the connection easily (Fig. 2.14). The connection can also include a cast in situ edge beam incorporated into the connection. This connection detailing also provides bracing to the lateral force-resistant frame DIN EN 1168: 2005-08 (Technical Comittee CEN/TC 229 2010). The reinforcement ratio of these ties can be calculated

using equations 2.7 and 2.8 provided by the EN 1992 1-04 (Technical Comiittee CEN/TC 250, 2008):

For peripheral ties: $F_{tie} = l_i q_1 \geq Q_2$=70 kN (2.7)

For internal ties: $F_{tie} = \frac{l_1+l_2}{2} q_3 \geq Q_2$ (2.8)

Where:

F_{tie} is the resistance force of the tie

l_1 and l_2 are the length of the end-span or consecutive spans

q_1 is 10kN/m, q_3 is 20 kN/m, approximately

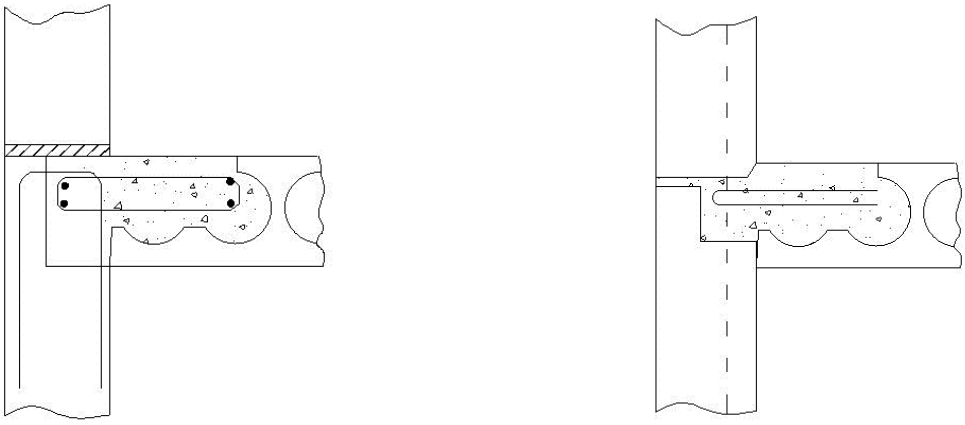

a) Enclosed tie for rigid connections b) Hairpin tie for flexible connections

Fig. 2.14: Tie connection of HCS to concrete supports - Reproduced from DIN EN 1168:2005-08 (Technical Comittee CEN/TC 229 2010)

Annex B of DIN EN 1168.08 recommends the type of grout, best practices and tolerances required for the construction of the joint. For instance, this code recommends profusely vacuuming the surface of shear keys and saw-cut slots/pockets to eliminate debris and dust that may interfere with joint bonding. Regarding the grout mixture, the maximum size of aggregate should be selected

accordingly to fit the space between the bar and the lateral face of the slabs. Also, this grout mixture should have a consistency that allows for filling the joint without settlement or formation of cavities and ensure proper bar cover. The minimum compressive strength of grout recommended is 20-25 MPa. The hardened grout should be normally cured (wet-cured) to ensure no cracks due to shrinkage. Also, minimum slabs spacing is set to fit the rebar in the shear key. The top spacing should be at least 30-mm wide to ensure enough space for grout placement, as shown in Fig. 2.15.

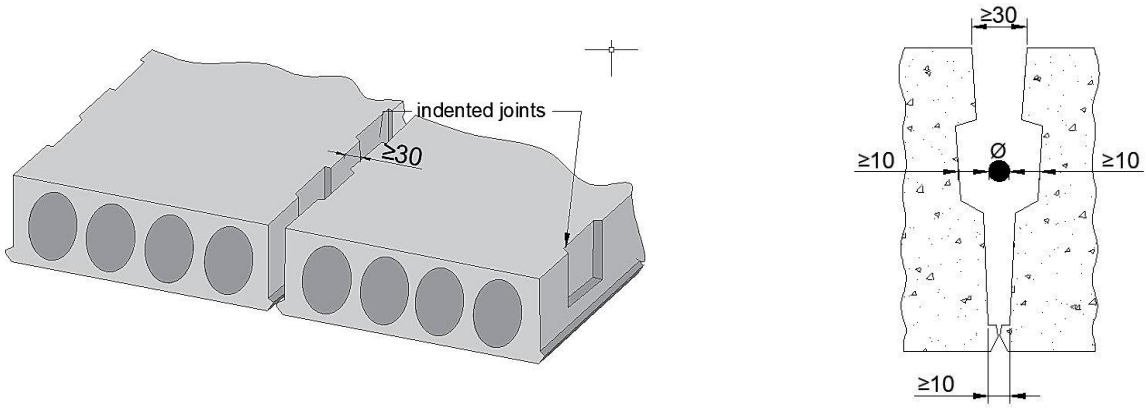

a) Spacing at top. Indented joints b) Tie placement at shear keys. Cross section

Fig. 2.15: Grouted shear key joints - Reproduced from DIN EN 1168-08 (Technical Comittee CEN/TC 229 2010).

2.6 Provisions in North American - Shear Friction Theory

2.6.1 Code provisions CPCI (CPCI 2017) and CSA A23.3-19 (CSA 2019a)

The CPCI (CPCI 2017) and CSA A23.3-19 (CSA 2019) codes recommend the equations from the shear friction theory to quantify the reinforcement ratio required to resist the in-plane forces. According to this theory, when cracks are expected to occur across a shear plane, steel reinforcement shall be provided to resist the shear stresses across that plane. If the cracks are narrow and tortuous, the interlock friction between concrete faces significantly contributes to

resisting shear stresses. In this case, the resistance to in-plane horizontal forces can be calculated with the following expression:

$$V_r = \lambda\phi_c(c + \mu\sigma) + \phi_s\rho_v f_y cos\alpha_f \quad (2.9)$$

When the cracks are excessively wide, and there is no friction interlock, the steel reinforcement carries the horizontal shear alone. In this case, steel reinforcement fails due to a kinking of the bar, since the contribution of concrete is zero ($V_c = 0$), then:

$$V_r = \phi_s\rho_v f_y cos\alpha_f \quad (2.10)$$

For direct tension stresses acting on the connection, all contribution of concrete shall be neglected, and the connection capacity is calculated as follows:

$$A_n = \frac{N_f}{\phi_s f_y} \quad (2.11)$$

Where:

λ = 0.8 for light-weight concrete, 1 for regular concrete, 1.2 for high-density concrete

ϕ_c is 0.65 for cast in-situ concrete, 0.7 for precast concrete

$\lambda\phi_c(c + \mu\sigma)$ shall not exceed $0.25\ \phi_c f'_c$

$\sigma = \rho_v f_y sin\alpha_f + \frac{N}{A_g}$ is the effective normal stress

N is the horizontal component of the shear force applied across an inclined plane with the same load factors as the shear force applied

ϕ_s is 0.85 for regular mild steel and 0.9 for high strength steel

$\rho_v = \frac{A_{vf}}{A_{cv}}$ is the ratio of shear-friction reinforcement

f_y is the fluency tension in reinforcing steel

α_f is the angle between the crack width and the shear displacement

Mejia-McMaster and Park (1994) employed this theory, and equivalent mathematical expressions, to predict the capacities of HCS bearing connections to concrete beams under horizontal in-plane monotonic loading. The connections tested by these authors were illustrated in Fig. 2.12 (a), 2.12 (b) and 2.12 (c) referred as connection types I, II and III, respectively. In general, the connections tested by Mejia-McMaster and Park (1994) exhibited more capacity than predicted (14 and 2% in connections type I and III). Connection II demonstrated an early failure (failed at 17% less capacity than predicted) due to splitting of the HCS, which provoked tie anchorage failure. Yet, these results demonstrated that shear friction equations are suitable for capacity prediction of monolithic HCS bearing connection with concrete topping reinforced with steel ties under monotonic pull-out forces.

However, to apply this theory, the failure mode must be clear. It was demonstrated previously that depending on the connection detail, failure may occur at different locations and for multiple reasons (LOSD, LOS, FS, OFS mechanisms) (Jensen 2006; Jensen et al. 2006; Jensen and Bull 2007). Some of these most common mechanisms of failure exhibit shear planes at different locations of the connection. For example, cracking could occur at the HCS (snapping due to lack of shear strength compared to the fixity of the connection), at the interface with the concrete beam (weak anchoring), at the topping (insufficient length in starter bars) or between the slabs and the topping (debonding). Therefore, these equations are useful to quantify the reinforcement ratio once the shear plane of failure was defined through experimental research. The CPCI website (CPCI 2021) offers a wide range of connection detailing that could be employed in bearing connections of HCS. However, these connections should be tested before assuming a plane of shear failure. Additionally, the shear friction theory does not account for the relative rotation that the bearing

connection suffers as a result of the deflection of the frame (Matthews 2004). Therefore, this theory cannot be applied alone to design HCS bearing connections in high-risk zones.

2.6.2. American Concrete Institute (ACI) 318-19 (ACI 2019)

The ACI 318-19 code (ACI 2019) also proposes the shear-friction theory to calculate the in-plane shear capacity of connections. However, this code added two clauses to the shear-friction equations. These clauses account for the materials involved in the connection and concrete cast at different times. Surface contact between dissimilar materials significantly affects the friction coefficient.

Other factors considered in the equations are the angle of load application which determines the cracking plane. The ACI 318-19 code (ACI 2019) states one expression for each specific situation. The most common case given in construction practice is in-plane loads acting 90-degrees perpendicular to the reinforcement, crack development appearance in 45-degrees and surface intentionally roughened. According to that code, the expression to calculate the horizontal-shear resistance is:

$$V_n = 0.8A_{vf}f_y + A_cK_1 * \sin(\alpha) \quad (2.12)$$

Where K_1 is 400-psi for normal-weight concrete, 200-psi lightweight concrete and 250-psi for sand concrete.

In the case of large crack widths, the shear-friction reinforcement is calculated as follows:

$$V_n = A_{vf}f_y\mu \quad (2.13)$$

when the shear-friction reinforcement is perpendicular to the shear plane.

$$V_n = A_{vf}f_y(\mu sin\alpha + cos\alpha) \quad (2.14)$$

in all remaining cases, where α is the angle between the shear-friction reinforcement and the shear plane.

CHAPTER 3 - EXPERIMENTAL PROGRAM

3.1 Test Program Overview

This research program aims at defining the capacity and mode of failure of the reinforcing bar connection of HCS to steel beams and masonry wall supports. The typical reinforcing bar connection was meticulously described in Chapter 1 and Sections 2.3.1.1 and 2.3.2.2 of Chapter 2. Twenty full-scale HCS bearing connections using "Z-bars" as connection reinforcement were assembled and tested until failure. These full-scale specimens imitate the construction practice in Canada for end and side bearing connections of HCS floors. The experimental program is divided into two phases. Phase I contains eleven specimens constructed with HCS supported on steel beams, where a reinforcing bar is inserted at HCS joints or pre-determined pockets to tie the slabs to the beam. In Phase II, which consists of nine specimens, similar connection detailing was used, but the supporting member was a masonry beam.

Test variables in this research are the type of bearing connection (End Bearing or Side Bearing denoted as "EB" or "SB," respectively), load direction (compression/pushing and tension/pulling, represented as "C" and "T") and load orientation (normal "N" or parallel "P" to the longitudinal axis of the supporting member). These test parameters were set to address all possible forces and bearing conditions acting on the HCS floor. Table 3.1 summarizes the specimen coding and test variables considered in this experimental program.

Table 3.1: Test specimens – Phase I

Type of support	Type of bearing	Specimen code	Load direction	Load orientation	Bend angle (°)
Steel Beam	End Bearing (Series I)	EB- S-CN-90	Pushing/Compression	Normal to support axis	90
		EB-S-CN-90R			90 R[1]
		EB-S-CN-45			45
		EB-S-CN-45R			45 R[1]
		EB-S-TN-90	Pulling/Tension		90
		EB-S-TN-45			45
		EB-S-CP-90	Pushing/Compression	Parallel to support axis	90
	Side Bearing (Series II)	SB-S-CN-90	Pushing/Compression	Normal to support axis	90
		SB-S-TN-90	Pulling/Tension		
		SB-S-CP-90	Pushing/Compression	Parallel to support axis	
		SB-S-TP-90	Pulling/Tension		

[1] R stands for reduced unbraced length in reinforcing bars with either 90 or 45-degree bar bends.

Table 3.2: Test specimens – Phase II

Type of support	Type of bearing	Specimen code	Load direction	Load orientation	Adhesive
Masonry Beam	End Bearing (Series III)	EB-M-CN-D	Pushing/Compression	Normal to support axis	No
		EB-M-CN-A			Yes
		EB-M-TN-D	Pulling/Tension		No
		EB-M-TN-A			Yes
		EB-M-CP-D	Pushing/Shear	Parallel to support axis	No
	Side bearing (Series IV)	SB-M-CN-D	Pushing/Compression	Normal to support axis	No
		SB-M-TN-D	Pulling/Tension		
		SB-M-CP-D	Pushing/Shear	Parallel to support axis	No
		SB-M-TP-D	Pulling/Shear		

The experimental program included additional test specimens to evaluate the effect of enhancing the connection detailing with few modifications. The first was to investigate the influence of the bend angle of the connection bar on HCS connections supported on steel beams. Two bar bend angles were considered: 45-degree bends (45) and 90-degree (90). Also, the effect of reducing the unrestrained portion in the connection bar, to be right against the flange of the steel beam, is assessed. In the specimens' name, this modification is denoted by the letter "R". In Phase II of testing, additional specimens were added to evaluate the effect of using adhesive (epoxy resin) to install the connection bar to masonry supports. Specimens with adhesive contain the letter "A" in their name, while specimens with "dry-fit" bars have the letter "D".

Based on material properties, the expected failure mechanisms are yielding of the reinforcing bar, followed by bond failure or grout crushing. Assuming no contribution from friction interlock between the HCS and the supporting member, the expected capacity of the connection bar is 40 kN, which is the yielding force of the 10M bar of Grade 400W.

3.2 Details of the Experimental Program

3.2.1 Test specimens

Test specimens were constructed using 203-mm thick HCS of 1,220-mm square segments. In end bearing specimens, the two slab segments were placed, while allowing a gap of 12-mm in between units to insert the connection bar. This recommendation appeared in the DIN EN 1168/2008-10 Standard (Technical Comittee CEN/TC 229 2010) and was taken from the construction practice. Therefore, these specimens measured 1,220-mm × 2,452-mm. In side-bearing specimens, only one slab segment was employed. In this case, the specimen measured 1,220-mm square. The slabs were supported on a 250 × 67-mm steel beam in Phase I of testing.

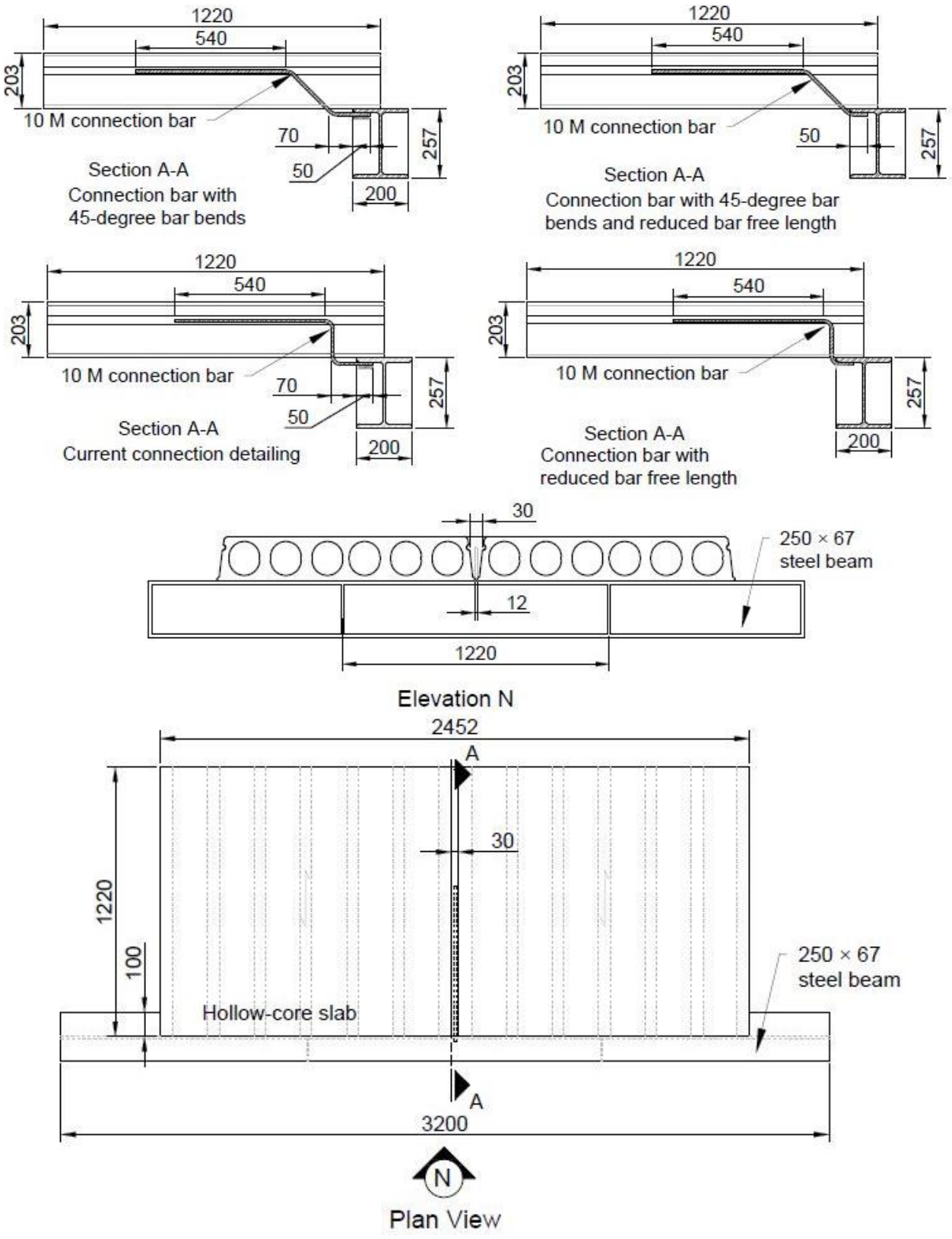

Fig. 3.1: Specimen details for Series I (Phase I)

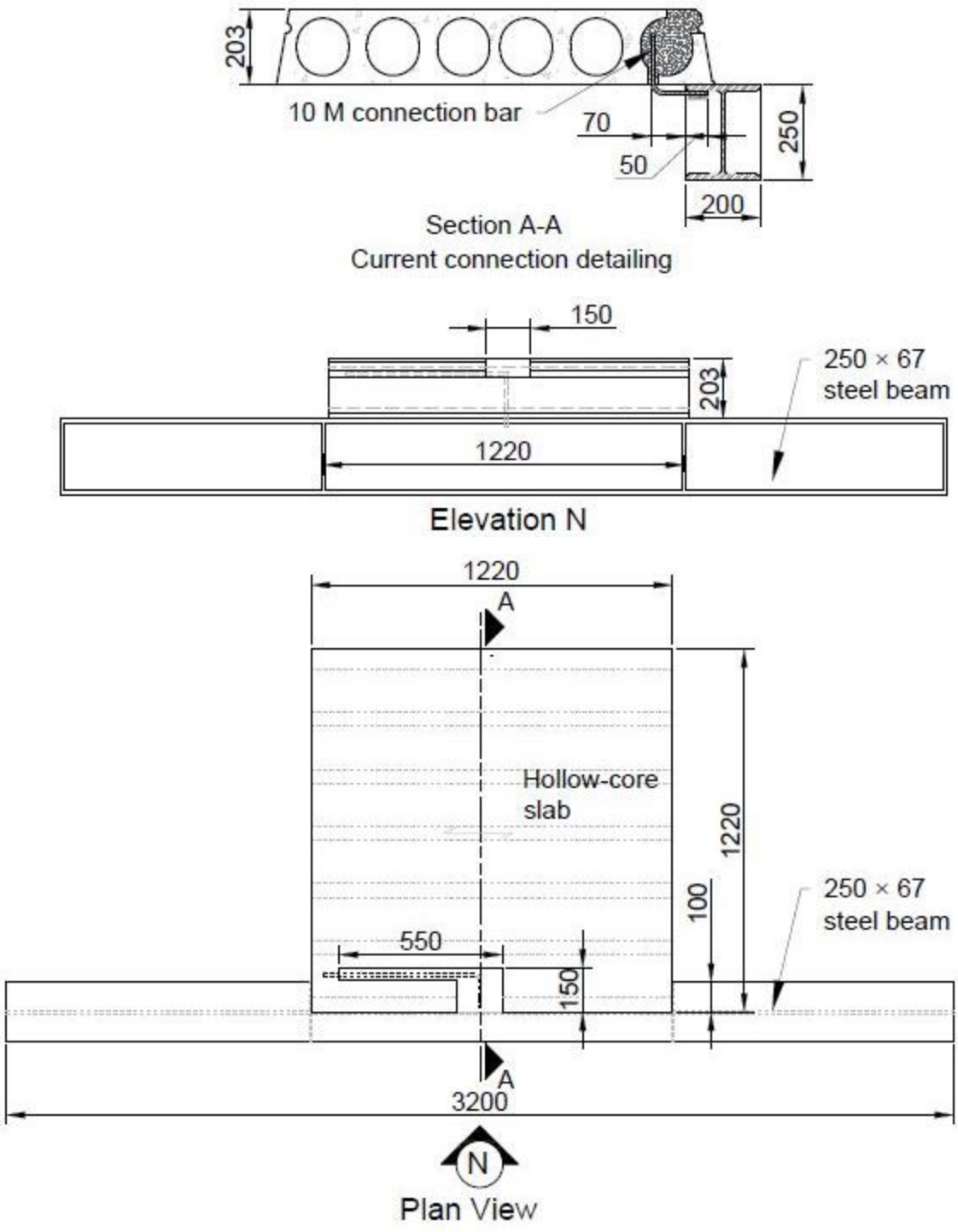

Fig. 3.2: Specimen details for Series II (Phase I)

Phase II involved a 2-course, 190-mm wise single wythe masonry beam of 3,200-mm length. This masonry beam mimics the construction practice of a typical bond beam at the top of a masonry

wall. Either steel or masonry beams was supported on two concrete blocks and tied to the laboratory strong floor allowing approximately 1,000 mm space between the floor and the bottom of the HCS. In both phases of testing, a minimum of 75-mm of seating length was provided to exceed code requirements and prolong the test. (CPCI 2017; CSA 2019). Figures 3.1 and 3.2

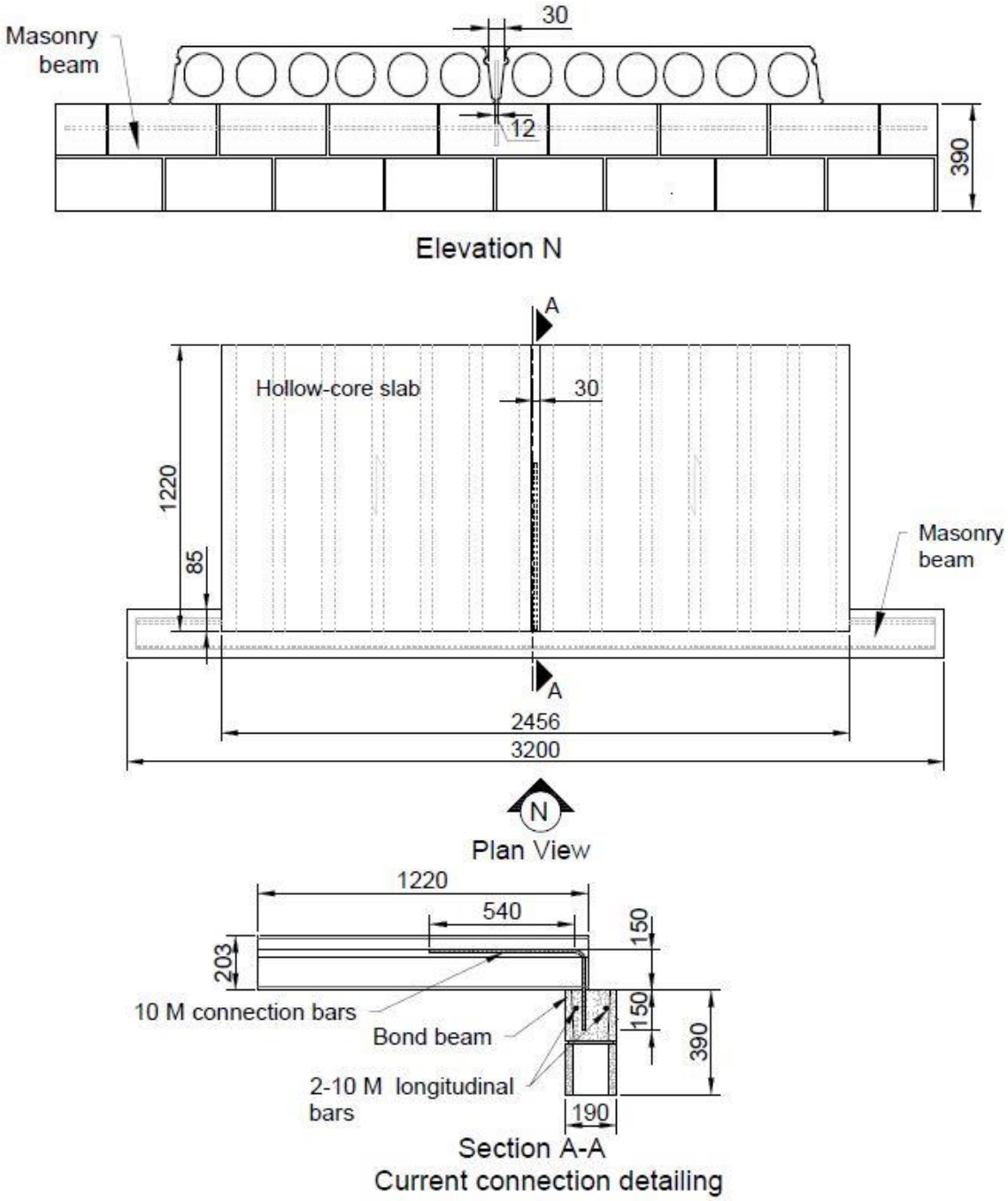

Fig. 3.3: Specimen details for Series III (Phase II)

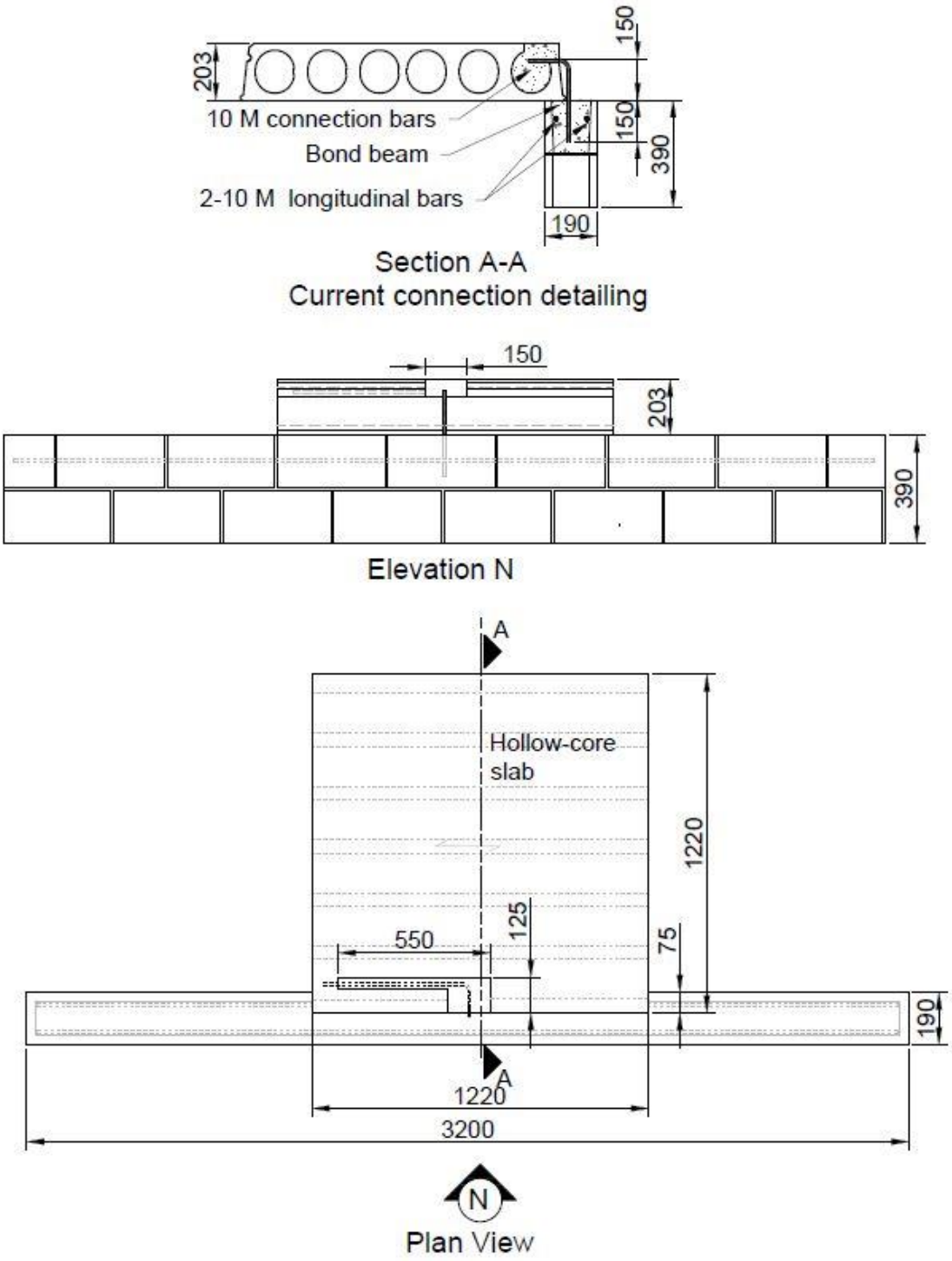

Fig. 3.4: Specimen details for Series IV (Phase II)

3.2.3 Material properties

3.2.3.1 Steel reinforcement

The connection bars were shaped, at a local workshop, using Grade 400W steel reinforcement. The mechanical properties of steel bars were obtained according to the ASTM A370-20 Standard (ASTM 2020a), as shown in Fig. 3.5 and Table 3.3.

Table 3.3: Material properties of steel reinforcing bars

Elasticity modulus [E] (MPa)	**Yielding strains [ε_y]**	**Ultimate strains [ε_u]**	**Yielding strength [f_y] (MPa)**	**Ultimate strength [f_u] (MPa)**
198,480	2,368	243,090	470	592

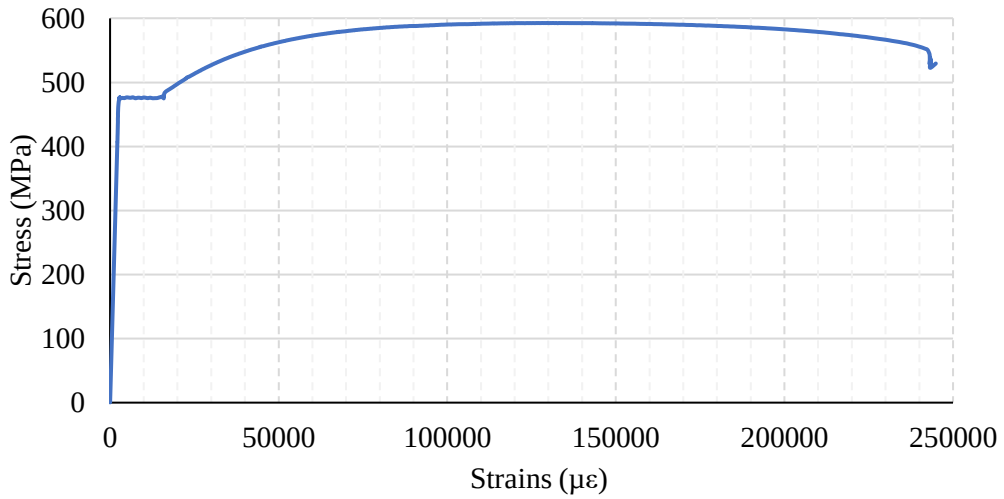

Fig. 3.5: Stress-strain relationship for steel reinforcing bars

3.2.3.2 Grout

The grout used to fill the HCS joints was mixed, placed, and cured in the Laboratory following the manufacturer specifications. First, the HCS shear keys and the specified cores were profusely air-blown with compressed air and vacuumed to remove dust. Grout poured in these joints was of

regular strength (20-25 MPa) according to the construction practice. The joints were filled in three layers that were tamped and vibrated using tamping rods and an electrical vibrator to avoid honeycombs, cavities or settlements and ensure proper bar cover. The mechanical properties of the grout were obtained based on ASTM C109/C109M-20b (ASTM 2020b) using 51-mm cubes. Compressive strength was obtained at 3, 7, 28 days of age (Table 3.4 and Fig. 3.6). The hardened grout and the grout cubes were normally wet-cured together for three days.

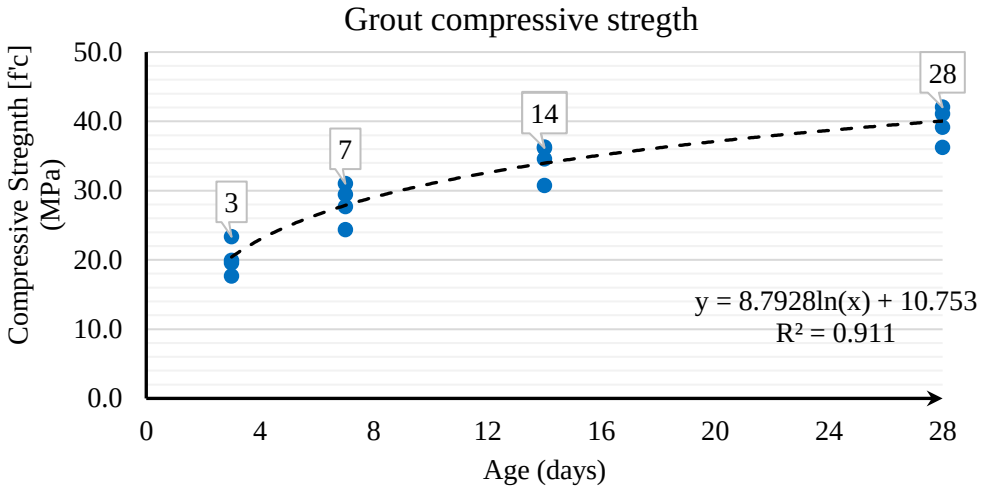

Fig. 3.6: Grout compressive strength growth with age

Table 3.4: Compressive strength for used grout

Age (days)	*3*	*7*	*14*	*28*	*Testing day*
Average Compressive Strength [f'$_c$] (MPa)	20.1	28.1	34.4	39.6	25.1
Standard deviation (MPa)	2.4	2.8	2.6	2.6	3.1

A local producer generously provided the HCS segments as in-kind contribution to this research. Manufacturer specifications indicated these HCS were cast with a target 28-day concrete compressive strength of 55-60 MPa. The prestressing steel reinforcement of the hollow-core

segments consisted of six high-strength steel strands in each web. Figure 3.7 illustrates the geometric properties of the HCS employed in this research. Pockets and openings were saw-cut and drilled in the Structures lab using heavy equipment (see Figure 3.8).

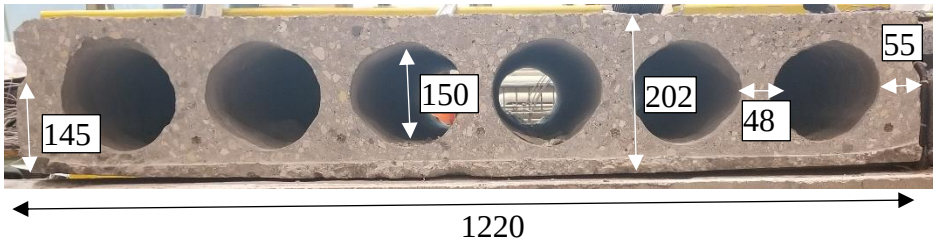

Fig. 3.7: HCS Cross section. (all dimensions in mm)

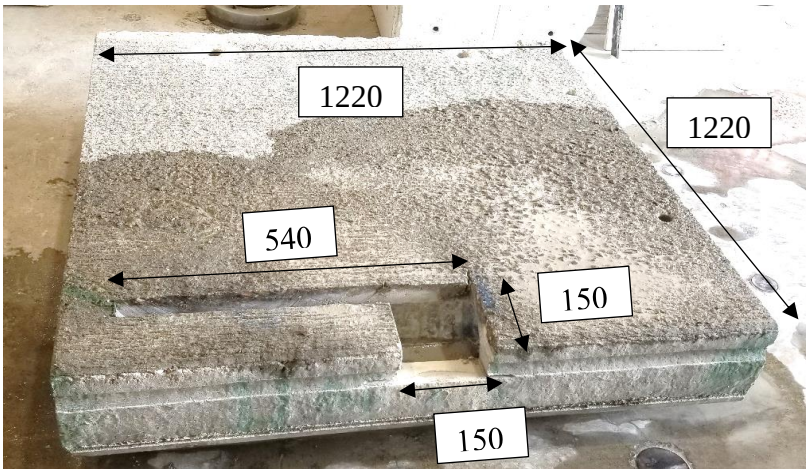

Fig. 3.8: Pockets and holes in HCS for construction of side bearing connection

3.2.3.4 Masonry support beam

The masonry beams were constructed by professional masons following the relevant standards and the process used in practice. Three types of masonry units were employed to construct these beams, as depicted in Fig. 3.9. The properties of the mortar used to construct the beam was obtained as per the ASTM C109/C109M-20b (ASTM 2020b). The mortar had an average compressive strength of 15.1 ± 0.5 MPa at 28 days, which complies with Annex A of CSA A179-04 (CSA 2014) and

the specifications of ASTM C270a (ASTM 2019) for Class S mortar. Furthermore, the properties of the grout used to fill the bond beam (top course) had an average compressive strength of 28.3 ± 2.1 MPa at 28 days. The bond beam had 2-10M reinforcing bars placed on top of the knockout webs of the bond blocks, as shown in Fig. 3.1b.

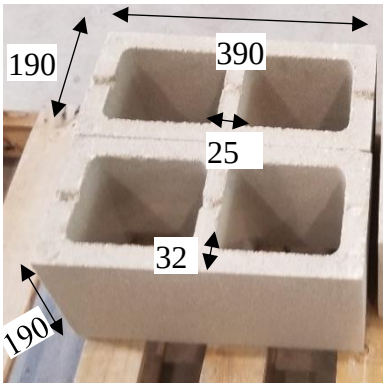

a) Plain end (corner units)[1]

b) Two-cell stretchers

c) Knockout web bond blocks

d) Masonry beams before grouting

Fig. 3.9: Construction of masonry beam

3.2.4 Loading scheme

The loading procedure consisted of either pulling or pushing the slabs away from or toward the supports, respectively, until provoking a failure. Therefore, the direction (pushing or pulling) and orientation (normal or parallel) of loading generates a compression, tension, or shear force in the reinforcing bar. No gravity load was added since it increases the friction between the HCS and the

supporting member. A similar loading protocol was applied in pull-out tests conducted by Mejia-McMaster and Park (1994) and later by Lam et al. (1998, 2002 and 2007) to test HCS bearing connections. The monotonic in-plane force was applied using a displacement-controlled actuator of 250-kN capacity. The loading rate was set to 5.2 mm/min to allow for load accommodation and a test duration of 15 minutes. Similar loading conditions were used by Herlihy (1999).

3.2.5 Test setup

The test setup comprised three main elements for testing the connection bar under push/pull forces. First, the HCS were attached to the actuator using two size 101.4 × 101.4 × 6.2 mm HS fastened together. These clamping beams were joined to a steel frame fixed to the tip of the actuator. Second, the slabs were supported on pinned-pinned supports at one end to carry half their self-weight and allow for free in-plane displacement. Third, the other ends of the slabs were supported on either the steel or the masonry beam that has the reinforcing bar connection. These beams were prestressed to the laboratory strong floor using Dywidag bars. The steel supporting beam had four stiffeners (two on each side) spaced at 1,220-mm using 6-mm thick plates. These plates were welded to the flanges and the web of the beams to resist possible flange torsion. In the case of masonry beam supports, the bond beam was tightly braced with horizontal steel supports, also spaced at 1,220-mm to resist torsion at the top course. Specimens tested to shear forces contained an additional component to limit HCS rotation due to non-concentric loading. This component consisted of two rollers installed at strategic locations to guide the lateral faces of the slabs. Fig. 3.10, 3.11, 3.12, 3.13 illustrate the test setup used in normal and parallel loading, in Phases I and II, respectively.

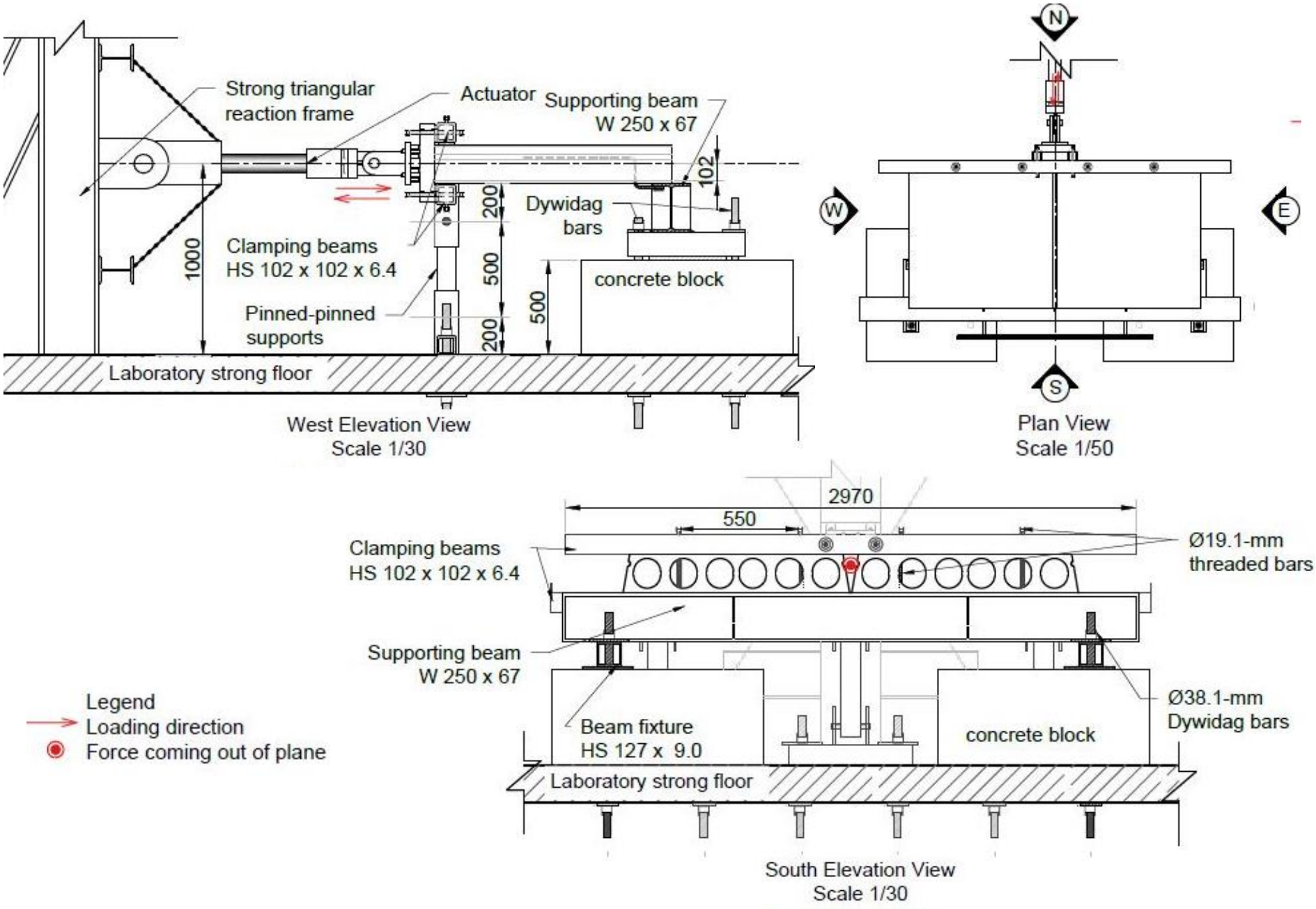

Fig. 3.10: Test setup for axial loading of specimens of Phase I

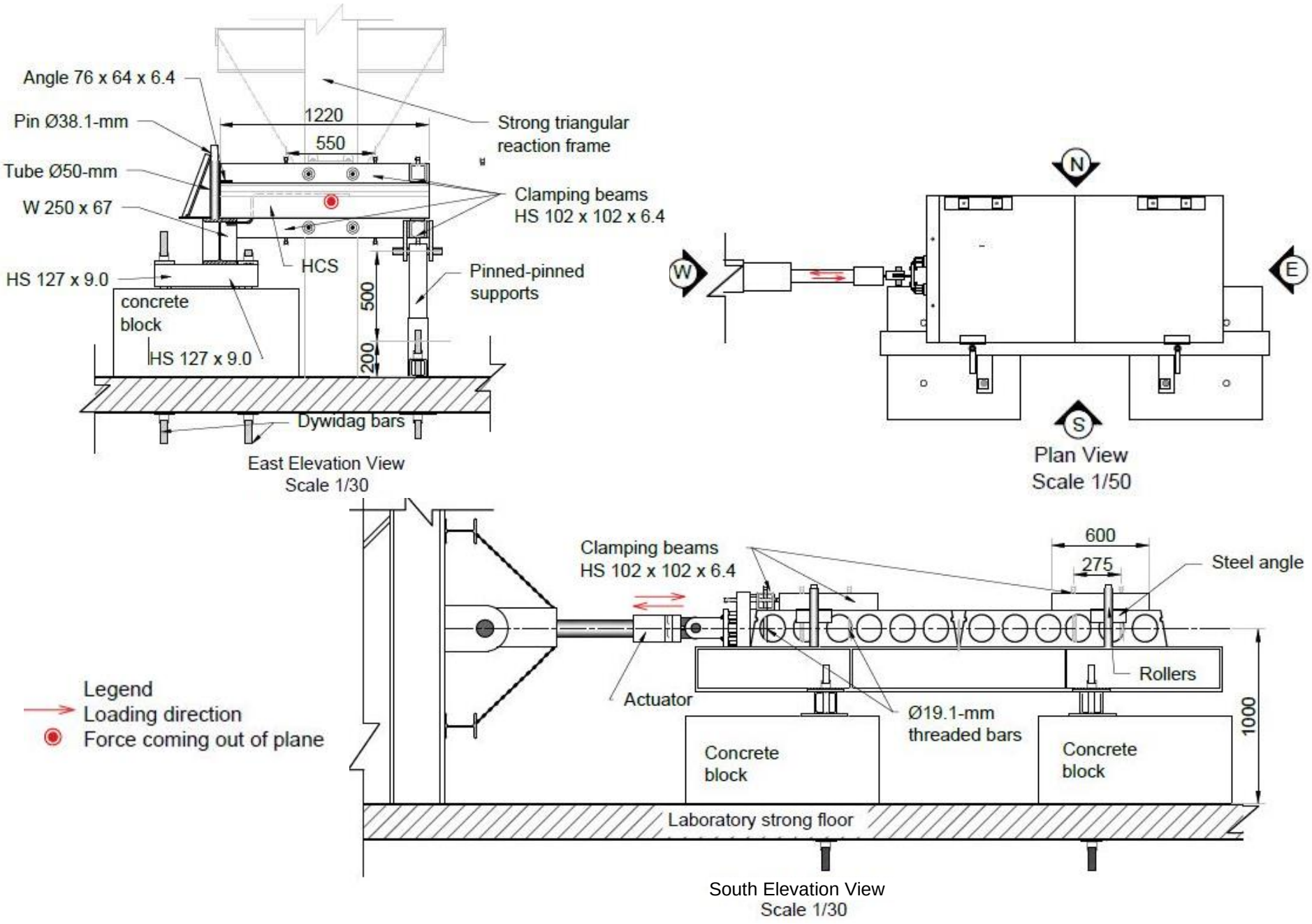

Fig. 3.11: Test setup for shear loading of specimens of Phase I

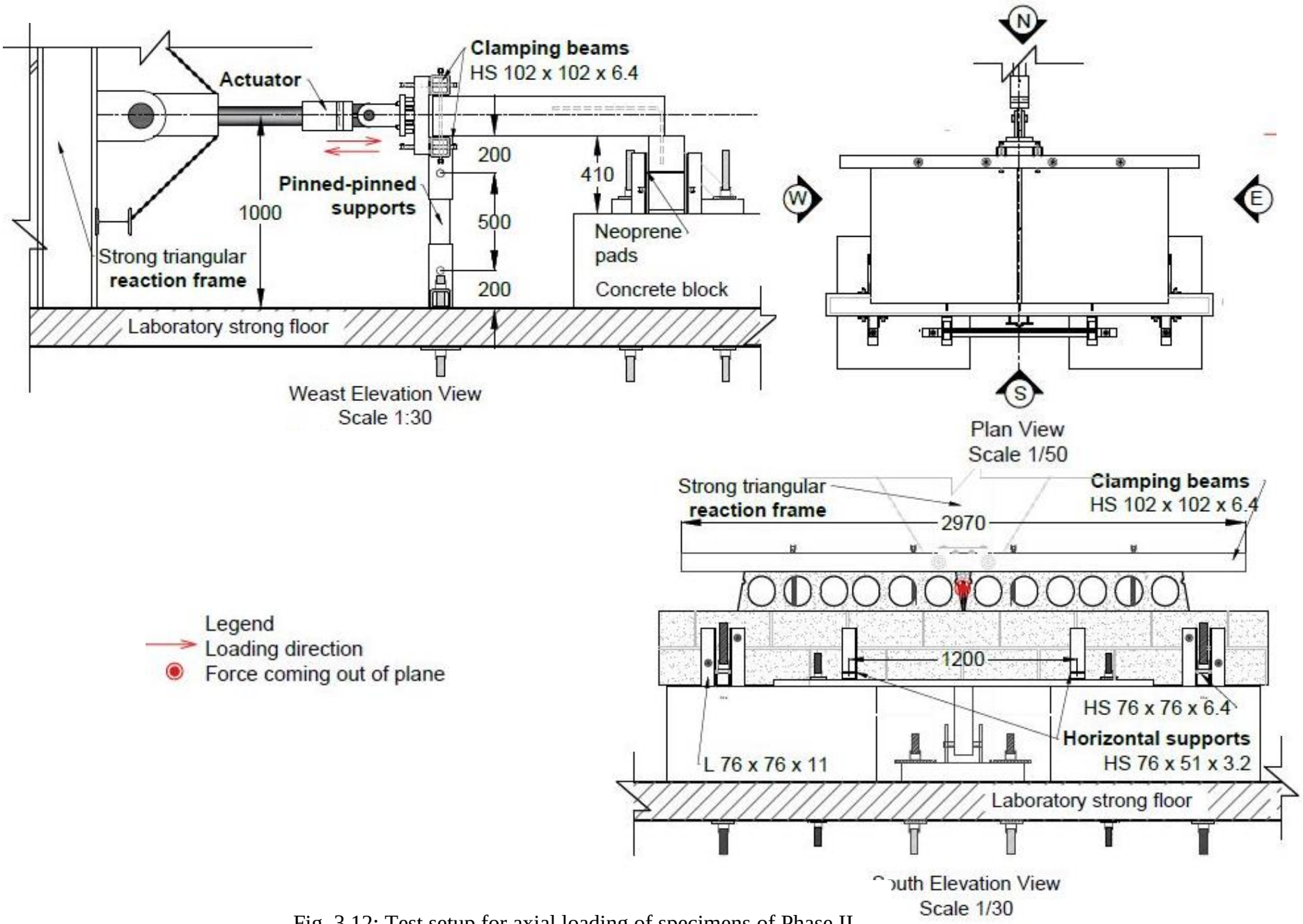

Fig. 3.12: Test setup for axial loading of specimens of Phase II

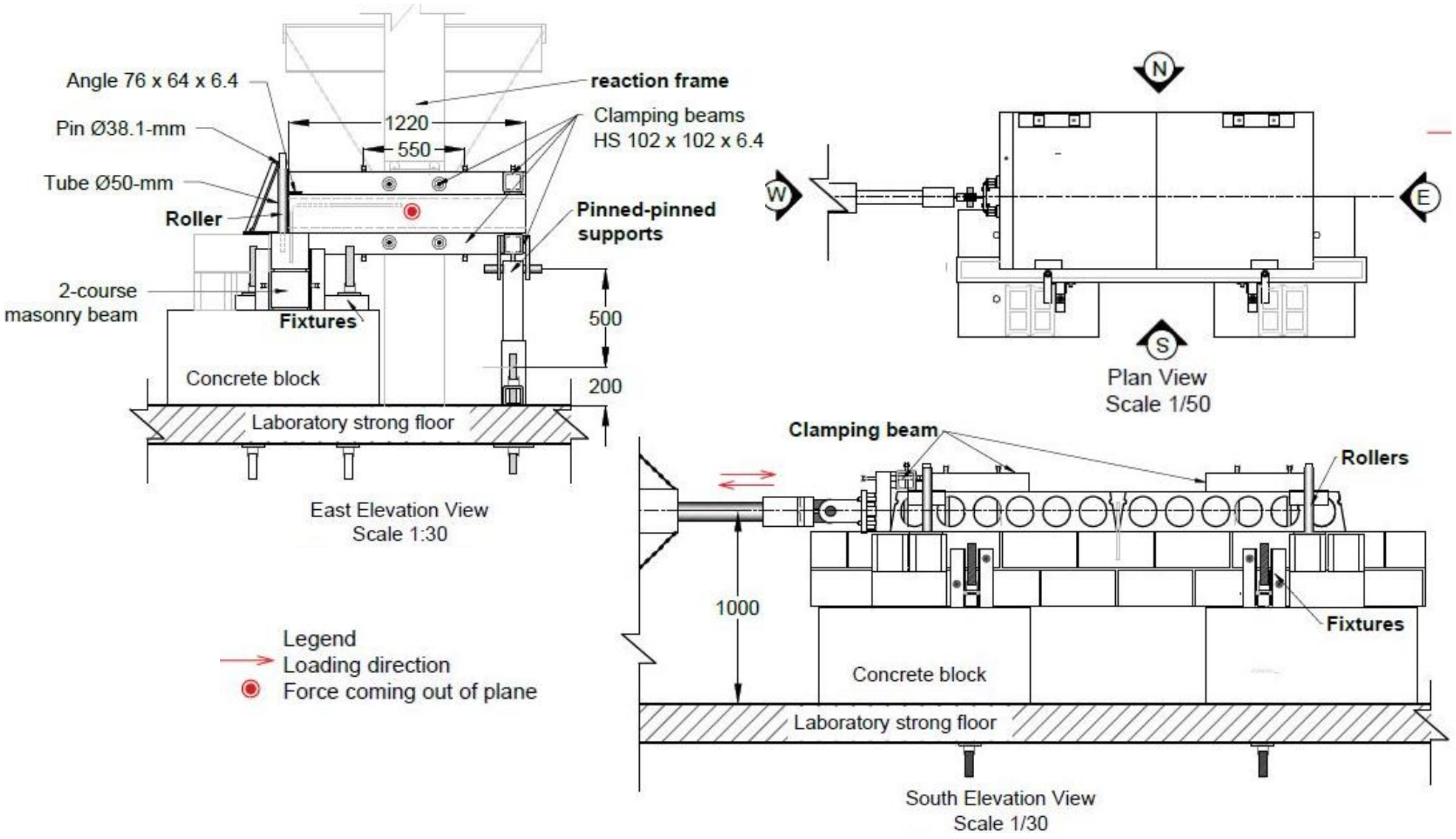

Fig. 3.13: Test setup for shear loading of specimens of Phase II

3.2.5 Instrumentation

Specimens were instrumented to monitor the applied load, slab displacements, strains in the reinforcing bar, and cracking in the bond beam. Three Linear Variable Displacement Transducers (LVDT's) of 150-mm stroke were installed at the mid-height of the HCS to measure slab displacements and account for floor rotations (Figs. 3.14 and 3.15). Two electric-resistance strain gauges were glued to the bends of the connection bar to monitor the load-strain relationship (Fig. 3.14 (a) and Fig. 3.15 (b)). The load was caught using a load cell installed at the tip of the actuator. A PI-gauge was installed to catch the cracking load at the mid-height of the masonry beam, where the connection bar was inserted (Fig. 3.15 (a)). These readings were collected through a Data Acquisition System plugged into a computer. Also, cracking patterns and concrete spalling, if any, were cautiously monitored during the testing and recorded on camera.

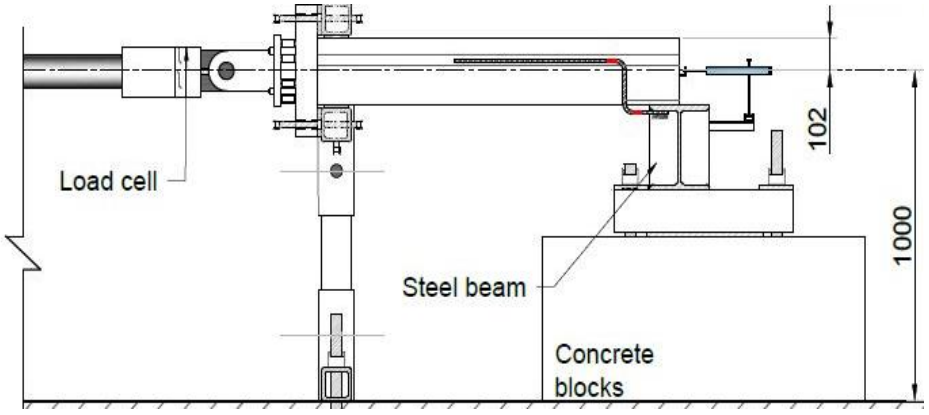

(a) Side Section A-A. of test specimens - End-Bearing connection

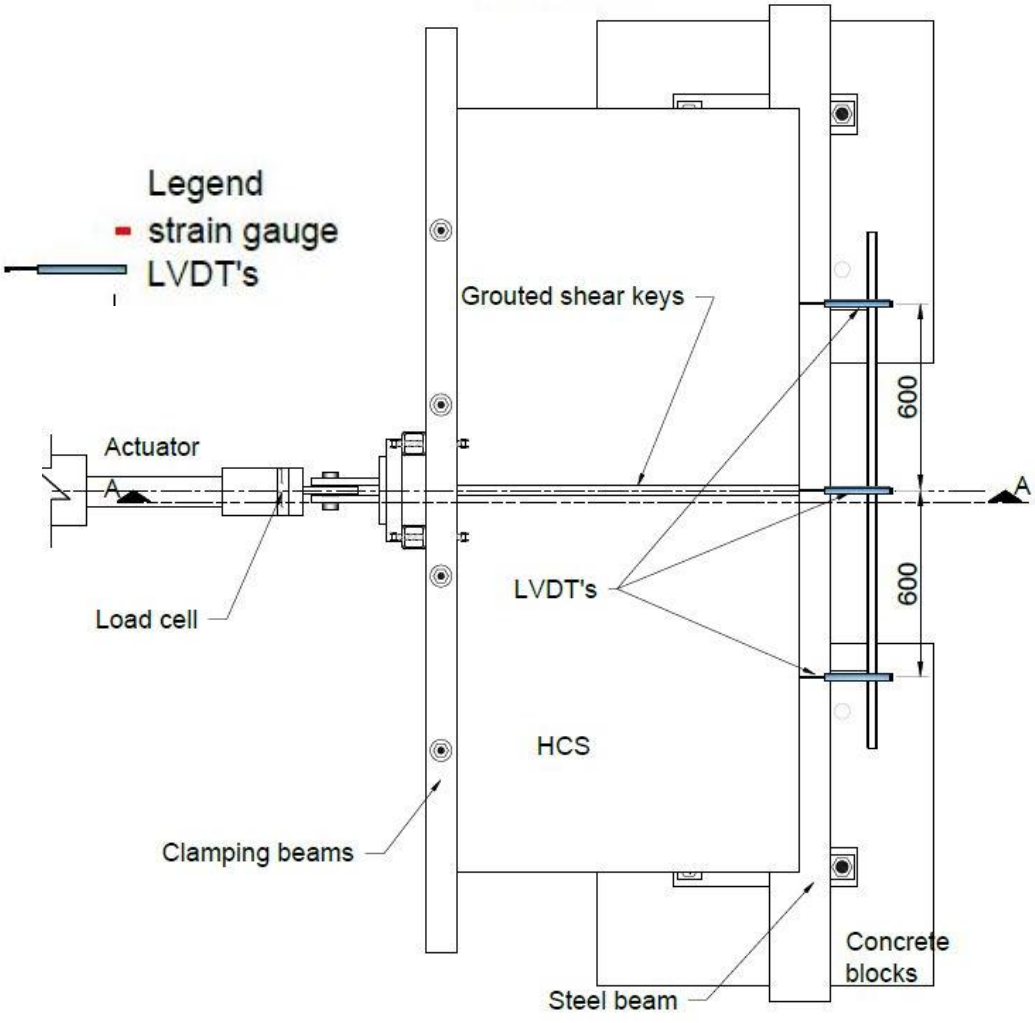

(b) Plan view of test specimens – End-Bearing connection

Fig. 3.14: Instrumentation for specimens supported on steel beam with "Z-shaped" bars. (Phase I)

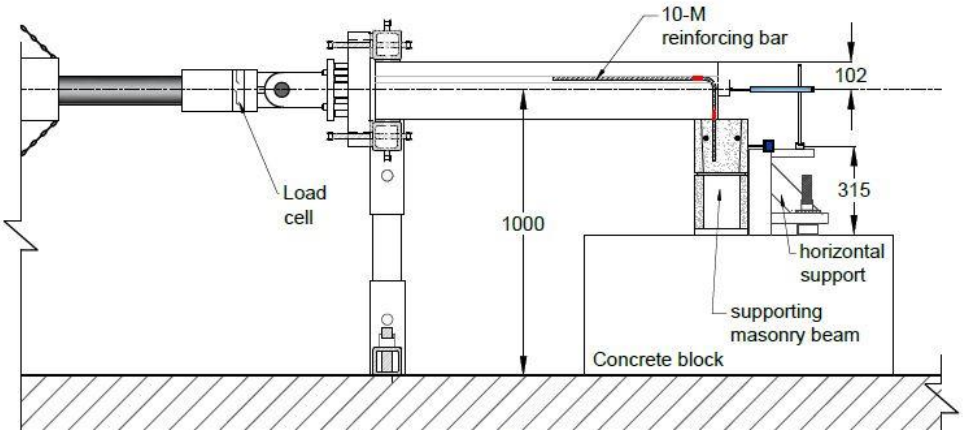

(a) Side Section A-A. of test specimens – End-Bearing connection

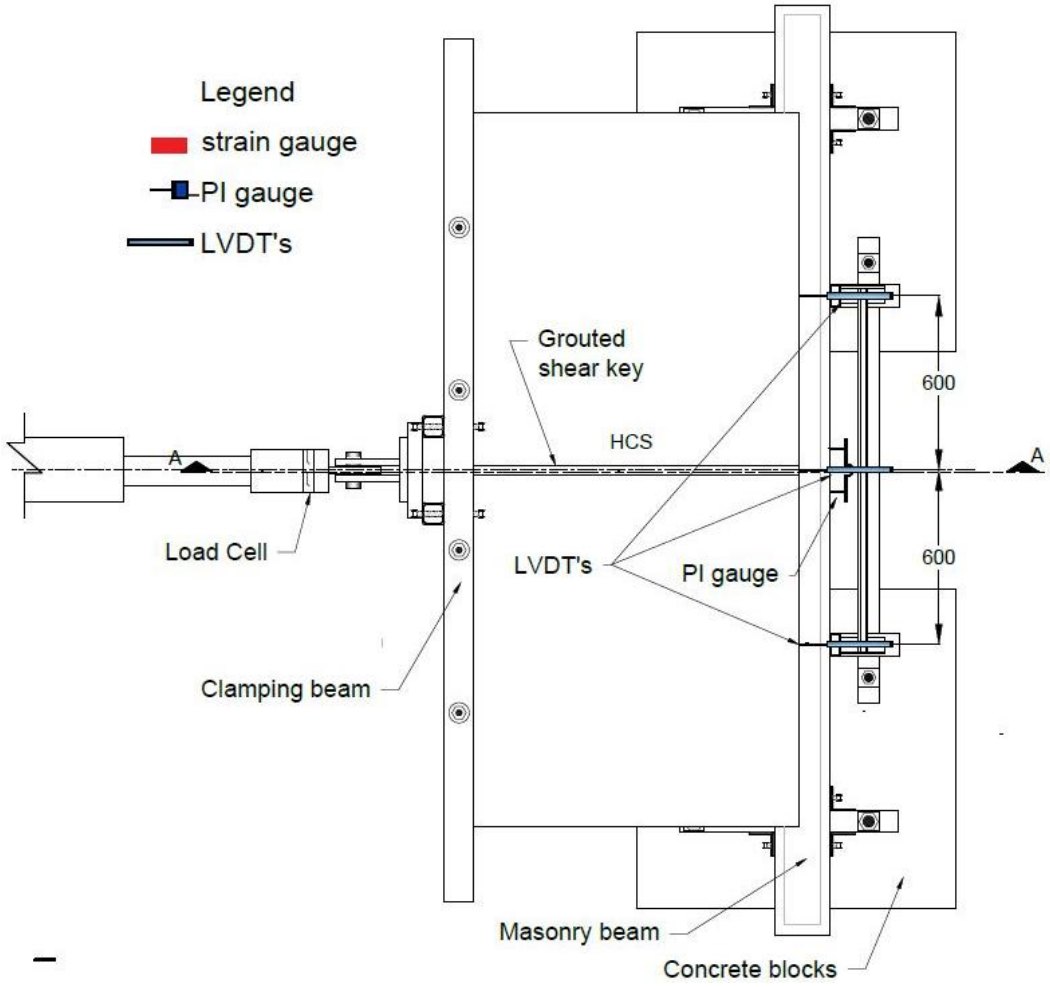

(b) Plan view of test specimens – End-Bearing connection

Fig. 3.15: Instrumentation for specimens supported on masonry beam with "L-shaped" bars. (Phase II)

CHAPTER 4: BEHAVIOUR OF REINFORCING BAR CONNECTION OF HOLLOW-CORE SLABS TO STEEL BEAMS UNDER IN-PLANE FORCES

Authors' Affiliations and Roles:

- **Susana Hernandez Brito**, M.Sc. Student, Department of Civil Engineering, University of Manitoba.
  Role: Methodology, Investigation, Formal analysis, Validation, Visualization and Writing-Original Draft.
- **Karam Mahmoud**, Post-Doctoral Fellow, Department of Civil Engineering, University of Manitoba.
  Role: Validation, Visualization and Writing-Review & Editing.
- **Ehab F. El-Salakawy**, Professor, Department of Civil Engineering, University of Manitoba.
  Role: Conceptualization, Methodology, Writing-Review & Editing, Supervision, Project administration, Resources and Funding acquisition.

Journal and Status: Canadian Journal of Civil Engineering, under review.

Reference:

Hernandez Brito, S., Mahmoud, K., and El-Salakawy, E. F. "Behaviour of Reinforcing Bar Connection of Hollow-Core Slabs to Steel Beams under in-plane Forces." Canadian Journal of Civil Engineering, Submitted in August 2021.

Note:

The content of the journal paper has been edited from the original manuscript by renumbering the sections, figures and tables to maintain the thesis organization. The specimen nomenclature also differs from test matrix presented in Table 3.1. The specimen nomenclature used in this chapter is explained in the list of abbreviations. In addition, the reference list has been moved to the end of the thesis, as indicated in the table of content.

4.1 Abstract

Hollow-core slab (HCS) floors supported on steel beams require the use of steel reinforcement as connections to avoid slab displacement caused by lateral loads. However, current North American design codes offer limited provisions on the design and behaviour of such connections. In this study, the results of an experimental investigation conducted on such connections to assess their capacity and mode of failure are presented. Eleven full-scale assemblies of HCS reinforcing bar connections to steel beams were tested to failure under monotonic in-plane loading (compression, tension, or shear). Test results revealed that connections tested under compression failed by bar buckling without yielding. Under tension, the connection bar reached close-to-yielding or yielding strains at the unrestrained portion of the bar, followed by grout splitting in the shear key or the grouted core. Finally, the mechanism of failure of specimens subjected to shear was governed by bar kinking and yielding.

Keywords: Hollow-core slabs; in-plane forces; integrity ties; end-bearing connection; side-bearing connections.

4.2 Introduction

Approximately 1.83 million m^2 of hollow-core slabs (HCS) are produced each year in Canada (Personal communication 2021). Designers often choose such HCS to cover long spans owing to their structural efficiency. The voids inside these slabs eliminate up to 50% of the concrete volume associated with using solid slabs of equal thickness, which results in relatively lighter elements. The use of prestressed concrete further reduces deflections and minimizes section height. Depending on the thickness, HCS can span up to 17 m without intermediate supports. Moreover, the HCS are convenient for construction purposes to allow for more floor clearance. The interior

cores are commonly employed for thermal and noise isolation or running mechanical, electrical and plumbing conduits. Therefore, these slabs are optimal for clear and open spaces in residential and office buildings.

Floors constructed with HCS are typically designed as continuous horizontal diaphragms, which transfer lateral loads to the supporting structure throughout their bearing connections. The load path from in-plane lateral loads (e.g., wind/seismic loads, accidental loads during construction, vibrations, or movements of the supports) generate in-plane axial and/or shear forces at the bearing connections of the HCS floor. Therefore, the steel reinforcement in HCS bearing connections to steel beams is necessary to tie the slabs to their supporting structure and to preserve the structural integrity of buildings utilizing such HCS floors (PCI 2015; CPCI 2017; ACI 2019; CSA 2019). The use of connection reinforcement impedes slabs displacements that can result in floor misalignments or loss of bearing of the units.

Current design codes, such as CSA A23.3-19 (CSA 2019) and ACI 318-19 (ACI 2019), refer to the bearing connection reinforcement as “integrity ties” owing to their main function in HCS floors. Accordingly, integrity ties shall ensure a minimum specified a tensile strength of 5.0 and 4.4 kN per meter length of the bearing length of HCS on the supporting beam, as per the CSA A23.3-19 (CSA 2019) and the ACI 318-19 (ACI 2019), respectively. These specifications are intended to ensure the minimum level of structural integrity of the HCS floor diaphragm. However, these requirements do not supersede acting lateral forces in HCS floor diaphragms. If the resultant tension forces from the in-plane forces on the diaphragm are greater than the code specified values, proper steel reinforcement must be provided to carry these forces. In addition, integrity ties in HCS floor diaphragms might be used to brace the top flange of the supporting steel beam, which carries the compressive stresses product of bending moments under gravity loads. In these situations, the

designer must provide a tie spacing that allows the ties to develop the nominal yield capacity while ensuring minimum floor integrity.

Based on the load transfer (web) direction of HCS, two types of connection to steel beam supports are identified according to the CPCI design manual (2017): end-bearing and side-bearing connections. In both types of connections, steel reinforcement is either welded or tied to the steel supporting beam on one side. On the other side, this reinforcement is either placed at the grouted joint between HCS, for end-bearing connections, or in a saw-cut openings or pockets on the side of the slab, for side-bearing connections. Commonly, the connection reinforcement or integrity tie consists of a 10M "Z-shaped" (400W) steel bar, as shown in Fig. 4.1. In practice, this connection bar has a minimum embedment length in grout of 450-mm to ensure adequate anchorage, while the other end, approximately 120-mm long, is welded to the underside of the top flange of the steel beam with a minimum welding length of 50-mm. This leaves a 70-mm long portion of the bar unrestrained.

In Manitoba and Western Canada, practitioners often employ a connection detailing composed of headed-stud connectors and "U-shape" hooks, or straight ties in interior connections, tied around the headed-stud connector. These headed-stud connectors are welded to the top flange of the beam. Then, the U-hooks are grouted in the shear key or the cut-pocket of the HCS depending on the type of bearing as described above. Other practitioners prefer to tie the slabs to the beam using welded steel sections (plates, channels, or angles) as an extension of the flanges of the beam. Then, expansion anchor bolts are used to connect the slab to the steel extension. This latter type of connection can be combined with other connection detailing in HCS floors. However, the connection detailing used in Eastern Canada, depicted in Fig. 4.1, is more commonly used because of their low cost, convenience, and fast installation.

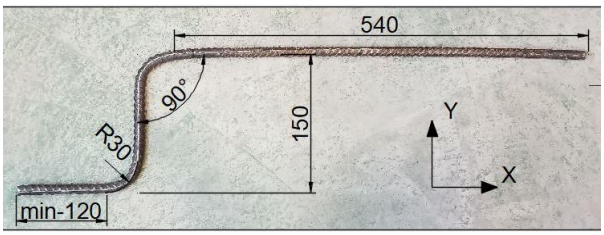

a) 90-degree bends for end bearing connection

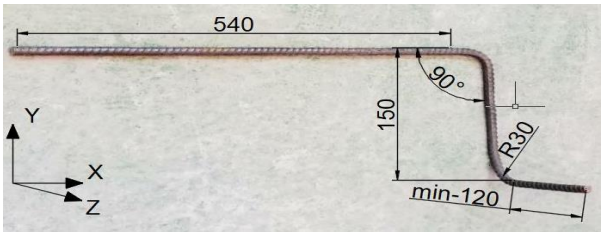

b) 90-degree bends for side bearing connection

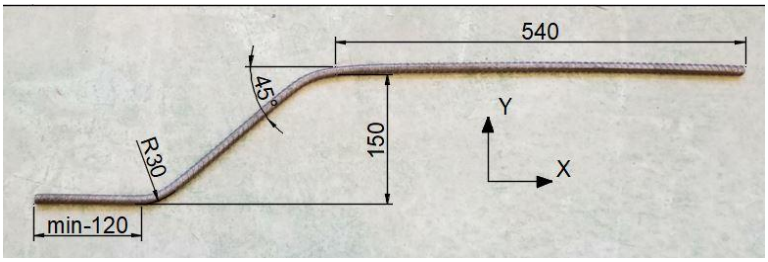

c) 45-degree bends for end bearing connection

Fig. 4.1: Connection bar details

Despite the importance of these ties to the overall structural integrity of the building, there is a noticeable gap in the literature and in the North American codes on the behaviour, expected capacity, and design provisions of the reinforcing bar connection. For instance, the CPCI design manual (CPCI 2017) and the CSA A23.3-19 standards (CSA 2019) suggest the equations based on the shear friction theory to calculate the reinforcement ratio necessary for HCS bearing connections. However, this concept might not be appropriate for this type of integrity tie, which is not monolithic and has an eccentricity regarding the points of load application and the resultant force. Research conducted to study HCS bearing connections to steel beams mainly covered the composite action of HCS with steel beams, using headed-studs and ties, as reinforcement, and concrete topping and void infill cast integrally (Lam 2007). Yet, HCS bearing connections to steel beams using a welded reinforcing bar as integrity tie have not been addressed. This study

investigates the behaviour and capacity of the reinforcing bar connection of HCS to steel beams, which are commonly used in Eastern Canada.

4.3 Experimental Program

4.3.1 Test specimens

Eleven full-scale specimens were assembled and tested under monotonic in-plane forces until failure. The specimens were divided into two series based on type of bearing. Series I, which contained seven specimens, was dedicated to investigating end-bearing connections, while Series II comprised four side-bearing specimens. The specimens were constructed using 203-mm thick HCS that were cut to 1,220-mm square segments. Each end-bearing specimen consisted of two HCS segments, while side bearing connections were constructed using one HCS segment. These HCS segments were supported on and connected to a 250 × 67 steel beam using a "Z-shaped", 10M steel reinforcing bar as indicated in Fig. 4.1. On one side, this reinforcing bar was welded to the underside of the top flange of the beam. Then, the other side was grouted to the joint (shear key) between HCS segments on the other side.

The test variables include the direction (pulling or pushing against supporting beam) and orientation (normal or parallel to the axis of the supporting beam) of the applied in-plane force. These test variables account for all possible in-plane horizontal forces and bearing types in HCS floors supported on steel beams. In addition, the effect of bar bends and reduced unrestrained length of the connection bar for end-bearing specimens was investigated.

The reinforcing bar, currently used in construction practice, is commonly shaped with 90^{o}-bend angles, as shown in Fig. 4.1 (a) and (b). However, an alternative 45^{o}-bend angle connection bar, was included in this study for end bearing connections (Fig. 4.1 (c)). Finally, reduced unrestrained

length connection bars for the 90º- and 45º-bend angles were introduced to evaluate their effect on the capacity of the connection. The details of these connections are shown in Fig. 4.2.

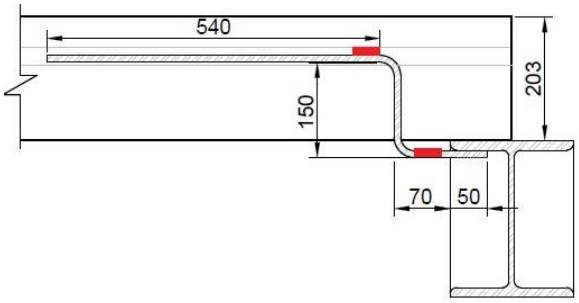

a) 90-degree bend bar - end bearing connection

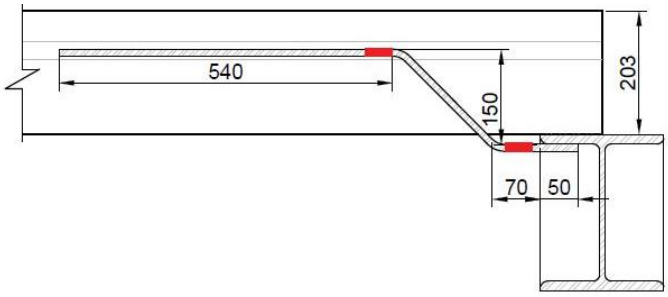

b) 45-degree bend bar - end bearing connection

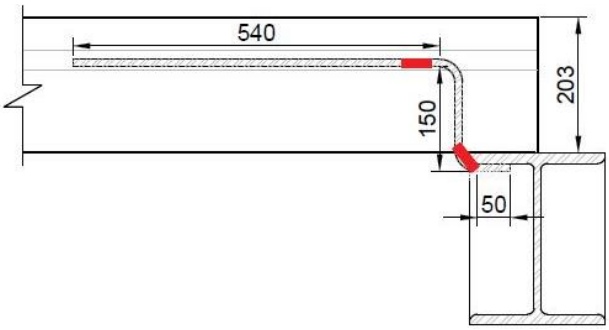

c) Reduced unrestrained bar length for 90-degree bend bar (EB-CN-90R)

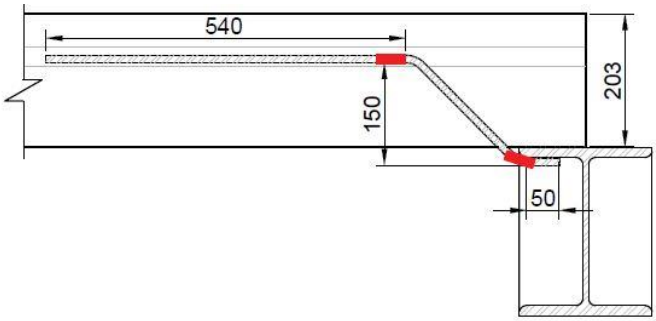

(d) Reduced unrestrained bar length for 45-degree bend bar (EB-CN-45R)

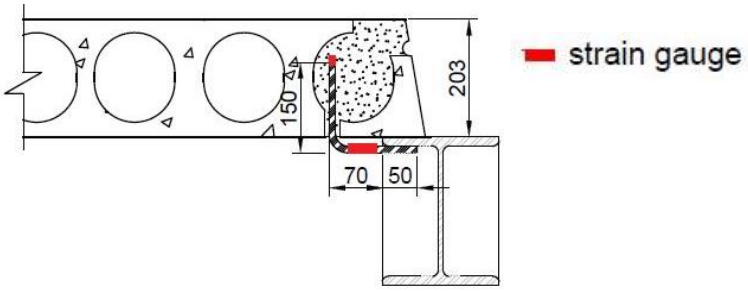

e) 90-degree bend bar for side bearing connections

Fig. 4.2: Steel bar connection detailing and locations of strain gauges (all dimensions in mm).

The specimen nomenclature consists of three parts. The first part refers to the type of bearing where “EB” and “SB” stand for end-bearing and side-bearing, respectively. The second part

consists of two letters denoting the load direction ("C" for compression/pushing or "T" for tension/pulling) and load orientation ("N" or "P" for normal or parallel to the longitudinal axis of the supporting beam, respectively). The last part of specimen nomenclature refers to the bend angles of the reinforcing bar ("45" or "90"-degrees). In addition, for the specimens with reduced unrestrained length, the letter "R" was added at the end of the nomenclature. Table 4.1 lists the test specimens.

A seating (bearing) length of 75 mm was provided in all HCS, which exceeds the minimum requirements of 50 mm as per the Canadian standards CSA A23.3-19 (CSA 2019) and CPCI design manual (CPCI 2017). This seating length was provided to ensure failure of the connection while the HCS remains bearing on the steel beam. Also, in case of end-bearing, the spacing (joint) between the two HCS segments was set to fit the connection bar tightly, as performed in the construction practice.

Table 4.1: Test Specimens

Type of bearing	Specimen code	Load direction/orientation	Bend angles (degrees)
Series I			
End Bearing	EB- CN-90	Pushing/Normal	90
	EB-CN-90R		90R*
	EB-CN-45		45
	EB-CN-45R		45R*
	EB-TN-90	Pulling/Normal	90
	EB-TN-45		45
	EB-CP-90	Pushing/Parallel	90
Series II			
Side Bearing	SB-CN-90	Pushing/Normal	90
	SB-TN-90	Pulling/Normal	90
	SB-CP-90	Pushing/Parallel	90
	SB-TP-90	Pulling/Parallel	90

* R stands for reduced unrestrained length of reinforcing bar with either 90- or 45-degree bends

4.3.2 Material properties

The tensile properties of the steel bars were obtained by standard tests according to the ASTM A370 (ASTM 2020a). The 10M steel bar has a strength and strain at yielding of 470 ± 8 MPa and 2,370 ± 40 με, respectively, with a modulus of elasticity of 199 GPa. A commercially available grout was used to fill in the joints between the HSC units or the cores of the slabs in which the 10M bar was embedded. This normal-strength grout (20-25MPa) was mixed, poured, and cured as per the manufacturer guidelines. The compressive strength of the grout mix tested according to the ASTM C109/C109M-20 (ASTM 2020b) on the day of testing was 25.1±3.1 MPa. The HCS were cast at the supplier facility using a concrete mix with a target 28-day compressive strength of 55-60 MPa.

4.3.3 Test setup and instrumentation

The test setup consists of three main elements: 1) clamping beams to attach the slabs to the actuator and distribute the in-plane forces uniformly along the edge of the slab; 2) pinned supports, which carry half the self-weight of the slabs and allow for the lateral displacement of the slab; and 3) the supporting steel beam, where the connection bar is welded. Figure 4.3 shows the details of the test setup. For specimens tested under parallel loading (shear), two rollers were welded to the beam to guide the slabs and prevent rotation, as shown in Fig. 3 (d).

The load was applied to the slab to generate an in-plane force that is normal or parallel to the supporting beam. The normal force was either pushing or pulling such the that the connection bar is under compression or tension forces, respectively. The parallel force was always pushing to generate a shear force in the connection bar. No gravity loads other than the self-weight of the slab was added to the loading scheme. Similar testing method was previously used by Mejia-McMaster and Park (1994). The monotonic load was applied using a hydraulic actuator with 500-kN load

and 130-mm stroke capacities. This actuator was mounted on a strong triangular reaction frame. A displacement-controlled loading rate of 5.0 mm/min was used to allow for load accommodation and test duration of about 25-30 minutes (Herlihy 1999), assuming a connection capacity of 40 kN.

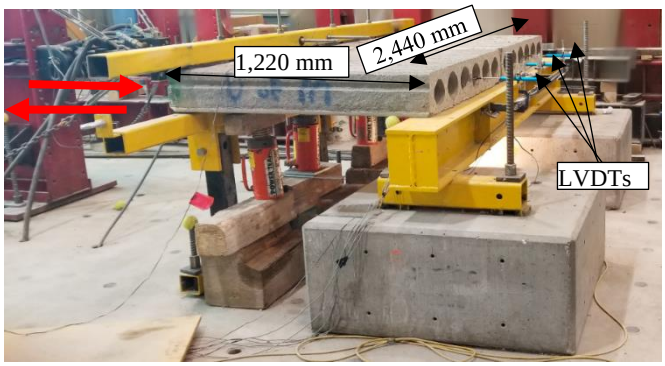

a) Normal load on end bearing specimen

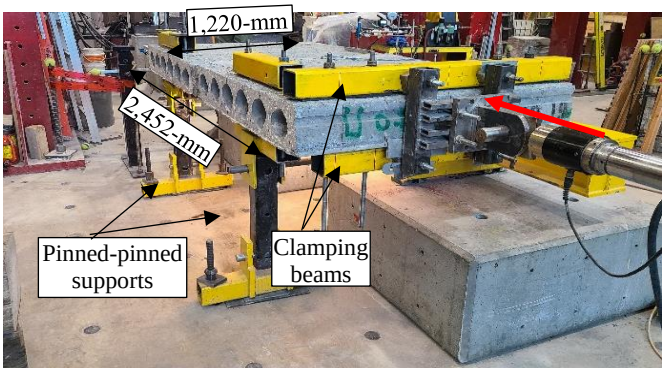

b) Parallel load on end bearing specimen

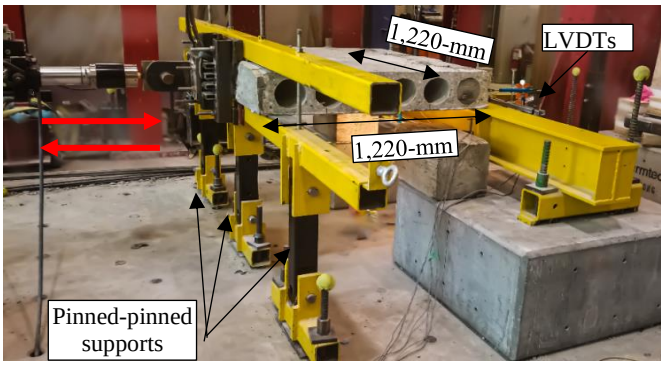

c) Normal load on side bearing specimen

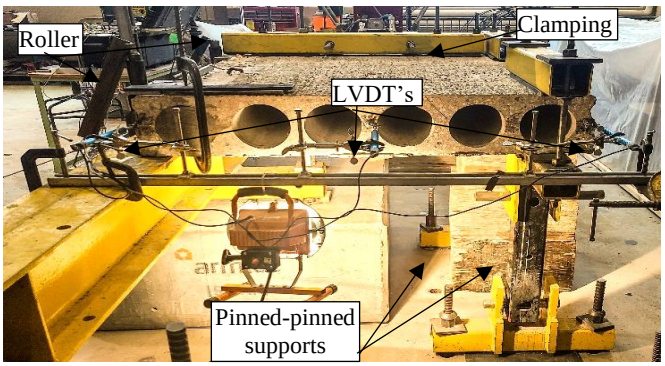

d) Parallel load on side bearing specimen

Fig. 4.3: Test setup and external instrumentation

The slab displacement was measured using linear variable displacement transducers (LVDTs), as shown in Fig. 4.3. The strains in the connection bar at its bends was measured by electrical strain gauges (Fig. 4.2). The applied load was recorded with a load cell installed at the tip of the actuator. The readings of these instrumentation were processed through a Data Acquisition (DAQ) System

and stored on a personal computer. In addition, cracking patterns, or spalling, if any, were carefully marked and recorded during testing.

4.4 Test Results and Discussion

This section introduces and discusses the experimental results in terms of mode of failure, capacity, measured strains, deflections, and overall structural integrity. In addition, the effects of decreasing the bend angle of the connection bar to 45-degree and/or reducing the unrestrained length of the bar are discussed. Table 4.2 lists a summary of the test results.

Table 4.2: Test results

Type of bearing	Specimen code	Load direction/orientation	Mode of failure	Capacity (kN)	Strains at peak load (με)	Slab displacement (mm)
Series I						
End Bearing	EB- CN-90	Pushing/Normal	Bar buckling	12.6	-1,050	3.9
	EB-CN-90R		Bar buckling	13.7	-1,460	4.0
	EB-CN-45		Bar bending	16.3	-1,010	3.9
	EB-CN-45R		Bar buckling	17.1	-2,770	3.9
	EB-TN-90	Pulling/Normal	Bar yielding & grout splitting	30.3	2,370	22.6
	EB-TN-45			53.2	24,980	21.8
	EB-CP-90	Pushing/Parallel	Bar yielding	15.3	8,080	60.3
Series II						
Side Bearing	SB-CN-90	Pushing/Normal	Bar buckling	11.4	900	3.5
	SB-TN-90	Pulling/Normal	Bar yielding & grout splitting	46.0	13,410	22.9
	SB-CP-90	Pushing/Parallel	Bar yielding	16.1	9,330	60.5
	SB-TP-90	Pulling/Parallel	Bar yielding	34.8	3,350	63.8

4.4.1 Mode of failure and cracking patterns

4.4.1.1 Specimens of Series I – end bearing connections

Loading normal to the axis of the supporting beam: The load direction, pulling or pushing, applied normal to the supporting beam resulted in different modes of failure in the connection bar.

Under tension forces (pulling), the Z-shaped bar failed by steel yielding at the unrestrained portion of the bar, followed by grout splitting. In addition, the bottom bend of the connection bar straightened and elongated, regardless of the bend angle (Fig. 4.4 (a) and (b)). The end bearing specimen with a 45-degree bent bar (EB-TN-45) exhibited bar yielding and later, bar necking (Fig. 4.4(b)). Afterwards, a single crack appeared at the grouted joint above the connection bar.

In contrast, the end bearing specimen with 90-degree bent bar (EB-TN-90) experienced an early cracking due to bond failure between the HCS and the grouted shear-key (Fig. 4.4(a)). A hairline crack was observed at approximately 83% of the maximum load in the grouted shear-key in specimen EB-TN-90. Near peak load, the connection bar reached close-to-yielding strains. The crack in the shear-key of both specimens (EB-TN-90 and EB-TN-45) started with grout spalling around the bar and propagated longitudinally across the shear-key. This crack extended across the slabs until grout splitting occurred.

Under compression forces (pushing/CN), the mode of failure of end-bearing specimens was governed by bar bending or buckling at the bottom bend (Fig. 4.4 (c), (d), (e) and (f)). In general, the connection bar did not yield before the maximum load, except for specimen EB-CN-45R, in which the connection bar developed yielding strains at the bottom bend before bar buckling. In all specimens, the peak load was attained at the onset of bar buckling. Then, the slabs gradually pulled the unrestrained (free) portion of the connection bar, provoking “dragging” in the bar. Strength degradation was observed thereafter through a gradual load reduction while the bar experienced further bending or buckling. No cracking was observed in the slabs or the grouted shear-key at any point during the test.

(a) EB-TN-90 (pulling/normal)

(b) EB-TN-45 (pulling/normal)

(c) EB-CN-90 (pushing/normal)

(d) EB-CN-45 (pushing/normal)

(e) EB-CN-90R (pushing/normal)

(f) EB-CN-45R (pushing/normal)

(g) EB-CP-90 (pushing/parallel)

Fig. 4.4: Mode of failure for end bearing specimens

All end bearing specimens with 90-degree bent bar (EB-S-CN-90, EB-S-CN-90R) buckled in the direction of the force until forming a 180-degree bend shape (Fig. 4.4 (c) and (e)). Finally, bar rupture occurred near the welding, because of the excessive deformation and buckling. Nevertheless, the rupture was observed after losing more than 50% of the peak load. Similarly, the connection bar with 45-degree bends in specimens EB-S-CN-45 and EB-CN-45R failed by bar bending and buckling under compression, respectively (Fig. 4.4 (d) and (e)). After reaching the peak load, the load dropped slowly as the bar experienced further deformations. In specimen EB-CN-45, the bar experienced a pushed-down effect of its unrestrained part, as shown in Fig. 4.4 (d). The connection bar deformed and bent downwards without reaching yielding. In contrast, the connection with a 45-degree bent bar and reduced unrestrained length (EB-CN-45R) yielded and later, buckled while pushing against the top flange of the supporting beam. This specimen was the only one tested under compression that reached yielding strain before the peak load. This connection bar also experienced dragging and strength degradation similar to the behaviour observed in connection bars with 90-degree bend after the peak load. This indicated that the combined effects of reducing the unrestrained length and decreasing the angle of bar bends improved the behaviour, where a more desirable mode of failure in the connection bar was observed.

Loading parallel to the axis of the supporting beam: The end bearing specimen tested under a pushing force (EB-CP-90) failed due to bar yielding followed by bar rupture near the weld (Fig. 4.4 (g)). At early stages of loading, the connection demonstrated bar kinking and elongation in the direction of the force followed by yielding and further deformation of the bar. Before the peak load, the connection bar experienced twisting, which resulted in bar shear off near the weld after undergoing excessive deformation.

4.4.1.2 Specimens of Series II – side bearing connection

Loading normal to the axis of the supporting beam: Under tension forces (pulling), the side-bearing specimen with the currently used connection detailing (SB-TN-90) experienced a similar mode of failure to EB-TN-45. After bar yielding and straightening, the grout started to crack, and the specimen failed by grout splitting (Fig. 4.5 (a)). However, the connection bar did not reach the necking stage and the cracking pattern was different from other test specimens. The crack was initiated around the connection bar but propagated transverse to the load application across the grouted core and extended to the top surface of the slab. Finally, grout and slab splitting occurred.

When tested under compression (pushing), the side bearing connection (SB-CN-90) demonstrated a similar failure mechanism to that of end-bearing counterpart specimen (EB-CN-90), however, no bar rupture occurred. The test was halted after a load drop of 70% of the maximum load and noticeable bar distortion (Fig. 4.5 (b)).

Loading parallel to the axis of the supporting beam: The side bearing connection (SB-CP-90), tested under pushing force, showed similar behaviour to its counterpart with end bearing. The connection bar failed owing to bar kinking and yielding with excessive deformation. However, in this specimen, no bar twisting, or bar rupture was observed (Fig. 4.5 (c)). Conversely, when tested under pulling, the connection bar in specimen SB-TP-90 failed because of bar yielding followed by bar twisting and necking near the welding point (Fig. 4.5 (d)). In both cases, the testing was also halted after significant bar deformation and no further strength gain.

(a) SB-TN-90 (pulling/normal)

(b) SB-CN-90 (pushing/normal)

(c) SB-CP-90 (pushing/parallel)

(d) SB-TP-90 (pulling/parallel)

Fig. 4.5: Mode of failure for side bearing specimens.

4.4.2 Connection load capacity

The expected capacity of 10M steel bars (Grade 400W) with a nominal yielding stress of 400 MPa is 40 kN (given that the bar cross-sectional area is 100 mm^2). Accordingly, installing one 10M connection bar in the grouted shear-key of the slabs, allowing for a bar spacing of 1.22 m, results in a connection capacity of 32.8 kN/m in tension (corresponding to the yielding load of the bar).

North American design codes (CSA A23.3-19 and ACI 318-19) specify a minimum capacity in tension for integrity ties of 5.0 and 4.4 kN/m of supported slab length, respectively. If the connection bar can develop the expected nominal tensile yielding strength, the connection capacity would be 6.6 times larger than the specified values given a spacing of 1,220 mm.

However, the required minimum capacity in the codes is set solely for tension forces acting on integrity ties. To date, there is no specification in the North American codes regarding the minimum strength required for integrity ties subjected to compression or transverse loading (shear). Given the reversible nature of the horizontal loads acting on a HCS floor (e.g., wind or seismic), compression and transverse (shear) forces are as likely to be acting on bearing connections as tension forces. The connection must resist these forces to ensure the structural integrity of buildings. Therefore, the magnitude of these limits in the codes might be considered a reference to the designer for the minimum expected integrity strength under either compression, tension, or transverse (shear) loading.

Figure 4.6 depicts the capacity for all test specimens. The figure also indicates the threshold of expected capacity based on the connection bar properties and the above-mentioned code limits.

4.4.2.1 Specimens of Series I – end-bearing connection

Loading normal to the axis of the supporting beam: The load direction affected the mode of failure and load capacity of end bearing connections. End bearing connections tested under tension (pulling) had a desirable mode of failure, where the connection bars yielded followed by cracking in the grouted shear-key. These connections reached a larger load capacity than their counterparts under compression forces. End bearing specimens EB-TN-45 and EB-TN-90 had a maximum load of 53.2 kN (45.9 kN/m) and 30.3 kN (24.6 kN/m), respectively. The relatively lower load capacity

in the latter specimen can be attributed to the early splitting failure between the slabs and grout. Both connection detailing met the threshold of minimum tensile capacity required by the ACI 318 (2019) and CSA A23.3 (CSA 2019) for integrity ties with supporting members other than bearing walls.

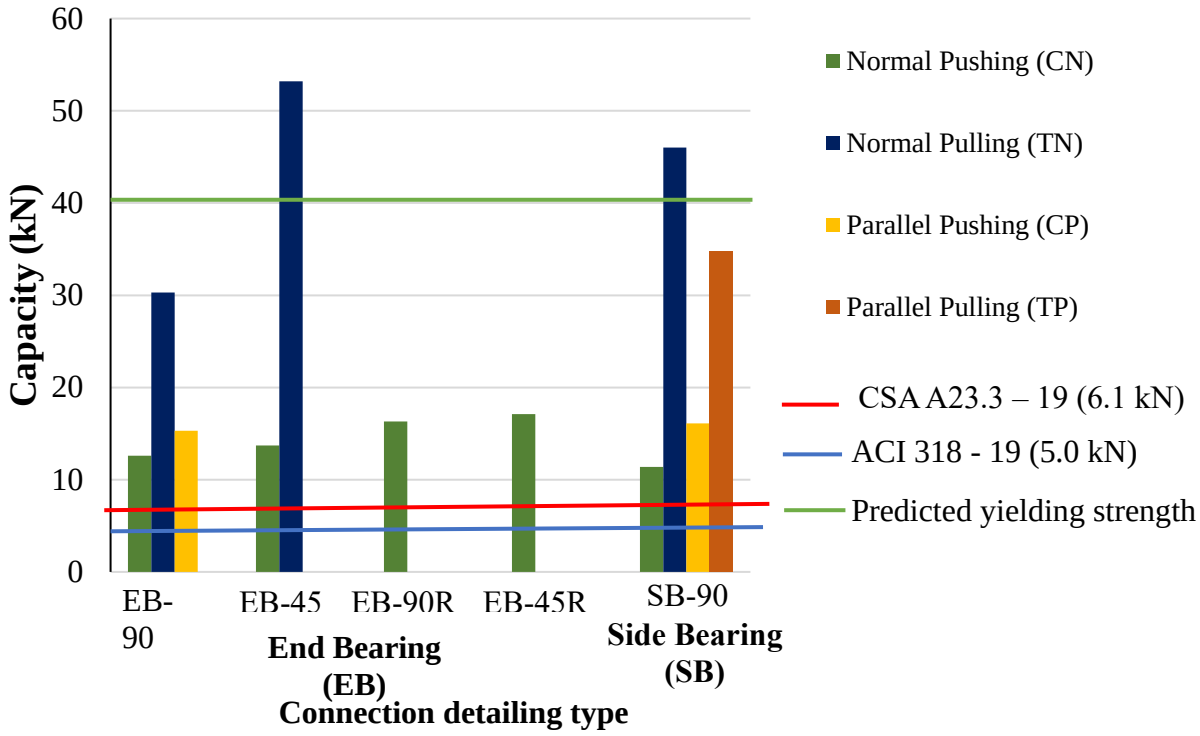

Fig. 4.6: Connection capacity of test specimens and code specifications for integrity ties with supporting members other than bearing walls

In contrast end-bearing connections tested under compression exhibited less than half the capacity of their counterparts under tension forces. Specimens EB-CN-90 and EB-CN-45 attained a maximum load capacity of 12.6 kN (10.3 kN/m) and 16.3 kN (13.4 kN/m), respectively. These results demonstrated that decreasing the bend angle from 90 to 45-degree resulted in a 29.4 % increase in the load capacity. However, minimizing the unrestrained length of the bar, in end-

bearing connections with either 90 or 45-degree bar bends, did not significantly increase the maximum load capacity. Specimens EB-CN-90R and EB-CN-45R reached a load capacity of 13.7 kN (11.2 kN/m) and 17.1 kN (14.0 kN/m), respectively. This represents 8.7 and 5.0% increase in the load capacity compared to their counterparts with the unrestrained length of 70 mm, respectively. Also, the combined effects of decreasing bar bends and bracing the bar against the beam resulted in a 35.7% increase in the load carrying capacity. In general, the values of maximum load capacity of end bearing connections tested under compression remain considerably lower than their counterparts tested in tension.

Loading parallel to the axis of the supporting beam: The capacity attained in the end bearing specimen (EB-CP-90) tested under parallel pushing load was in the range of values of load capacities of its counterpart tested under axial forces. Although this specimen reached yielding, the maximum load capacity attained was 15.3 kN (12.5 kN/m).

4.4.2.2 Specimens of Series II– side bearing connection

Loading normal to the axis of the supporting beam: Similar to specimens of Series I, the capacity of side bearing specimens under normal loading depends on the loading direction. Larger load capacity was observed in specimens under tension compared to those tested under compression. While the side bearing specimen tested under tension forces (SB-TN-90) reached a capacity of 46.0 kN (37.7 kN/m), the peak load for specimen tested under compression was 11.4 kN (9.3 kN/m).

Loading parallel to the axis of the supporting beam: Side bearing specimens tested under parallel loading also exhibited larger load capacity when being pulled than when being pushed. Specimen SB-TP-90 tested under pulling attained a maximum load capacity of 34.8 kN (28.5 kN/m). In

contrast, the side bearing connection SB-CP-90, tested under pushing, reached a load capacity of 16.1 kN (13.1 kN/m), which is less than half the capacity of its counterpart tested under a pulling force.

The values of load capacity, depicted in Fig. 4.6, demonstrate that either in end or side bearing connections (Series I and II), the connection bar is more vulnerable under pushing forces, regardless of the load orientation (parallel or normal to the supporting beam) than under pulling forces. In addition, the relatively low values of load capacity resulted from the eccentricity of the load application in respect to the point of resultant force at the bottom bend of the connection bar. In the case of specimens tested under normal pushing (compression), which showed the lowest load capacities, no matter the bearing type, the load eccentricity triggered an early bending/buckling of the connection bar since the bar was unrestrained at this portion.

4.4.3 Strains in the connection bar

Figures 4.7 and 4.8 present the load-strain relationship for the connection bar at the unrestrained bend in specimens from Series I and II, respectively. It is to be noted that the strain gauge attached to the grouted side of the connection bar did not read strains larger than 400 με in any specimen. As such, its readings are not presented in this paper. The following section discusses the load-strain relationship of the connection bars at the unrestrained bend of the bar.

4.4.3.1 Specimens of Series I – end bearing connection

Loading normal to the axis of the supporting beam: Under tension (pulling) force, the connection bar in end bearing specimens showed an initial linear elastic stage, followed by a reduction in slope at the onset of bar yielding (Fig. 4.7). Specimen EB-TN-45 first yielded at 70% of the peak load. However, the connection bar in EB-TN-90 experienced less deformation due to the early bond failure of the connection. At the peak load, the measured tensile strains under tension forces with

90-degree (EB-TN-90) and 45-degree bent bars (EB-TN-45) were 2,370 and 24,980 με, respectively. The latter tensile strains value confirms that the connection bar in EB-TN-45 reached the necking stage, as mentioned earlier. Both end bearing specimens offered ample warning before maximum load capacity under tension, which also explains the larger capacity compared to their counterparts under pushing force.

Under compression (pushing) forces, the length of unrestrained bar at the bottom bend in end bearing connections affected the load-strain behaviour (Fig. 4.7). The end-bearing specimen with a 45-degree bend bar (EB-CN-45) exhibited an initial linear elastic load-compressive strain behaviour, which resulted from the connection bar being pushed downwards by the slabs (Fig. 4.4 (d)). At peak load, the connection bar attained -1,000 με at the bend. After this point of loading, strength degradation was observed along with strain reduction. In contrast, reducing the unrestrained length of the bar in specimen EB-CN-45R delayed the onset of bar buckling and strength degradation at the bottom bend due to the bar leaning against the top flange of the supporting beam. After the linear elastic stage with compressive strains, the connection bar yielded while buckling near the flange of the supporting beam. Fig. 4.4 (d) illustrates the bar buckling and the distortion of the bar around the flange of the beam. This connection bar maintained the peak load almost steady until approximately -3,360 με. Finally, a drop in the load with increasing tensile strains was observed. Specimens with 90-degree bar bends tested under compression (EB-CN-90 and EB-CN-90R) had similar load-strain behaviour. At the maximum load, the measured strain in the connection bar in EB-CN-90 and EB-CN-90R, were -1,050 and -1,460 με, respectively.

Loading parallel to the axis of the supporting beam: The end bearing specimen under pushing load (EB-CP-90) showed tensile strains while testing (Fig. 4.7). The bar elongation in the direction of the force caused such tensile strains. The unrestrained bend of the connection bar yielded at

approximately 9.1 kN (60% of the capacity). After undergoing significant deformation, bar twisting started at approximately 87% of the peak load and the specimens failed by bar rupture. The maximum strain measured at the unrestrained bend was 8,080 με before bar rupture near the welding. Compared to its counterparts subjected to normal pulling, the figure shows a significantly lower slope before reaching a similar maximum load. This behaviour demonstrated a weaker response of the connection to parallel forces compared to normal ones.

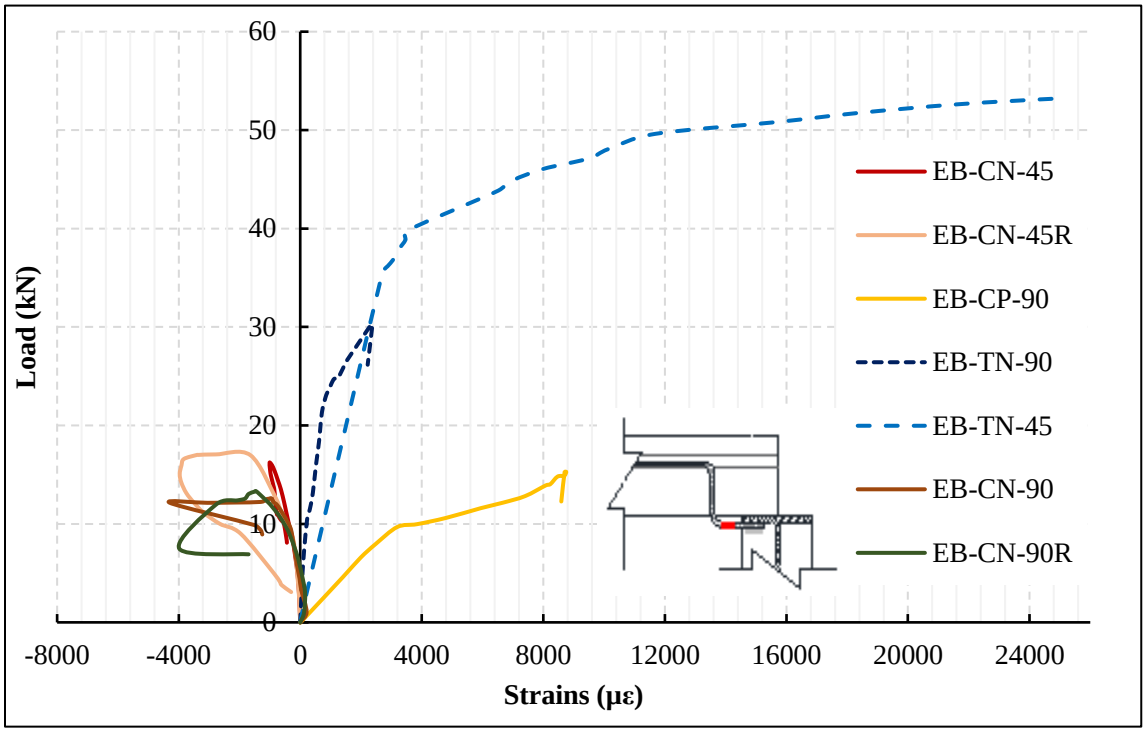

Fig. 4.7: Load-strain relationship for the connection bar of Series I (end bearing specimens)

4.4.3.2 Specimens of Series II – side bearing connection

Loading normal to the axis of the supporting beam: The side bearing specimen (SB-TN-90) under tension force had a similar load-strain relationship to end bearing specimens. The connection bar of this specimen yielded at approximately 79% of the peak load and reached 13,400 με at the peak load (Fig. 4.8). On the other hand, when tested under compression forces, the load-strain

relationship of the connection bar showed an initial linear-elastic behaviour up to bar buckling. According to the strain measured at peak load (900 με), bar buckling does not necessarily mean the bar has yielded. After buckling, strength degradation and tensile strains occurred as an effect of bar drifting by the slab displacement. In the post-buckling stage, the trend of the load-strain relationship for SB-CN-90 and its counterparts with end bearing (EB-CN-90 and EB-CN-90R) agree with the findings of Dhakal and Maekawa (2002) and Mander et al. (1984), where it was reported that the stress-strain relationship depends on the unrestrained length of the steel bar and the bar diameter. As the unrestrained portion of the bar increases, the post-buckling slope is more negatively abrupt. Typically, peak load occurs at yielding or bar buckling (Mander et al. 1984; Dhakal and Maekawa 2002). Overall, the load-strain relationship of the connection bars tested under compression forces demonstrated that there is no strength gaining after bar buckling.

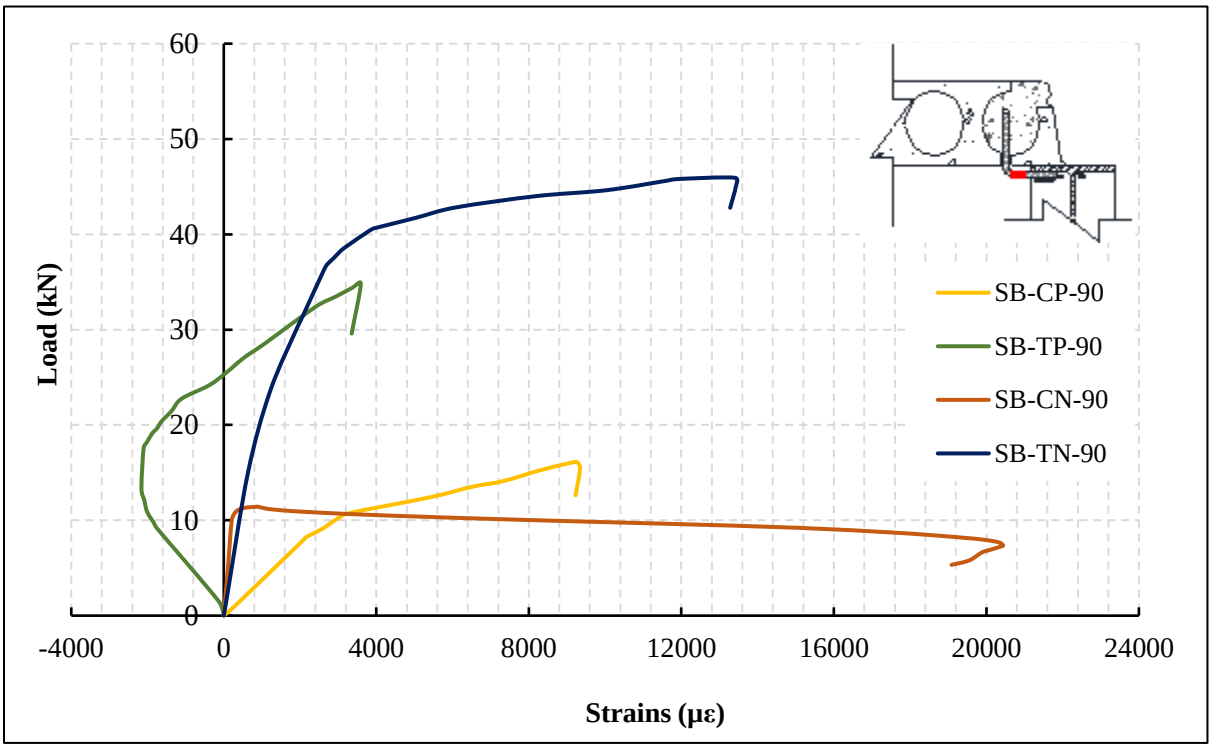

Fig. 4.8: Load-strain relationship for the connection bar of Series II (side bearing specimens)

Loading parallel to the axis of the supporting beam: The load-strain relationship for the connection bar in the side bearing specimen tested under a pushing force (EB-CP-90) is almost identical to its counterpart with end bearing (Fig. 4.8). After the initial linear elastic stage, yielding in the connection bar occurred at 7.8 kN, which represents 60% of the maximum load capacity. At peak load, the measured strain in the connection bar was 9,330 με. The side bearing specimen tested under pulling forces (SB-TP-90) underwent an initial phase of compressive strains since the connection bar was welded at an angle that was not perfectly perpendicular to the flange of the supporting beam (Fig. 4.8). Once the bar straightened, tensile stresses were observed until yielding. Finally, the specimen reached a tensile strain of 3,350 με at peak load. However, Fig. 4.5 (d) shows neck formation near the welding of the bar, which indicates an even larger strain occurred in that portion.

Under parallel loads, the load-strain relationship of connection bars from series II showed lower slopes of the curves compared to their counterparts tested under normal loading from series I. Hence, the connection bar showed a stiffer response to axial loading than when subjected to shear loading.

4.4.4 Displacement of the slab

4.4.4.1 Specimens of Series I – end bearing connection

Loading normal to the axis of the supporting beam: End bearing connections subjected to normal loads had comparable initial linear elastic load-displacement relationships (Fig. 4.9), regardless of load direction. Then, the load-displacement graphs diverged at bar buckling for specimens under compression (EB-CN-90, EB-CN-90R, EB-CN-45 and EB-CN-45R); while specimens under tension (EB-TN-90 and EB-TN-45) had a slope reduction at larger values of load.

In specimens under tension, this difference in the slope following the initial elastic stage is associated with the straightening and elongation of the unrestrained bend of the connection bar, and the cracking observed in specimen EB-TN-90. In general, the specimen with 45-degree bent connection bar (EB-TN-45) exhibited a steeper slope compared to their counterparts with 90-degree bends (EB-TN-90), which implies a stiffer response of the connection. Since the specimen with 45-degree bend attained 43.2% more load than the specimen with 90-degree bend, the connection bar with a 45-degree bend exhibited more stiffness besides the higher load capacity. These two specimens failed at very similar slab displacement (22.6 mm and 21.8 mm in EB-TN-90 and EB-TN-45, respectively). These relatively low values of displacement at failure suggest that the 50-mm seating length is sufficient to avoid loss of bearing of the slabs when the bearing connection bar undergoes tensile stresses.

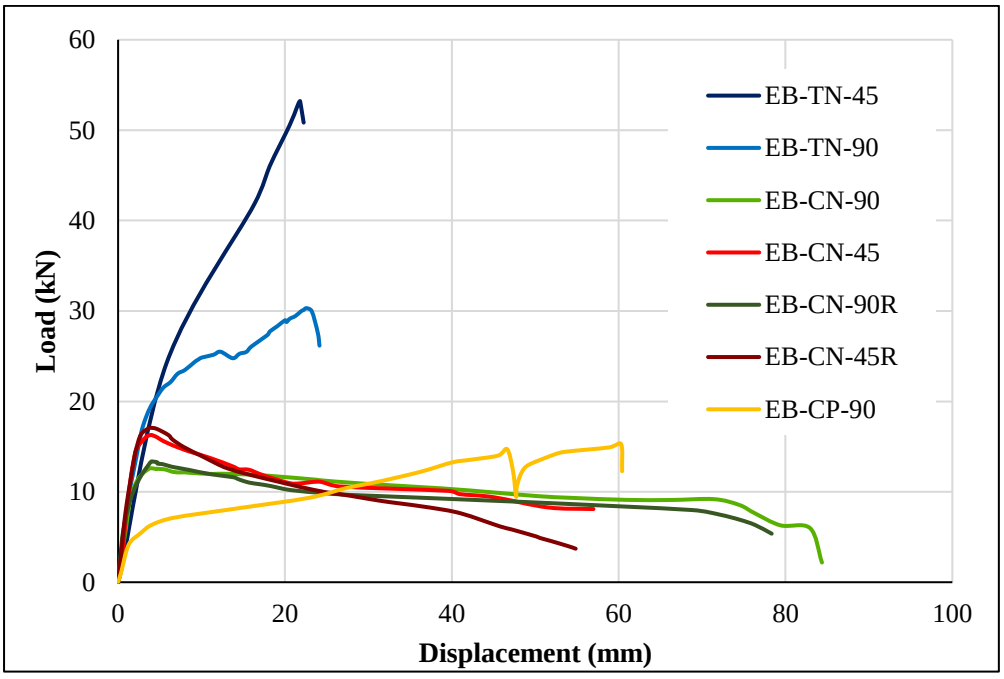

Fig. 4.9: Load-slab displacement relationship for end bearing specimens (Series I) tested under normal and parallel forces

The load-slab displacement behaviour of end bearing specimens tested under compression forces did not significantly vary with changing the bend angle or reducing the unrestrained length of the bar. The measured displacement was similar for the four specimens with alternative connection detailing, as shown in Fig. 4.9. At peak load, the measured slab displacement of specimens EB-CN-90, EB-CN-90R, EB-CN-45 and EB-CN-45R was 3.9, 4.0, 3.9, and 3.9 mm, respectively.

Loading parallel to the axis of the supporting beam: The end bearing specimen (EB-CP-90) tested under pulling force exhibited a linear elastic initial stage, followed by a considerable slope reduction after bar yielding (Fig. 4.9). A load drop occurred in EB-CP-90 was due to bar twisting, which ended with bar rupture. At peak load, the measured slab displacement was 61.5 mm, which exceeded the minimum recommended seating length in the CSA A23.3-19 (CSA 2019) of 50-mm or l_n/180, where l_n is the clear span between slab supports. Although there is no potential risk of loss of bearing of the slabs in the side bearing case, the maximum load capacity of the connection is attained after experiencing excessive displacements. This results in lower stiffness of the connection and an undesirable behaviour, where floor misalignments can occur during construction at relatively low load values.

4.4.4.2 Specimens of Series II – side bearing connection

Loading normal to the axis of the supporting beam: For side bearing connections under tension (SB-TN-90), the load-slab displacement relationship (Fig. 4.10) has a similar trend to specimens EB-TN-90 and EB-TN-45, where the connection experienced lower stiffness at bar yielding. Like its counterparts with end bearing, the measured slab displacement at the end of the test was 22.9 mm. It can be observed that the side bearing connection exhibited a stiffer behaviour in comparison to the end bearing connection with 90-degree bent bar. As discussed earlier, this was due to the early bond failure of the end bearing specimen.

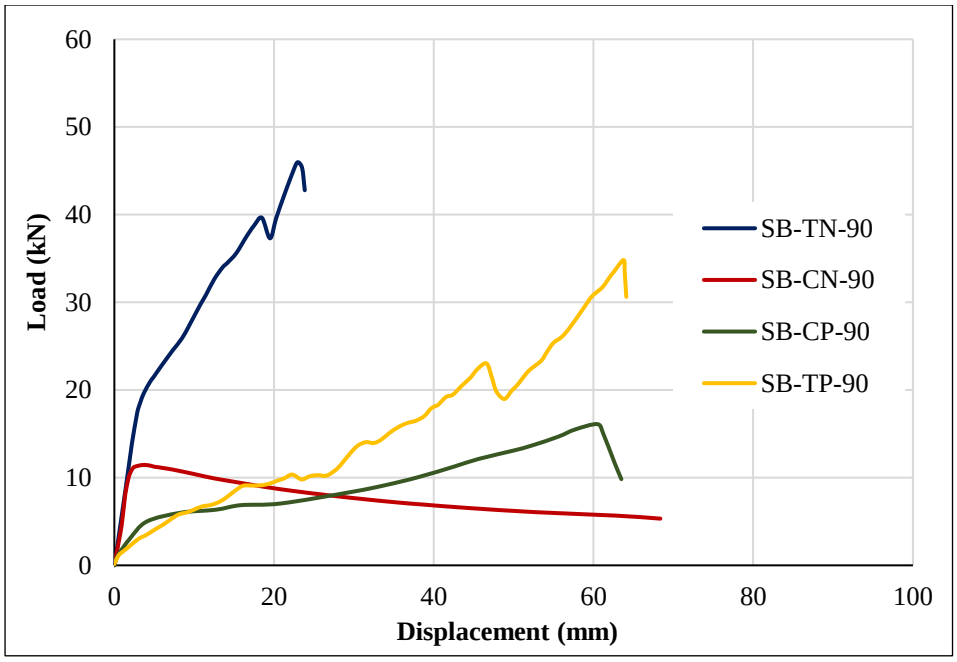

Fig. 4.10: Load-slab displacement relationship for side bearing specimens (Series II) tested under normal and parallel forces

When subjected to compression (pushing) force, the load-slab displacement graph of the side bearing specimen (SB-CN-90) followed an identical trend to its counterpart end bearing specimen. The linear-elastic relationship experienced an abrupt change after the peak load, resulting from bar buckling and loss of capacity (Fig. 4.10). Also, the measured slab displacement near the peak load was approximately 3.5 mm. Moreover, the curve overlaps with its counterpart under tension forces (SB-TN-90) in the initial linear elastic stage. Given that the load capacity was similar to that of the end supported specimens and its counterpart under tension, no significant change in the stiffness can be noted in the pre-peak stage.

Loading parallel to the axis of the supporting beam: The side bearing specimen under parallel pushing force (SB-CP-90) showed a load-slab displacement curve that is similar to the end bearing

specimen EB-CP-90 in terms of the slope at all loading stages (Fig. 4.10). This indicates no significant variation in the stiffness because of the bearing type.

In contrast, the side bearing connection (EB-CP-90) under pulling exhibited a steeper load-displacement curve before failure compared to its counterpart tested under a pushing force (Fig. 10). Initially, this specimen had a linear-elastic stage followed by a load drop at the onset of the bar twisting. Finally, the load capacity was reached at a displacement of 63.8 mm.

4.5 Conclusions

Based on the test results of steel connection bars under in-plane forces, the following conclusions can be drawn:

- The connection detailing tested met the minimum tensile capacity specified by the North American standards and codes (CSA 2019, ACI 2019) for integrity ties under tension forces (normal to the support).
- Specimens tested under tension (pulling normal to support) forces or parallel loads (regardless of load direction) reached yielding or close-to-yielding stresses before the peak load. After yielding, the specimens tested under tension forces failed due to grout splitting. However, specimens tested under parallel loads (pushing or pulling) experienced relatively large deformations and yielding under relatively lower loading levels, and no grout or slab cracking were observed after yielding.
- Specimens with connection bar tested under compression forces (normal to support) did not show yielding before the peak load, except for EB-CN-45R, which had a 45-degree bend angle and less unrestrained length of the connection bar. The mode of failure in the specimens tested under compression was governed by bar bending/buckling.

- Compared to the original connection detailing, the combined effects of restraining the bar against the beam and decreasing the bend angle to 45-degree resulted in a 35.7 % increase in the load capacity under normal pushing (compression). Although the capacity of the connection remained less than that of the predicted based on material properties, the mode of failure was more ductile compared with the rest of the connections tested under compression.
- There is no significant difference in the behaviour of the end-bearing and side-bearing connections with similar connection detailing when tested under pushing or pulling forces, applied either normal or parallel to the supporting beam.
- The eccentricity between the load application and the unrestrained bend of the connections bar provoked a reduction of the load capacity of the connection bar tested under pushing forces. This eccentricity in the load path triggered the early bending/buckling of the bar.

CHAPTER 5 - BEHAVIOUR OF REINFORCING BAR CONNECTION OF HOLLOW-CORE SLABS TO MASONRY WALLS UNDER IN-PLANE FORCES

Authors' Affiliations and Roles:

- **Susana Hernandez Brito**, M.Sc. Student, Department of Civil Engineering, University of Manitoba.
  Role: Methodology, Investigation, Formal analysis, Validation, Visualization and Writing-Original Draft.
- **Karam Mahmoud**, Post-Doctoral Fellow, Department of Civil Engineering, University of Manitoba.
  Role: Validation, Visualization and Writing-Review & Editing.
- **Karl Truderung**, Structural Engineer, Associate, Tower Engineering Group, Canada.
  Role: Validation and Writing-Review & Editing.
- **Ehab F. El-Salakawy**, Professor, Department of Civil Engineering, University of Manitoba.
  Role: Conceptualization, Methodology, Writing-Review & Editing, Supervision, Project administration, Resources and Funding acquisition.

Journal and Status: Precast/Prestressed Concrete Institute Journal, under review

Reference:

Hernandez Brito, S., Mahmoud, K., Truderung, K., and El-Salakawy, E. F. "Behaviour of Reinforcing Bar Connection of Hollow-Core Slabs to Masonry Walls under in-plane Forces". PCI Journal, Submitted in September 2021.

Note:

The content of the journal paper has been edited from the original manuscript by renumbering the sections, figures and tables to maintain the thesis organization. The specimen nomenclature also differs from test matrix presented in Table 3.2. The specimen nomenclature used in this chapter is explained in the list of abbreviations. In addition, the reference list has been moved to the end of the thesis, as indicated in the table of contents.

5.1 Abstract

Integrity ties are necessary in hollow-core slab (HCS) floors as connections to prevent floor displacements under lateral loads and maintain the overall structural integrity of buildings. In Eastern Canada, the integrity tie for HCS on masonry walls usually consists of a 10M, L-shaped, steel bar, which is hammered into the supporting wall and grouted to the slabs. However, current North American design codes do not offer sufficient provisions to determine the capacity or predict the mode of failure of these ties/connections. This paper introduces the results of testing nine full-scale reinforcing bar connection assemblies under monotonic in-plane forces (compression, tension and shear) until failure. Test parameters in this study included direction and orientation of the in-plane loading, the bearing type of the HCS, and the use of adhesive. Test results showed that connections with dry-fit bars tested under compression failed by bar yielding followed by masonry beam crushing. In addition, the mode of failure under tension forces was governed by the loss of bearing of the slabs due to bar pull-out and cover spalling. Under shear forces, the connection failed by bar yielding. Finally, the connections with adhesive had a similar mode of failure to their counterparts with dry-fit bars, but these did not show bar pull-out from the masonry beam, demonstrating higher stiffness.

Keywords: Hollow-core slabs; in-plane forces; integrity ties; end-bearing connection; side-bearing connections.

5.2 Introduction

Hollow-core slabs (HCS) are commonly selected to span large areas in residential and industrial buildings, where clear and open spaces are required. In 2016, it was estimated that more than 50 million square meters of HCS floors have been constructed since 1962 in Canada (Personal contact

2021). These slabs have a relatively light weight and shallow cross-section, compared to other precast-prestressed solid slabs with similar load-carrying capacity. The voids in HCS eliminate up to 50% of the concrete volume in the geometric centre of the section, where the slabs do not carry flexure allowing for longer spans, reduced deflections and section height.

HCS floors are typically designed to act as continuous horizontal diaphragms, where lateral in-plane loads (e.g., winds, earthquakes, accidental loads during construction) are transferred to lateral force-resisting walls throughout their bearing connections. There are two types of bearing connections – end-bearing, where the slabs transfer the gravity loads onto the masonry walls, and side-bearing, where the edge of the slabs overlap into the masonry wall. Depending on their direction, lateral in-plane loads result in axial and/or shear forces in HCS bearing connections. Besides horizontal load transfer to supporting members, the use of steel reinforcement in bearing connections is intended for structural integrity and preventing slab displacements that could result in floor misalignments, loss of bearing or even a progressive collapse. Furthermore, the connection reinforcement provides lateral bracing for the axially loaded supporting members, by connecting bearing walls into the floor diaphragm.

Due to the main function of this connection reinforcement, current North American design codes, CSA A23.3-19 (CSA 2019) and ACI 318-19 (ACI 2019) refer to them as "integrity ties", in which the tie resistance shall be governed by yielding of the steel component, assumed to be a reinforcing bar for HCS connections. Accordingly, these codes require minimum threshold design loads to achieve structural integrity via tension ties that connect the HCS diaphragms to the end walls of the building. For structures up to two storeys high, the CSA code requires connections between the HCS diaphragm and elements being laterally supported to be designed for a minimum factored tensile resistance of not less than 5.0 kN/m, with ACI requiring a slightly lower minimum force of

4.4 kN/m. However, for structures that are three or more storeys high, and are constructed with precast concrete bearing walls, the CSA A23.3 (CSA 2019) and ACI 318 (ACI 2019) codes require a minimum factored tensile resistance of 14 or 22 kN/m of supporting wall length, respectively for longitudinal tension ties in end-bearing connections. These ties are represented with an "L" in Figure 5.1.

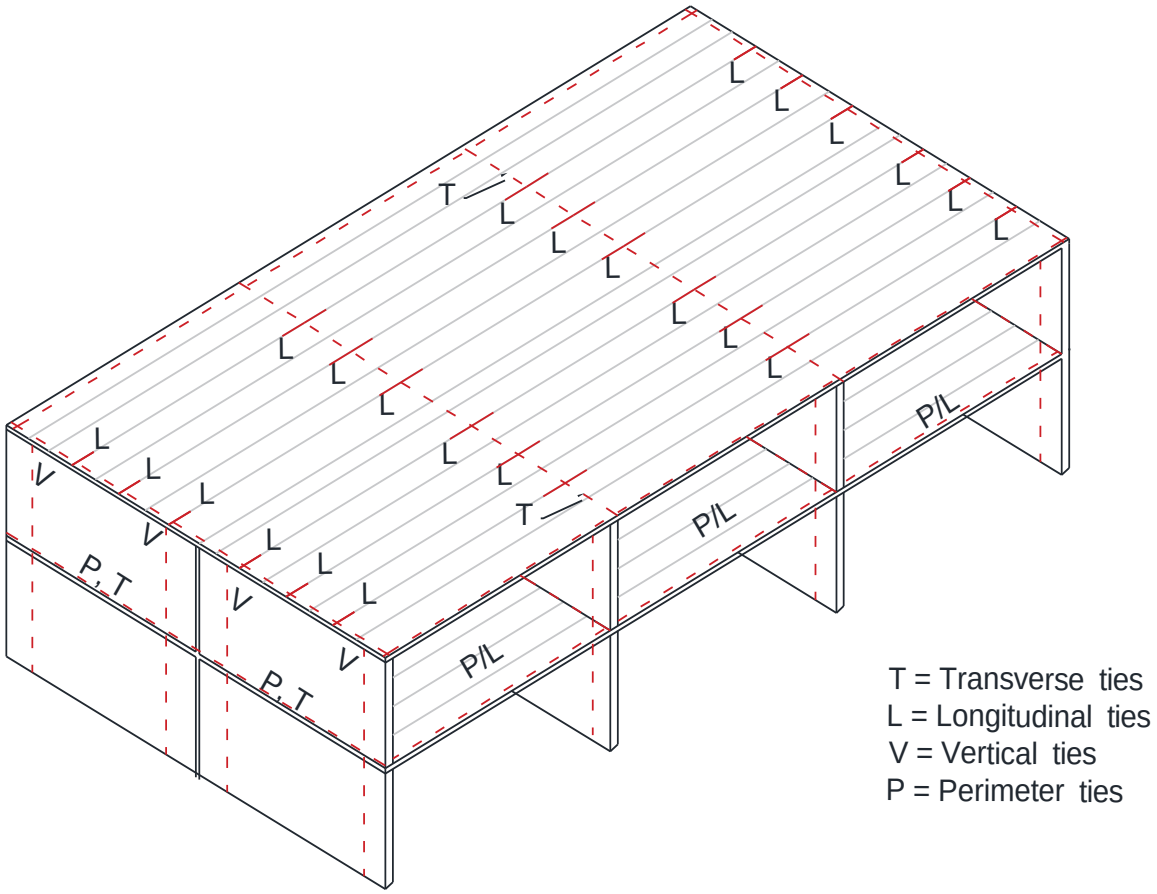

Fig. 5.1: Typical arrangement of integrity ties in HCS floor diaphragms supported in precast concrete walls - Reproduced from ACI 318 (ACI 2019).

A possible reason for the lower CSA A23.3-19 (CSA 2019) design tensile resistance value of 14 kN/m in comparison with the design value in the ACI 318 (ACI 2019) of 22 kN/m, could be that

a 10M reinforcing bar placed at every second HCS slab joint (at a spacing of 2,440 mm) would require a minimum factored resistance of 34 kN per bar, which is exactly the factored resistance of a single 10M bar in tension. For a hybrid structure such as a multi-level building constructed with masonry walls and HCS, there are no specific design provisions that apply, however it would be logical that the minimum recommended tension tie force thresholds noted in the CSA A23.3 (2019) and ACI 318 (2019) codes could be reasonably applied, based on the number of storeys in the building.

For design calculations, the tie spacing selected depends on the individual capacity of each tie. Although these code minimum force requirements are intended for integrity ties under tension or pulling forces exclusively, compression and shear forces act equally on HCS floors due to the reversible nature of lateral loads (e.g., wind, load, accidental loads). Hence, HCS connections must be able to resist compression, tension, or shear forces to provide a complete load path between critical elements throughout the building under response from lateral loads, and still maintain a minimum level of structural integrity.

5.3 Background and Motivation

In Eastern Canada, an integrity tie typically consists of an "L-shaped" 10M steel reinforcing bar of Grade 400W, as shown in Fig. 5.2. This connection bar is hammered 150 mm into the masonry wall from one end and grouted to the shear keys or side cores of the HCS on the other end. A tight hole is drilled on top of the masonry wall, required to achieve a strong fixation of the embedded portion of the vertical leg of the bar, via direct bar contact with the masonry grout and without using a binding material such as epoxy. In end-bearing connections, one connection bar is inserted between HCS (spacing of 1,220 mm), while in side-bearing connections, bars are inserted (maximum spacing of 3,000-mm) into side pockets. These pockets are saw-cut slots that are pre-

ordered to the manufacturer of the slabs. It is a common practice to provide a minimum embedment length in grout of at least 450-mm to ensure a strong anchorage of the rebar to the HCS.

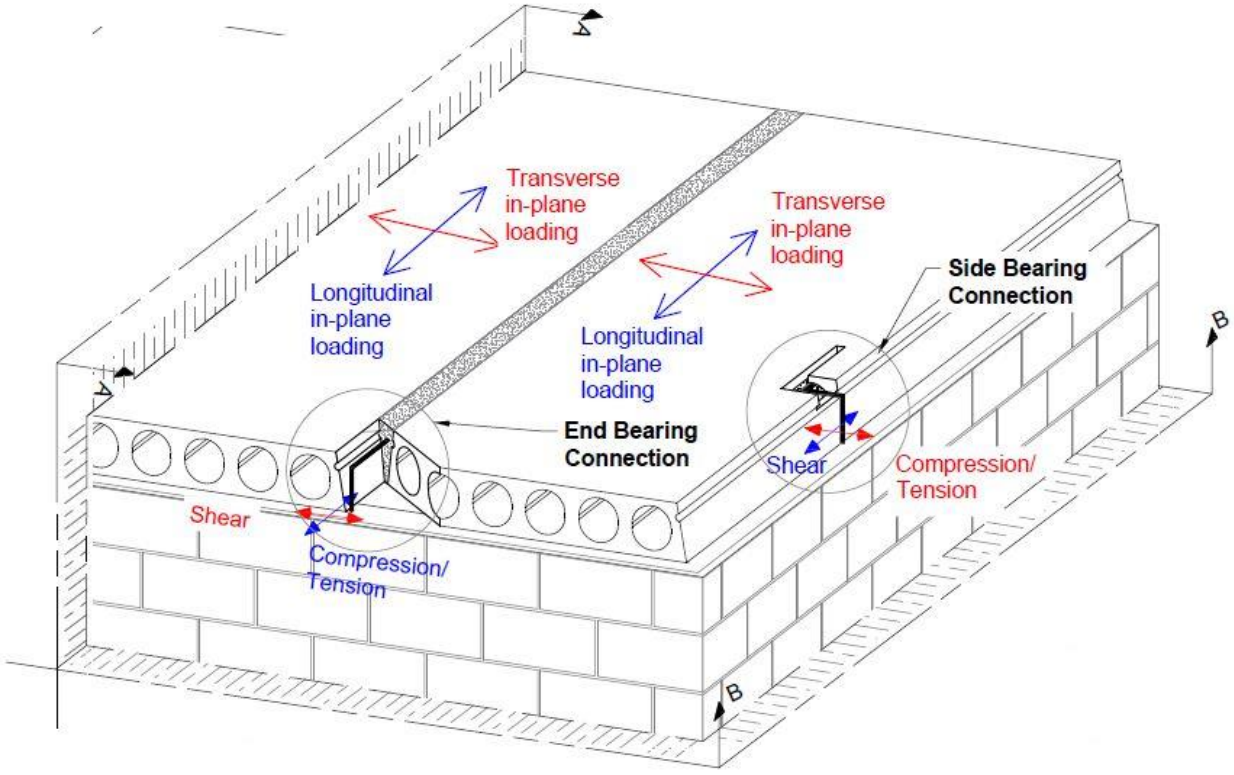

a) End- and Side-bearing connections of HCS supported on masonry walls

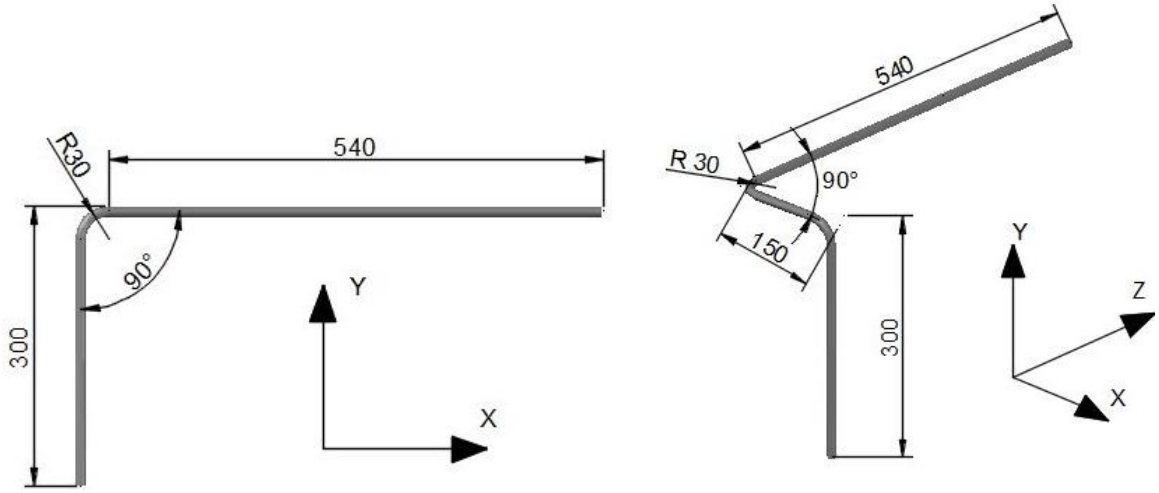

b) End-Bearing c) Side-Bearing

Fig. 5.2: Connection bar details

Another typical bearing connection detailing consists of grouting one end of the L-shaped bar to the shear keys or side pockets of the HCS while leaving its other end exposed and facing up to be inserted in the next masonry course constructed above the HCS (PCI 2015; CPCI 2019). Then, that course of masonry blocks is filled with grout around the connection bar (Fig. 5.3 (a)). As an alternative to "L-shaped" ties, U-shaped hooked bars can also be employed as connection for HCS to supporting masonry walls. In this case, the steel hooks are tied to the longitudinal steel reinforcement of boundary elements cast at the top of masonry wall and cast integrally. Afterwards, the other end of the hooks is grouted to the shear keys or pockets of the HCS (Fig. 5.3 (b)).

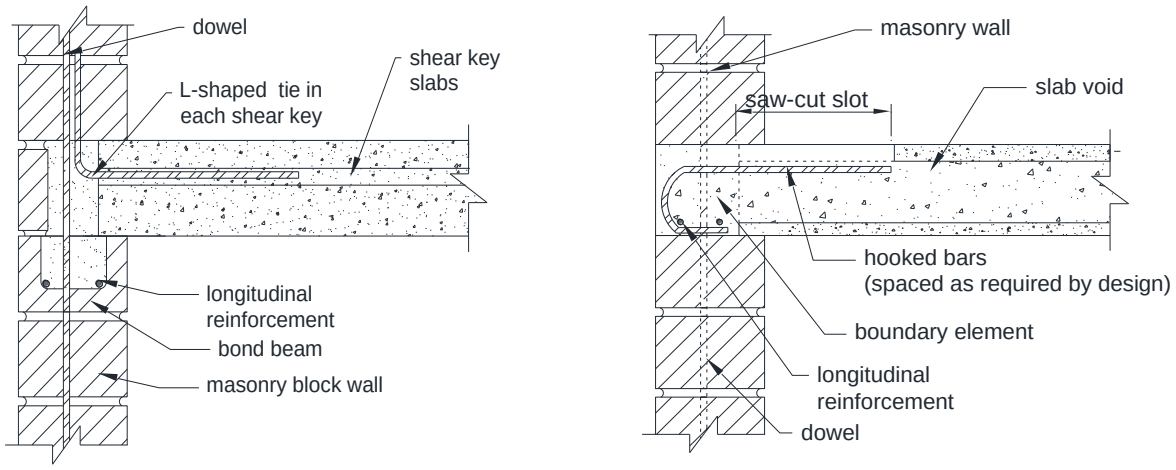

a) L-shaped tie grouted to masonry blocks b) Hooked bars locked to longitudinal reinforcement

Fig. 5.3: Connection detailing for end-bearing connections - Reproduced from PCI-15 (PCI 2015)

Despite the wide utilization of the reinforcing bar connection in Eastern Canada, current design codes and guidelines (PCI 2015; CPCI 2017; ACI 2019; CSA 2019) do not offer a design methodology or sufficient provisions for their design and construction. These standards suggest using the shear friction theory to determine the horizontal-load capacity of HCS bearing connections. However, due to the eccentricity between the entry and exit points of lateral loads in

the overall connection system (from the HCS grout key into the masonry wall at the base of the slab below), shear friction may not be appropriate for analysis of such connections – see Figure 5.4. In addition, no attention was given to investigate the behaviour of HCS bearing connections to masonry wall supports. Previous studies (Mejia-McMaster and Park 1994; Herlihy 1999; Matthews et al. 2001; Lindsay et al. 2004; MacPherson et al. 2005) covered the seismic performance of HCS diaphragms supported on concrete beams, where the bearing connections were cast integrally and behaved compositely.

To the author's knowledge, no research has been conducted on the lateral resistance of HCS bearing connections to masonry walls, using the Eastern Canada detailing for integrity ties. Therefore, it is deemed necessary to investigate the capacity and the mode of failure of the reinforcing bar connection under in-plane forces.

5.4 Experimental Program

5.4.1 Test specimens

Nine full-scale assemblies of HCS reinforcing bar connections to masonry beams, divided into two series, were tested under in-plane monotonic forces until failure. These testing series were arranged according to the bearing type (Table 5.1), where Series I corresponded to end-bearing connections (five specimens), while Series II was dedicated to side-bearing connections (four specimens). The specimens were constructed with 203-mm thick HCS, cut to 1,220-mm square segments. For end-bearing connections, two of these segments were employed to assemble the connection, whereas side-bearing connections involved a single segment of HCS. The slabs were supported on a two-course, 190-mm wide single wythe masonry beam of 3,200-mm length, which simulated the typical bond beam constructed with U-masonry blocks at the top of the wall. The longitudinal reinforcement of the masonry beam consisted of two 10M steel bars, placed inside the U-blocks,

which were filled with grout. In this study, the masonry beam was made of 190 × 190 × 390 mm masonry blocks of three shapes (plain end units, two-cell stretchers, and knockout web bond blocks). The masonry beams were constructed by certified masons to reproduce similar quality to the construction practice.

Table 5.1: Specimen Details

Type of connection	Specimen Code	Load Orientation	Load Direction	Adhesive
End-Bearing (Series I)	EB-CN-A	Normal to support axis	Pushing/Compression	Yes
	EB-CN-D			No
	EB-TN-A	Normal to support axis	Pulling/Tension	Yes
	EB-TN-D			No
	EB-CP-D	Parallel to support axis	Pushing/Compression	
Side-Bearing (Series II)	SB-CN-D	Normal to support axis	Pushing/Compression	No
	SB-TN-D		Pulling/Tension	
	SB-CP-D	Parallel to support axis	Pushing/Compression	
	SB-TP-D		Pulling/Tension	

The HCS in both series were connected to the masonry beam using an L-shaped 10M connection bar or integrity tie, as described previously, and indicated in Figs. 5.2 and 5.4. After drilling the beam with an appropriate bit diameter, the hole was blown with compressed air and thoroughly vacuumed. Next, the bar was hammered into the masonry beam. An adhesive (epoxy resin) was incorporated in two of the end-bearing specimens to bond the bar to the masonry beam. In this case, before hammering the bar into the hole, the hole was injected with the adhesive using a specialized gun, as required by the supplier. Once the connection bar was installed on the masonry beam, the slabs were erected while providing a minimum seating (bearing) length of 75-mm, which

is industry standard. This value of seating length exceeded the minimum required length of 50-mm according to Canadian Standards (CPCI 2017; CSA 2019) to prolong the test and ensure failure while the slabs are still supported. Slab spacing was set to fit tightly the connection bar, as performed in practice. Finally, the connections were grouted. The HCS segments were provided by a local Canadian Precast Concrete Quality Assurance (CPCQA) certified precast manufacturer, and the components were constructed and assembled at the Heavy Structures Laboratory of the University of Manitoba.

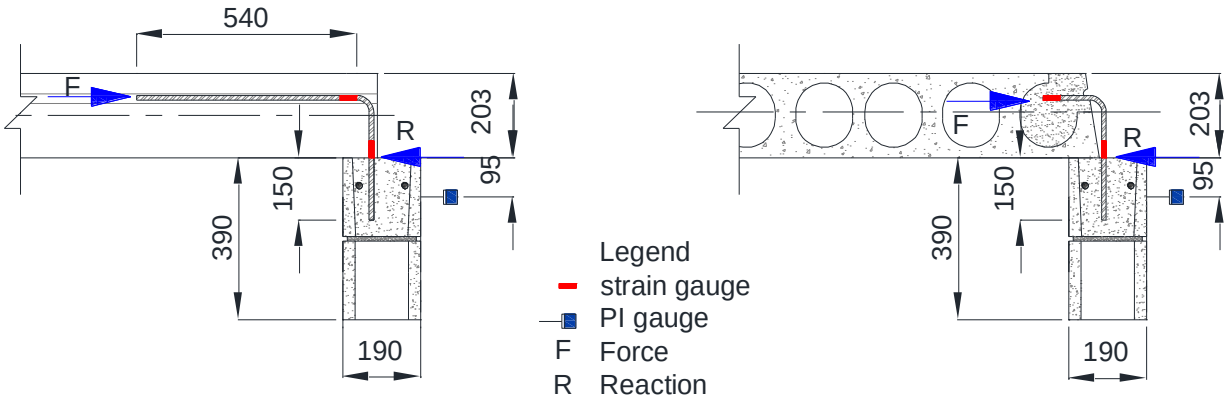

a) End-Bearing connection b) Side-bearing connection

Fig. 5.4: Steel bar connection detailing, locations of gauges and force eccentricity

Test variables in this study were bearing type (end-bearing or side-bearing), load direction (pulling or pushing against the masonry beam), load orientation (normal or parallel to the longitudinal axis of the masonry beam). These test variables were individually implemented to address all possible scenarios of axial and shear in-plane forces acting in HCS bearing connections to masonry walls. Additionally, the effect of using an adhesive (epoxy resin) to enhance bar bonding to the masonry beam was examined in two of the end-bearing connections.

The specimen nomenclature contains three parts. The first part represents the bearing type of the HCS: end-bearing “EB” and side-bearing “SB”. The second part has two letters representing the

load direction ("C" for compression/pushing or "T" for tension/pulling), and the load orientation (applied normal "N" or parallel "P" to the masonry beam). Finally, the last part of the specimen nomenclature refers to the method of installing the bar in the masonry beam, where "D" stands for dry fit bars (hammered), while "A" corresponds to connection bars bounded with adhesive. Table 5.1 list a summary of the specimen nomenclature and test variables.

5.4.2 Material properties

Standard tests were carried out on steel bars to determine their tensile properties, in accordance with ASTM A370-20 (ASTM 2020a). The steel bars had a yielding strength, yielding strain, and modulus of elasticity of 470 ± 8 MPa 2,370 ± 40 με, and 199 GPa, respectively. Due to the lack of provisions for the construction of bearing connections in North American standards, industry-standard normal-strength grout (20 – 25 MPa) was used. Grout cubes of 51-mm were cast and tested, as per ASTM C109/C109M-20 (ASTM 2020b), to obtain the grout strength on the day of testing. The average grout strength obtained was 25.3 ± 3.1 MPa. The mixing, placement and curing of this normal-strength grout were carried out according to the manufacturer's guidelines. The masonry beam was filled with a similar normal-strength grout mix, provided by a local supplier. Finally, the HCS were cast at the supplier plant, using a concrete mix with a target 28-day design compressive strength of 55-60 MPa.

5.4.3 Test setup and instrumentation

The test setup contained four main components: (a) pinned-pinned supports to allow for lateral displacement while carrying half the self-weight of the HCS, (b) clamping beams to distribute the in-plane forces from the actuator along the edge of the HCS, (c) a 3,200-mm long masonry beam, and (d) two vertical restraints to brace the masonry beam and avoid undesired torsion at the top course of blocks (Fig. 5.5). The masonry beam was fixed to the laboratory's strong floor using

four steel fixtures and Dywidag bars prestressed to the floor. Two rollers were attached to the masonry beam to guide the slabs and avoid slab rotation.

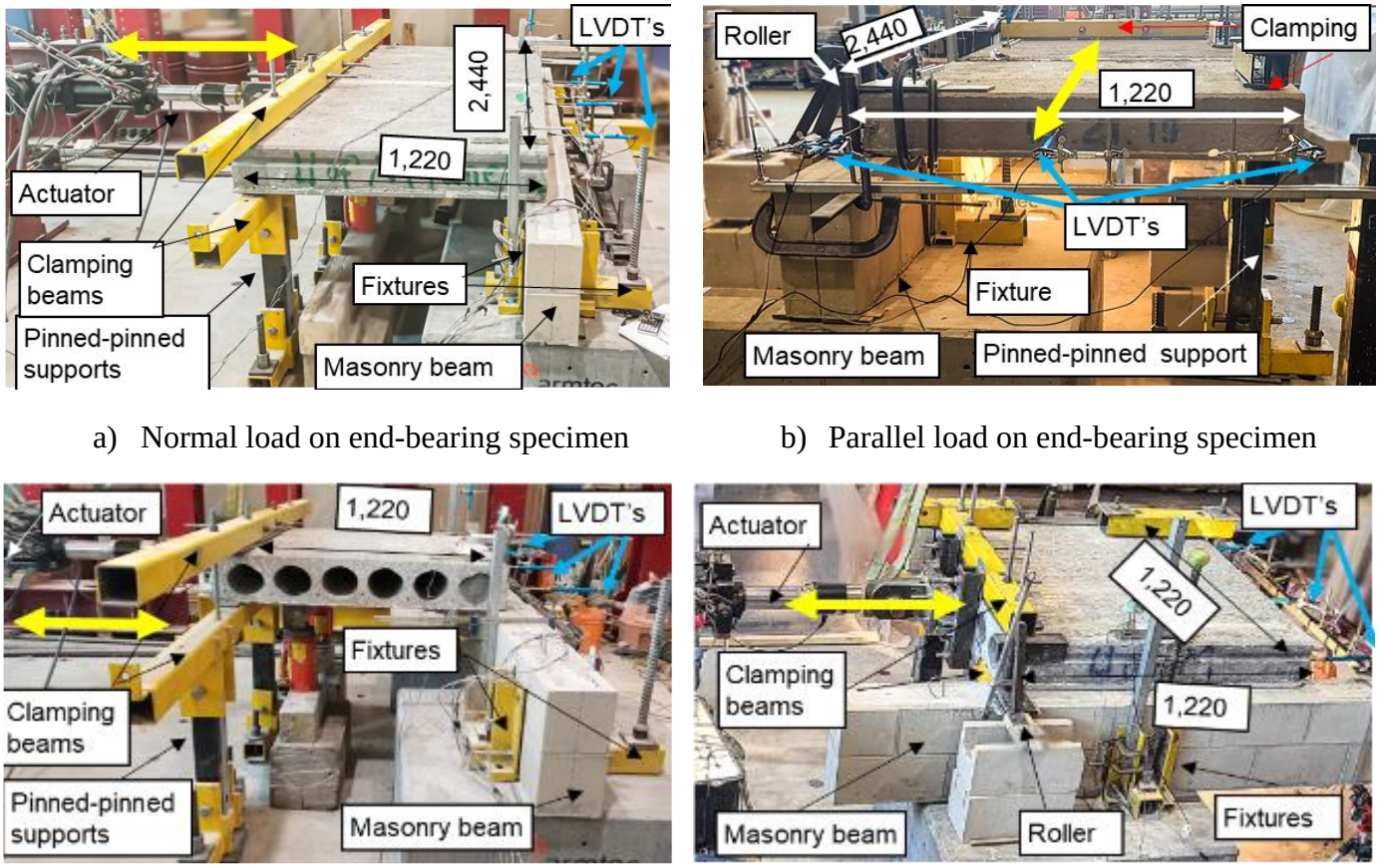

a) Normal load on end-bearing specimen

b) Parallel load on end-bearing specimen

c) Normal load on side-bearing specimen

d) Parallel load on side-bearing specimen

Fig. 5.5: Test setup and external instrumentation

The slabs were either pulled or pushed in a parallel or normal orientation to the axis of the masonry beam. Hence, under normal forces the connection bar resisted axial compression or tension, depending on the loading direction, while under parallel forces it was subjected to shear. The loading scheme did not include additional gravity loads, other than the self-weight of the HCS, to simulate the lower-bound loading scenario with minimum friction between the HCS and the masonry beam.

An actuator with load and stroke capacities of 500 kN and ±130-mm, respectively, was mounted on a strong triangular reaction frame and hinged to the test setup. The monotonic load was applied at a rate of 5.0 mm/min to allow for gradual load application and to complete the test within 25-30 minutes, given the expected nominal connection capacity of 40 kN, in direct tensile yielding of the rebar. Similar testing conditions were employed previously by Herlihy (1999).

Slab displacement was measured by linear variable displacement transducers (LVDT), as shown in Fig. 5.5. Electrical strain gauges were used to measure strains in the connection bar at its bends and at the beam top surface. The crack width was monitored with PI gauges (Fig. 5.4). Also, a load cell connected to the actuator was used to record the load. Readings from these sensors were processed through a Data Acquisition (DAQ) System. In addition, cracks or spalling, if any, were carefully marked and photographed during the test.

5.5 Test Results and Discussion

5.5.1 Mode of failure and cracking patterns

In this section, test results are discussed in terms of mode of failure, capacity, measured strains in the connection bar, cracking loads, slab displacements and overall integrity. Test results were summarized in Table 5.2.

5.5.1.1 Specimens of Series I – end-bearing connections

Loading normal to the axis of the masonry beam: The mechanism of failure of end-bearing specimens subjected to normal forces depended on the loading direction, pushing or pulling. Under compression forces (pushing), the end-bearing connection with dry-fit bars (EB-CN-D) failed by bar pull-out, yielding, followed by masonry beam crushing.

Table 5.2: Test results

Type of bearing	Specimen code	Load direction/ orientation	Mode of failure	Cracking Load (kN)	Yielding Load (kN)	Peak Load (kN)	Strains at peak load (με)	Slab displacement[3] (mm)
End-Bearing (Series I)	EB-CN-A	Normal/ Pushing	Bar yielding and beam crushing	11.4	27.3[1]	29.0	650	8.7
	EB-CN-D		Bar pull-out, yielding and beam crushing	4.5	20.1	25.1	16,000	84.4
	EB-TN-A	Normal/ Pulling	Bar cover spalling, and loss of bearing	7.5	10.6	10.6	2,100	36.4[4]
	EB-TN-D		Bar cover spalling, bar pull-out and loss of bearing	5.9	-	9.2	325	5.4
	EB-CP-D	Parallel/ Pushing	Bar yielding and pull-out	13.8	18.1	25.9	10,870[2]	112.0
Side-Bearing (Series II)	SB-CN-D	Normal/ Pushing	Bar pull-out, yielding and beam crushing	8.2	18.2	21.2	18,650	83.1
	SB-TN-D	Normal/ Pulling	Bar pull-out and loss of bearing	5.0	-	9.1	110	60.8
	SB-CP-D	Parallel/ Pushing	Bar yielding and pull-out	-	12.1	17	15,960[5]	82.5
	SB-TP-D	Normal/ Pulling	Bar yielding and pull-out	-	7.2	7.8	4,910	17.6

[1] Post-peak value

[2] Measured at a load of 17.1 kN less than the peak load.

[3] Slab displacement at peak load.

[4] Value measured in the second peak

Masonry beam cracking Bar yielding and pull-out

a) EB-CN-D (pushing)

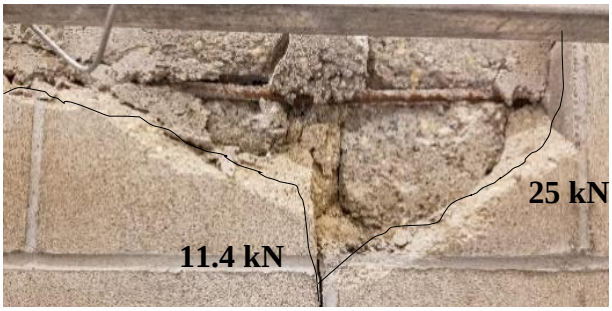

Masonry beam cracking and spalling Bar yielding

b) EB-CN-A (pushing)

Masonry beam cracking and cover spalling Bar deformation and pull-out

c) EB-TN-D (pulling)

Masonry beam cracking and spalling Bar yielding

d) EB-TN-A (pulling)

Fig. 5.6: Mode of failure for end-bearing specimens under normal forces

Initially, at a load of 4.5 kN, the masonry beam experienced vertical cracking in the tension side of the central masonry block at the location of the connection bar (Fig. 5.6 (a)). A second crack appeared at a load of approximately 17.0 kN at the vertical (head) mortar joints of the central masonry block. While the cracks propagated and widened, the connection bar experienced gradual pull out and bending in the direction of the force since, at this point, the bar lost the tight fit with the development of cracks. Fig. 5.6 (a) depicts the final shape of the connection bar, where the straight side inserted in the masonry beam deformed into a 90-degree bend. Then, the cracks propagated and connected to form a V-shape, provoking spalling where the load dropped. Yet, the connection bar reached yielding and ultimately the beam crushing occurred at a load of 25.3 kN.

The mode of failure of the specimen with adhesive tested under compression (EB-CN-A) was governed by spalling of the masonry block side face followed by bar yielding and strength degradation. Similar to its counterpart with dry-fit bar, the vertical crack at the central block behind the bar and at the mortar head joints occurred at a load of approximately 11.4 and 25 kN, respectively (Fig. 5.6 (b)). Once the spalling of the side surface of the masonry block initiated, a small load drop of 1.7 kN was observed. Then, the bar yielded and maintained the load steady. Afterwards, strength degradation occurred associated with more severe spalling, which ended with beam crushing. No bar pull out was observed during the test for the compression specimen with the adhesive.

In contrast, specimens EB-TN-D and EB-TN-A tested under tension forces (pulling/TN) failed due to loss of bearing of the slabs, preceded by masonry beam spalling. The cracking patterns observed on the tension face of the masonry beam were similar to their counterparts tested under compression forces. However, initial vertical cracks formed at a load of 5.9 and 7.5 kN at the central block in specimens EB-TN-D and EB-TN-A, respectively (Fig. 5.5 (c) and (d)). These

connected to the cracks formed at the head joint (mortar) locations, at a load of 8.2 and 9.0 kN in specimens EB-TN-D and EB-TN-A, respectively, and spalled the bar cover in both specimens. While the specimen with dry-fit bar experienced bar pull-out and strength degradation following the cover spalling, the connection bar with adhesive (EB-TN-A) reached close-to-yielding strains and a second peak of 10.6 kN. Similar to their counterparts tested under compression forces, the masonry beam in the specimen with the adhesive under tension (EB-TN-A) showed more damage than its counterpart with the dry-fit bar (EB-TN-D) before the loss of bearing of the slabs. This indicated that the bar with adhesive had a better load transfer mechanism, regardless of load direction.

Loading parallel to the axis of the masonry beam: Under parallel pushing forces, the mode of failure of the end-bearing specimen (EB-CP-D) was characterized by bar yielding and bar pull-out. At a load of 13.8 and 15.3 kN, hairline cracks formed at the central block of the masonry beam and at the head joints, respectively (Fig. 5.7). However, these cracks did not further propagate or connect. Afterwards, the bar yielded while experiencing gradual pull-out. Fig. 5.7 illustrates the shape of the connection bar, which adopted a 90-degree bend shape, similar to the connection bar in specimen EB-CN-D tested under normal pushing (compression) force, as shown in Fig. 5.6 (a).

In general, although specimens with dry-fit bars (EB-CN-D, EB-CP-D and EB-TN-D) experienced bar pull-out, the connection bar did not detach completely from the beam. As the bar deformed and gradually yielded and pulled-out in the direction of the load, the portion that was still inside the hole acted as a lock-key mechanism, resisting the load. The longitudinal steel reinforcement in the top course of the masonry beam contributed to this lock-key mechanism by enclosing the bar and tightening/controlling the cracks until more severe spalling occurred.

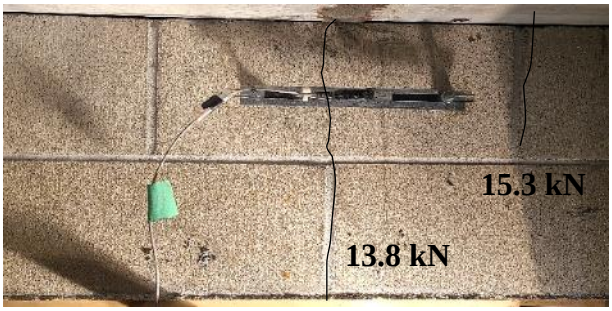

Masonry beam cracking

Bar yielding

Fig. 5.7: Modes of failure for the EB-CP-D under parallel pushing (shear) force

5.5.1.2 Specimens of Series II – side-bearing connection

Loading normal to the axis of the masonry beam: The mode of failure of side-bearing connections had great similarity to its counterparts with end-bearing type, regardless of load direction. Under compression forces, the side-bearing connection (SB-CN-D) failed due to bar pull-out and yielding, followed by masonry beam crushing. Initially, cracks formed in the masonry beam at a load of 8.2 and 17.9 kN in its center and mortar head joints, respectively (Fig 5.8 (a)). With the increasing load, these cracks further propagated and connected to each other while the bar underwent pull-out and yielded. Ultimately, the masonry beam crushed.

Under tension (pulling), the side-bearing connection (SB-TN-D) also failed because of bar pull-out and loss of bearing without reaching yielding. The bar pull-out was preceded by the formation of cracks at a load of 5.0 and 6.0 kN at the center block and masonry head joints, respectively (Fig. 5.8 (b)). Nevertheless, the cracks did not connect to each other before the loss of bearing of the slab, which evidenced a weaker load transfer mechanism to the masonry beam compared to its counterpart with end-bearing type.

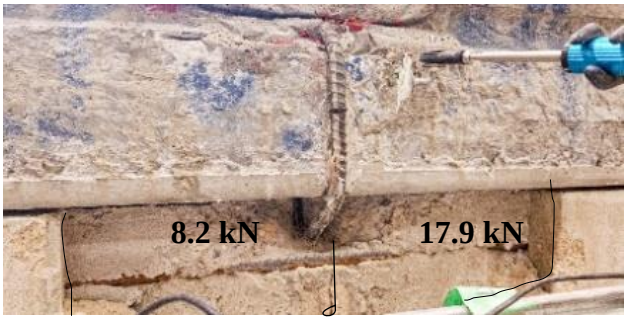

Masonry beam cracking Bar yielding

a) SB-CN-D

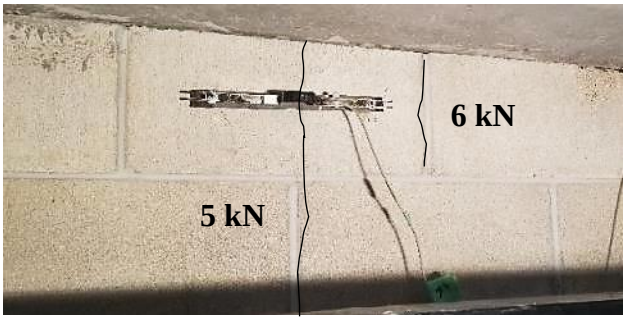

Masonry beam cracking Bar deformation

b) SB-TN-D

Fig. 5.8: Mode of failure for side-bearing specimens under normal forces

Loading parallel to the axis of the masonry beam: The mode of failure of side-bearing connections was governed by bar yielding and pull-out, regardless of the loading direction. No cracks formed in the masonry beam or the HCS while testing these specimens, which demonstrated a weak load-transfer mechanism to the masonry beam. The pictures in Figs. 5.9 (a) and (b), corresponding to the side-bearing connections under pushing (SB-CP-D) and pulling (SB-TP-D), respectively, implied that both connection bars had almost identical shapes at the end of testing, as result of bending in the direction of the force. In these specimens, the connection bars formed a 45-degree bend shape in the direction of the force, which significantly differed from their counterparts with end-bearing.

a) SB-CP-D

b) SB-TP-D

Fig. 5.9: Mode of failure by bar yielding for side-bearing specimens under parallel forces

5.5.2 Connection load capacity

In this study, a grade 400W, 10M steel L-bar was used to connect the HCS to the masonry beam. For a bar area of 100-mm^2 and a nominal yield strength of 400 MPa, the expected nominal load capacity per bar location is 40 kN, without the application of the 0.85 material resistance factor for steel bar. For end-bearing connections, typical industry practice is to place one 10M connection bar at every grout key joint location, resulting in a bar spacing of 1220 mm for standard-width HCS.

For structures up to two storeys, applying the CSA A23.3 code minimum structural integrity tension tie load of 5.0 kN/m to the 10M L-bar connections spaced at 1,220 mm requires a minimum tensile capacity of 6.1 kN per connection bar. For structures of three storeys or more with precast bearing walls, applying the code requirements results in a minimum tensile strength of 6.1 and 17.1 kN for buildings with up to two storeys and with three storeys or taller, respectively. If the 10M L-bars are able to develop the full yield capacity of the reinforcing bar in tension (40 kN), then the nominal capacity of the bars would be over twice the required tensile capacity for three-

storey buildings. Also, the minimum structural integrity force of 17.1 kN per bar would remain in the elastic range, at just below 50% of the nominal yield capacity for a 10M bar.

However, the code limits (ACI 2019; CSA 2019) only refer to the minimum required load capacity of structural integrity ties under tension. The designer must still verify the diaphragm tension loads resulting from the lateral load analysis and compare these tension forces with the code-specified minimum structural integrity forces. Since diaphragm lateral loads are reversible, in-plane compression and transverse (shear) forces could also be applied to the HCS floors. If these forces are not adequately addressed, the structural integrity of the floor could be compromised.

Fig. 5.10 illustrates the recorded capacity of all specimens. This figure also depicts code limits from ACI 318-19 (2019) and CSA A23.3-19 (2019) as the threshold of expected capacity for all specimens, based on a bar spacing of 1,220 mm.

5.5.2.1 Specimens of Series I – end-bearing connection

Loading normal to the axis of the masonry beam: The behaviour of end-bearing connections tested under normal forces resulted in significant differences in the maximum load capacity, depending on the loading direction. While connections tested under compression forces (pushing) showed a more desirable mode of failure, featuring bar yielding and masonry beam crushing, the failure of specimens under tension (pulling) was governed by cover spalling and loss of bearing (seating). Therefore, the capacity of the specimens tested under compression was considerably larger than that of their counterparts under tension. When tested under compression forces, the maximum load attained was 29.0 kN at a displacement of 8.7 mm, and 25.1 kN at a displacement of 84.4 mm in specimens EB-CN-A and EB-CN-D, respectively. Despite the use of adhesive, which resulted in a 15.5 % increase in the maximum load, the connection did not achieve the nominal yield capacity of 40 kN for a 10M bar in compression.

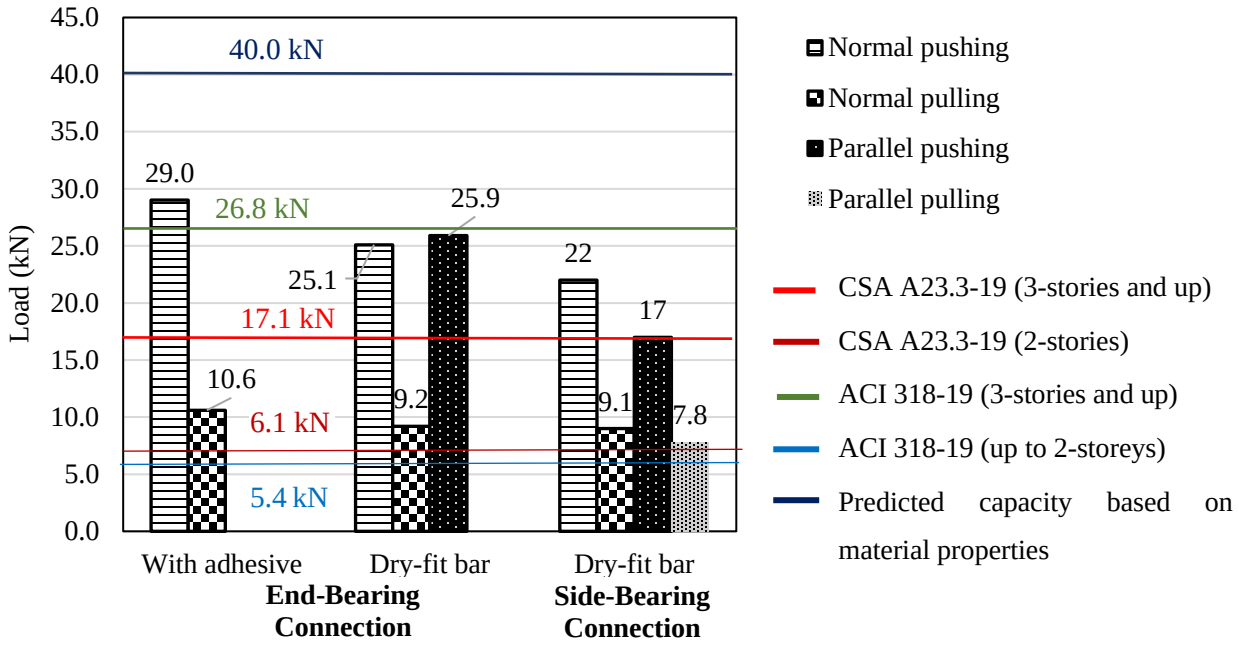

Fig. 5.10: Connection capacity of test specimens

In contrast, end-bearing specimens tested under tension had significantly less capacity compared to their counterparts under compression. Specimens EB-TN-A and EB-TN-D reached a maximum load of 10.6 kN at a displacement of 36.4 mm in the second peak, and 9.2 kN at a displacement of 5.4 mm, respectively. Both values were below the minimum threshold tension force of 17.1 kN recommended in CSA A23.3 (2019) for buildings of three or more stories but are still above the minimum threshold force of 6.1 kN for a structure with two storeys or less. In addition, the use of adhesive resulted in a 15.2 % load increase in the connection capacity compared to the specimen with dry-fit bars.

5.5.2.2 Specimens of Series II– side-bearing connection

Loading normal to the axis of the masonry beam: The capacity of side-bearing specimens under normal forces also was affected by the loading direction. The peak load in direct compression was 2.46 times higher than the tested capacity in direct tension. Whereas specimen SB-CN-D,

subjected to a pushing force, failed at a peak load of 22 kN at a displacement of 83.1 mm, and specimen SB-TN-D, under pulling force, achieved a peak load capacity of only 9.1 kN at a displacement of 60.8 mm.

Loading parallel to the axis of the masonry beam: Under parallel forces, the loading direction also generated disparities in the capacity of side-bearing connections. The load capacity of the specimen tested under pushing (SB-CP-D) was 2.26 times that of its counterpart tested under a pulling force (SB-TP-D). While specimen SB-TP-D peaked at 7.8 kN under pulling at a displacement of 17.6 mm, specimen SB-CP-D was able to reach a load of 17.0 kN, but at a displacement of 82.5 mm.

For this connection subjected to pushing and pulling forces, it would be expected that the peak failure loads and displacements would be similar. However, there was a large difference in both the peak load and corresponding displacements between SB-TP-D and SB-CP-D. This is most likely due to that the drilled hole in specimen SB-TP-D had a slightly larger diameter, which compromised the tight fit of the connection bar with the masonry beam. This implies that the dry-fit drilled connection is sensitive to the installation, with a snug fit being critical to the load resistance.

The disparity of capacity displayed in Fig. 5.10 evidenced that either end- or side-bearing connections are more susceptible to a failure under pulling forces than pushing forces, regardless of load orientation. It should be noted that none of the connection bars attained the nominal tensile yield capacity of 40 kN, regardless of loading direction/orientation or bearing type.

However, the tested tensile capacities of the end-bearing connections represent lower-bound, conservative values since no gravity loads were added. The clamping effect of gravity loads on the

end-bearing connection from long spans HCS coupled with the weight of upper storey walls would likely delay the large lateral displacements observed during testing and result in larger load capacities. In addition, the increased compressive strength of cast-in-place or precast concrete walls in comparison with masonry-block wall and grout strength would also increase the load capacity of the connection, at which the dowels would crack the wall surface under tension loading.

5.5.3 Strains in the connection bar

Figures 5.11 (a) and (b) illustrate the load-strain relationship of the connection bar in end- and side-bearing connections, respectively. Strains were measured at the top surface of the masonry beam, as indicated in the figures. An additional strain gauge was placed at the grouted bend of the connection bar. However, the readings of this strain gauge were smaller than 450 με in all tested specimens. Hence, those results are not presented herein. The following section discusses the load-strain relationship for the connection bar at the interface between the HCS and the masonry beam.

5.5.3.1 Specimens of Series I – end-bearing connection

Loading normal to the axis of the masonry beam: Under compression, the connection bars in end-bearing specimens, EB-CN-D and EB-CN-A, showed an initial linear elastic stage with compressive strains in the range of -100 to -300 με, respectively, followed by reversed tensile strains. These tensile strains were caused by the slab pulling-out the connection bar while being pushed. Then, both strain curves started to diverge and experienced a different peak for each connection, which was associated with the onset of concrete cover spalling. At this time, the longitudinal reinforcement in the masonry beam acted as dowels, interlocking the cracked faces of the masonry blocks and the grout. Consequently, the connection bars in both specimens were able to develop larger strains in the post-peak stage. For specimen EB-CN-D without adhesive, at 80% of the peak load, the connection bar reached yielding while the beam showed considerable damage.

At peak load, the measured tensile strains were 16,000 με, which demonstrates great ductility before failure.

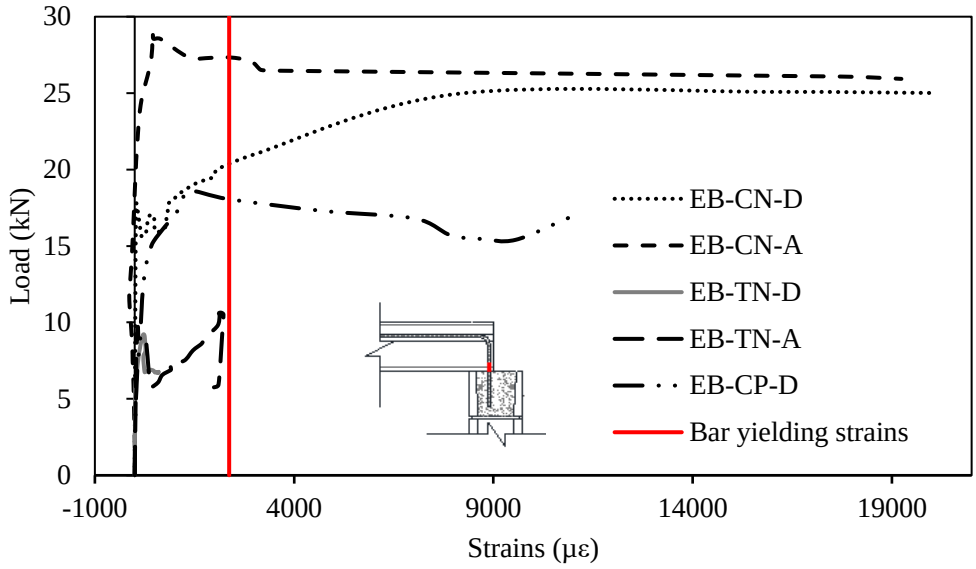

a) Series I (end-bearing specimens)

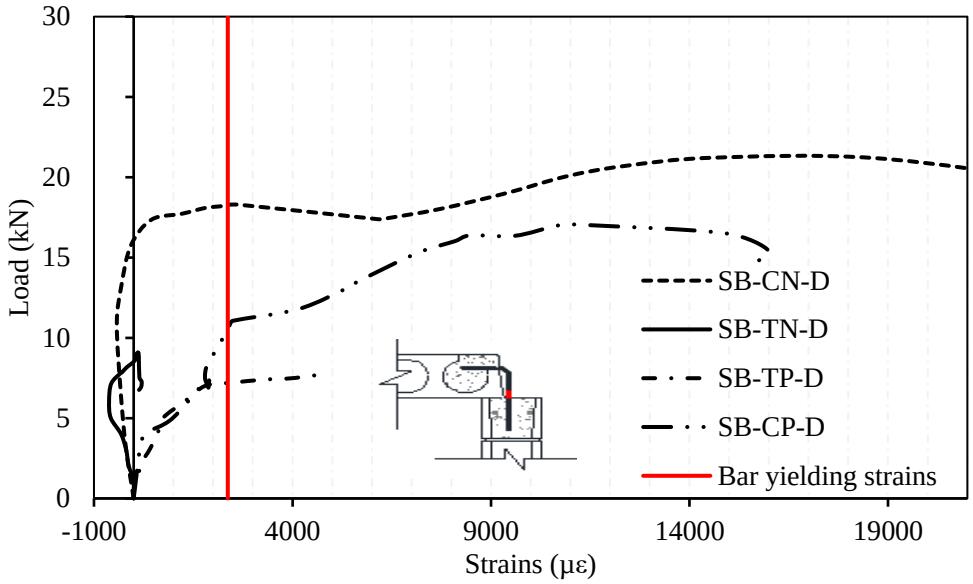

b) Series II (side-bearing specimens)

Fig. 5.11: Load strain relationships

On the other hand, the connection bar with adhesive (EB-CN-A) reached the peak load of 29.0 kN at a strain of only 650 με. Following a small load drop of 1.7 kN (5.9 %), the bar yielded at a load of 27.3 kN and maintained this load relatively steady until 3,380 με. Afterwards, the connection experienced a slight decrease in strength associated with large strains up to 19,000 με. After this point, the strain gauge malfunctioned, but a load reduction was observed while the masonry beam experienced more severe spalling until it crushed. Although this connection with adhesive (EB-CN-A) resisted larger loads, it offered less ductility than its counterpart without adhesive (EB-CN-D). This may be attributed to the stronger load transfer mechanism when an adhesive is used versus the dry-fit method since the masonry beam in specimen EB-CN-A survived a larger load and more damage in the masonry beam at than specimen EB-CN-D at bar yielding.

In contrast, the measured strains in the connection bars of end-bearing specimens tested under tension (pulling) forces, EB-TN-D and EB-TN-A, were considerably lower at the peak load. The first peak, triggered by the onset of cover spalling, occurred when the measured strains in were 325 με and 380 με in specimens EB-TN-D and EB-TN-A, respectively. Afterwards, the load dropped, and the curves diverged. Whereas the dry-fit connection bar (EB-TN-D) experience concrete cover/grout spalling and bar pull-out, leading to strength degradation without any further strain increase; the connection bar with adhesive (EB-TN-A) had a second peak where the measured strains reached 2,110 με. Even though the load did not significantly increase compared to the first peak, the use of adhesive delayed the failure and demonstrated more ductility. Table 3.3 offers the load-tensile strains and load-displacement relationships for end-bearing connections with dry-fit bars and adhesive at a load of 6.1 kN, which is the threshold of minimum tensile capacity for 10M L-shaped integrity ties in two-storey buildings. These values might be of interest to the designer.

Table 5.3: Tensile strains and slab displacement for integrity ties at 6.1 kN of load (CSA 2019)

End-bearing specimen	**Tensile strains at 6.1 kN (με)**	**Displacement under tension at 6.1 kN (mm)**
EB-TN-D	125	2.3
EB-TN-A	185	1.0

Loading parallel to the axis of the masonry beam: When subjected to parallel pushing forces, the bar in the end-bearing connection (EB-CP-D) exhibits a similar load-strain behaviour to its counterpart tested under normal pushing (EB-CN-D). After the initial linear elastic stage, the connection bar yielded at 70% of the peak load (Fig. 5.11 (a)). The post-peak descending part of the graph resulted from bar pull-out, where the bar continued accumulating strains while bending in the direction of the load. A second peak occurred at a load of 25.9 kN, which is not shown on the curve since the strain gauge malfunctioned after reading 10,870 με at a load of 17.1 kN. However, this indicates great ductility and ample warning before failure.

5.5.3.2 Specimens of Series II – side-bearing connection

Loading normal to the axis of the masonry beam: The connection bar in the side-bearing connection tested under compression (pushing) forces (SB-CN-D) initially developed compressive strains, similar to its counterpart with end-bearing type (Fig. 5.11 (b)). These compressive strains achieved up to -425 με and then shifted to tensile strains at a load of approximately 13.2 kN. Afterwards, the connection bar yielded at 85.8% of the peak load. A small load drop followed, which was because of initial concrete cover spalling and bar pull-out. At the second peak, the strains in the connection bar were 18,650 με.

On the other hand, similar to its counterpart with end-bearing type, SB-TN-D under tension (pulling) forces developed considerably smaller strains and lower capacity compared to SB-CN-

D. The connection bar initially experienced compressive strains, resulting from a slight bar inclination when it was inserted, which provoked the slabs to push the bar against the beam. These compressive strains reached -620 με. Once the connection bar recovered the vertical position after further slab pulling, the bar experienced tensile strains. However, the connection bar developed only 110 με when the HCS had been pushed to their end of bearing. This may be attributed to the bar pull-out.

In general, test results demonstrated that the connection bar tested under normal pushing forces demonstrated ample warning before attaining the maximum load capacity, regardless of bearing type. In contrast, when the connection bar is subjected to pulling normal forces, it developed considerably lower strains, resulting in a low lateral capacity and lack of ductility before failure.

Loading parallel to the axis of the masonry beam: When subjected to parallel forces, the connection bars of side-bearing specimens, SB-CP-D and SB-TP-D, had a bilinear load-strain relationship under either pushing or pulling (Fig. 5.11 (b)). Both connection bars experienced tensile stresses due to bar pull-out and bending in the direction of the force. After the initial linear elastic stage, the curves showed a slope reduction at bar yielding in both specimens. While the connection bar subjected to pushing (SB-CP-D) yielded at 63.5% of the peak load, the connection bar in the specimen under pulling (SB-TP-D) yielded at 92.3% of the peak load. The latter connection bar (SB-TP-D) experienced large deformation and bending but did not significantly increase the load-carrying capacity in the post-yielding stage.

Although the connection bars reached yielding under pushing forces, regardless of load orientation or bearing type, the yielding load was considerably smaller than the predicted direct tension value of 40 kN, based on material properties (Table 5.2). Under pulling forces, the capacity of the connection bars was even lower, where the yielding load was close to one-fourth of the predicted

value, or the bars did not yield. These relatively low yielding load resulted from the eccentricity of the applied in-plane force with respect to the location of the connection bar (interface of the slabs with the masonry beam, as indicated in Fig 5.4). This load eccentricity provoked the bar bending and early yielding.

Bar bending in the direction of the force was due to bar pull-out in the case of dry-fit connections, and due to grout spalling in the case of connections with adhesive, which left part of the bar exposed. Depending on other factors related to the connection detail, such as bar cover in grout and formation of initial cracks in the masonry beam, the onset of bar bending in the direction of the force occurred earlier. When cracks appeared at the reinforcement location, the tight fit of the bar was compromised, leading to bar pull-out, bending and thereof, yielding at earlier stages. Side-bearing connections were more vulnerable to this effect as these had a segment of the bar not embedded in grout, causing relatively lower yielding loads.

Reducing the connection eccentricity of load path by aligning the connection bar to be in-plane with the HCS would put the bar into more direct tension, resulting in a higher lateral capacity and a lower lateral displacement. This can be achieved by hooking the connection bar into the boundary reinforcement of the HCS diaphragm or by tying a hooked connection bar directly behind the vertical dowel of the masonry wall. Ideally the connection between the HCS and the masonry wall could be detailed such that the connection bar will be able to develop its full yield capacity in tension. This would also meet the design intent of the North American design codes for structural integrity reinforcement.

5.5.4 Displacement of the slab

Figures 5.12 (a) and (b) present the load-slab displacement relationship of bearing connections for Series I and II, respectively. The curves repeatedly show bumps in their slopes in specimens with

adhesive, which are associated with cycles of bar yielding and pull-out, or masonry beam cracking and load accommodation, which provoked small load drops in the ascending load-displacement relationship.

5.5.4.1 Specimens of Series I – end-bearing connection

Loading normal to the axis of the masonry beam: The load-displacement relationships of bearing connections under normal forces, EB-CN-A, EB-CN-D, EB-TN-A and EB-TN-D, initially exhibit linear elastic behaviour with comparable slopes (Fig. 5.12 (a)). The graphs diverged at their first peak load. For the specimen under compression (pushing) forces with dry-fit bars (EB-CN-D), the first peak, caused by the development of additional cracks, was the beginning of bar pull-out and yielding. This caused a slope reduction and provoked excessive slab displacement (84.4 mm) at peak load. However, its counterpart with adhesive (EB-CN-A) tested under compression forces attained a larger peak load of 29.0 kN at a displacement of 8.7 mm at the end of the linear elastic stage. This indicated a stiffer response when incorporating the adhesive to the connection. The post-peak stage in the latter specimen showed strength degradation, where the load decreased while the displacement increased rapidly. The changes in the slope become more negatively abrupt as the beam suffered more spalling, until finally beam crushing occurred.

Under tension (pulling) forces, end-bearing specimens, EB-TN-D and EB-TN-A, reached the first peak of 9.1 at a displacement of 3.5 mm, and 9.9 kN at a displacement of 5.4 mm, respectively. While the connection with a dry-fit bar, EB-TN-D, suffered strength degradation after the peak load due to cover spalling, the connection with the adhesive, EB-TN-A, experienced a second peak of 10.6 kN at a displacement of 36.4 mm. However, both specimens demonstrated low stiffness as these allowed excessive slab displacements under low values of load.

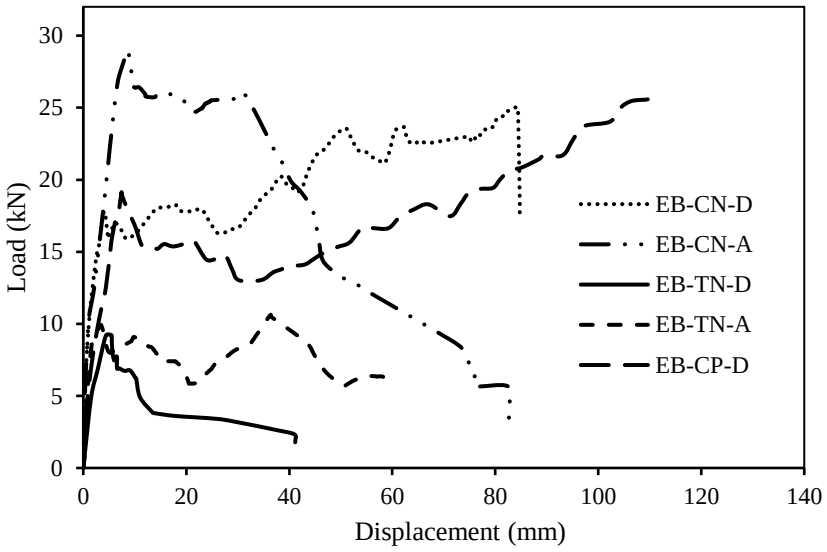

a) End-bearing specimens under normal and parallel forces

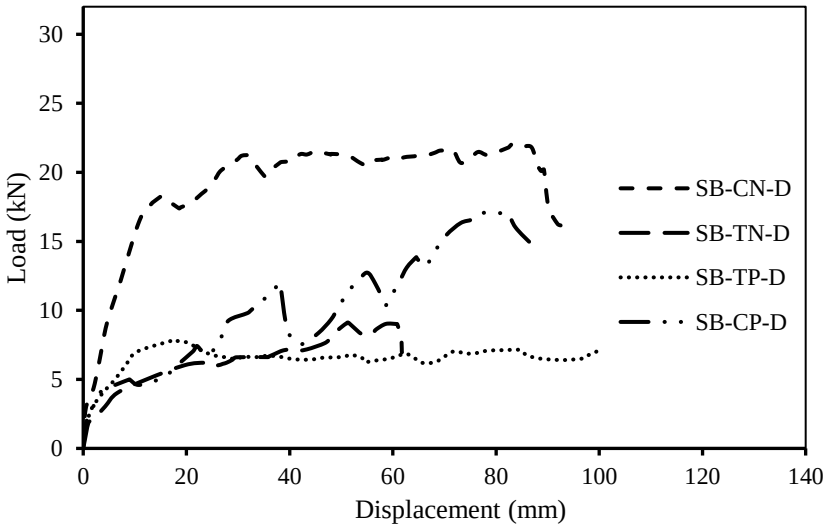

b) Side-bearing specimens under normal and parallel forces

Fig. 5.12: Load-slab displacement relationships

Loading parallel to the axis of the masonry beam: Under pushing forces, the connection bar in the end-bearing specimen, EB-CP-D, exhibited a similar load-slab displacement relationship to its counterpart under normal pushing (compression) forces (Fig. 5.12 (a)). After the initial linear

elastic stage, a slope reduction and series of bumps followed due to bar pull-out and yielding. At peak load, the displacement of the slab was 112 mm.

The excessively large displacement values at peak load in end-bearing connection under compression (pushing) and shear forces, EB-CN-D and EB-CP-D, reflected the lack of stiffness of the connections with dry-fit bars because of bar pull-out. Although there is no potential hazard of suffering bearing loss under compression forces, such large displacement after the second crack might cause floor misalignments, bumping with adjacent units and overall loss of integrity.

In the construction practice, the slabs supported on masonry have a minimum seating length of the greater of 50 mm and l_n/180, where l_n is the clear span between supports of the HCS, as per Canadian Standards (CPCI 2017; CSA 2019). During the construction of these specimens, this value was exceeded to ensure a controlled failure. However, the slabs displaced considerably under tension (pulling) forces in specimen EB-TN-D, once the concrete cover was lost. This could result in loss of bearing of the slabs under relatively low values of load. In these specimens, incorporating an adhesive mitigated the lack of stiffness and delayed the loss of bearing but did not allow to increase the load to the acceptable values for integrity ties in three storey buildings or taller.

5.5.4.2 Specimens of Series II – side-bearing connection

Loading normal to the axis of the masonry beam: The load-displacement curves in side-bearing specimens exhibited significantly lower slope compared to their counterparts with end-bearing type (Fig. 5.12 (b)). The reason for the stiffness disparities stems from the variations in the connection detailing between end- and side-bearing connections. The bars in end-bearing specimens were enclosed in between the two slabs and fully embedded in the grout, while the bar in side-bearing specimens was partially unrestrained and external to the slab. The latter configuration significantly reduced the stiffness of side-bearing connections.

Out of the four graphs in Fig. 5.12 (b), the curve for the side-bearing connection tested under compression (pushing) normal forces (SB-CN-D) presented the steeper slope. This resulted from the bar leaning against the HCS under the pushing loads. Following the initial linear elastic stage, the connection suffered bar pull-out, bar yielding, and slope reduction. In this specimen, the measured slab displacement was 83.1 mm when beam crushing occurred at the peak load. In contrast, under tension (pulling) forces, the connection bar in specimen SB-TN-D was completely unrestrained, which provoked the bar pull-out and compromised the load transfer to the supporting beam, evidenced by the few cracks and no spalling observed before the loss of bearing. The test was stopped when the displacement reached 60.8 mm.

Loading parallel to the axis of the masonry beam: Although the side-bearing connection under pushing force (SB-CP-D) had a steeper load-displacement curve compared to the specimen under pulling forces (SB-TP-D), both connections allowed excessive displacements and bar pull-out (Fig. 5. 12 (b)) and demonstrated low stiffness. The test of specimens SB-CP-D and SB-TP-D was stopped once the slabs displaced 100 mm and 88 mm, respectively and no further load increase occurred.

In general, SB-TP-D tested under parallel pulling (shear) forces can be considered the most critical load-case scenario with the most undesirable mode of failure since the connection bar had the lowest peak and yielding loads, and the bar continues to pull out easily, leading to the largest slab displacement measured. As noted earlier in the report, the drilled hole for the bar dowel in slab SB-TP-D was not as snug to the bar as for slab SB-CP-D, which is the likely explanation for the much lower peak load.

5.6 Conclusions

Based on the analysis of test results, the following conclusions can be drawn:

1. The mode of failure depended on the load direction under axial in-plane loads. Under compression (pushing) forces, the connections failed by grout crushing preceded by bar bending and yielding, while under tension (pulling) forces, the connections failed by masonry beam spalling followed by loss of bearing of the slabs without bar yielding.
2. Regardless of load direction and type of bearing, the mode of failure of connections tested under parallel (shear) forces was governed by bar pull-out, bending and yielding associated with excessive slab displacement.
3. The configuration of the L-shaped connection detailing, used in this study, generated load eccentricities when in-plane forces acted on the HCS, resulting in bar bending and a reduction of the load capacities in relation to predicted load capacities based on bar yielding under an axial load path.
4. The tested capacity of end-bearing connections under tension (pulling) forces met the tensile strength specified in North American for resisting the structural integrity forces for a building of up to two storeys but did not satisfy the specifications for buildings of three or more stories (CSA 2019; ACI 2019).
5. All bearing connections tested under tension had slab displacements larger to 50-mm without developing the full yielding capacity of the connection bars, which results in a potential risk for HCS loss of bearing and does not meet the intent of the code of reaching bar yielding under tension forces without losing the bearing.
6. The dry-fit connection bars allowed excessive bar displacements (up to 112 mm) before reaching the ultimate load capacity, which might result in floor misalignments.

7. The connection bar with adhesive reached 15.2% more capacity under tension forces and 13.3% under compression forces than its counterparts with dry-fit bars, respectively. In addition, the connections with adhesive showed a better load transfer to the supporting beam evidenced by the severe spalling in the supporting beam at larger peak loads.
8. The end bearing connection detailing demonstrated higher stiffness evidenced by the steeper slopes in the load-displacement graphs compared to side-bearing connections because of having the bar completely embedded in grout.

Testing on end-bearing connections under tension loads with connection bar in-plane with the HCS grout keys should be investigated, including a portion of the wall extending above and below the level of the HCS, to reflect the load response of an intermediate level bearing wall accurately. Tests could be performed with and without a clamping force acting on the wall at the connection, to evaluate the effect of gravity loads, transferred from upper floors, on the connection response.

CHAPTER 6 - CONCLUSIONS AND FUTURE WORK

6.1 Summary

This thesis introduced the results of testing twenty full-scale reinforcing bar connections of HCS to either steel or masonry wall supports to investigate their capacity and mode of failure. The assembled specimens simulated the common construction practice in Eastern Canada, where HCS bearing connections are reinforced using size 10M steel bars of Grade 400W inserted at the shear keys and side pockets of the slabs. These specimens were tested to failure under monotonic in-plane axial and shear forces. Test parameters in this study were the bearing type, the orientation and direction of loading, and the use of alternative connection detailing such as smaller bend angles, reduced free length of the bar or incorporating an adhesive to enhance bar bonding. Test results were discussed in terms of maximum load capacity, mode of failure, strain variations in the connection bar and slab displacements. Especial emphasis was placed on the differences and similarities in the behaviour between end and side bearing connections. Also, the effect of load orientation/direction and connection modifications was fully unveiled. Finally, the tested capacity of connection bars was compared against North American code specifications for integrity ties in HCS floors. The most important findings are hereby presented.

6.2 Conclusions

6.2.1 Phase I: Specimens supported on steel beams under axial and shear loading

1. The connection bars tested under normal pulling (tension) experienced yielding strains in the range of 2,370 to 24,980 με, when grout splitting occurred at peak load, which offered a ductile mode of failure of the connection under tension forces.

2. Connection bars with 90-degree bends tested under normal pushing (compression) and parallel loads (shear) did not demonstrate a desirable mode of failure. Connection bars tested under compression developed strains in the range of 900 to -1,490 με before the peak load, which indicates no yielding when bar bending initiated.
3. The connection bars, tested under shear, yielded before reaching the ultimate capacity but experienced extensive displacements (up to 61.5 mm), which could provoke floor misalignments.
4. The connection bar tested under tension reached load capacities close to load predictions. These capacities for end-bearing connections exceeded the tensile strength requirements for integrity ties in structures other than those supported on bearing walls as per the North American codes (ACI 2019 and CSA 2019).
5. The tested end- and side-bearing connections present no risk of loss of bearing of the slabs under direct tension since the peak load was reached at a displacement of approximately 22.5-mm, which is less than the minimum bearing length for HCS (50 mm).
6. Connections tested under pushing/parallel (shear) and pushing/normal (compression) forces demonstrated less than 50% of the capacity of their counterparts tested under pulling forces. Therefore, the reinforcing bar connection is more susceptible to fail under compression and pushing/parallel (shear) forces compared to the case of tension or pulling/parallel (shear) forces.
7. Compared to the original connection detailing, the combined effects of restraining the bar against the beam and decreasing the bend angle to 45-degree resulted in a 35.7 % increase in the load capacity under normal pushing (compression). Although the capacity of the connection remained less than that of the predicted based on material properties, the mode

of failure was more ductile compared with the rest of the connections tested under compression.

6.2.2 Phase II: Specimens supported on steel beams under axial and shear loading

1. The mode of failure of connections tested under axial forces depended on the loading direction. Under compression (pushing) forces, the connections failed by grout crushing preceded by bar bending and yielding with strains larger than 16,000 με. Under tension (pulling) forces, the connections failed by masonry beam spalling followed by slabs loss of bearing with strains less than 2,110 με.
2. Regardless of load direction and type of bearing, the mode of failure of connections tested under parallel (shear) forces was governed by bar pull-out, bending, and yielding, at excessive displacements.
3. The tested capacity of end-bearing connections under tension (pulling) forces met the tensile strength specified in North American for resisting the structural integrity forces for a building of up to two storeys but not for buildings of three or more stories (CSA 2019; ACI 2019).
4. All bearing connections tested under tension had slab displacements larger than 50-mm without developing the full yielding capacity of the connection bars, which could result in a potential risk for HCS loss of bearing. This does not meet the intent of the code of reaching bar yielding under tension forces without missing the bearing.
5. The dry-fit connection bars experienced bar pull-out and allowed excessive slab displacements (up to 112 mm) before reaching the ultimate load capacity, which might result in floor misalignments besides poor stiffness.

6. The connection bar with adhesive reached 15.2% more capacity under tension forces and 13.3% under compression forces than its counterparts with dry-fit bars, respectively. In addition, the connections with adhesive showed a better load transfer to the supporting beam evidenced by the severe spalling in the supporting beam at larger peak loads.
7. The end bearing connection detailing demonstrated higher stiffness evidenced by the steeper slopes in the load-displacement graphs compared to side-bearing connections because of having the bar completely embedded in grout.
8. The configuration of the L-shaped connection detailing, used in this study, generated load eccentricities when in-plane forces acted on the HCS, resulting in bar bending and a reduction of the load capacities in relation to predicted load capacities based on bar yielding under an axial load path.

6.3 Recommendations for Construction Practice

Based on the analysis of test results, the following recommendations might be of interest to the designer:

1. For reinforcing bar connections in HCS supported on steel beams, reducing the bar bends to 45-degrees, and pushing the bar against the flange of the supporting beam will result in a more ductile mode of failure and larger capacity at no additional cost.
2. For reinforcing bar connections in HCS supported on masonry walls, the use of an adhesive to bind the bar to the supporting masonry beam as an alternative to the dry-fit method will result in larger capacity and better safety for buildings with up to two floors.

6.4 Recommendations for Future Works

6.4.1 Specimens supported on steel beams under axial and shear loading

The following are suggested for future work on HCS bearing connections supported on steel beams:

1. Investigate connection detailing while accounting for minimal load eccentricities and bar full cover in grout. In this investigation, it was noted that load eccentricities in Z-shaped connection bars triggered an early bar bending/buckling failure where the grout had little contribution under pushing forces. For instance, welding the connection bar to the upper side of the top flange of the beam and grouting integrally the connection might significantly improve the mechanism of failure of the connection.
2. Investigate the effect of larger reinforcement ratios in bearing connections (e.g., employing 15M bars instead of 10M connection bars).
3. Investigate the mode of failure and capacities of integrity ties in end-bearing connections grouted to the open cores of the slabs. This connection detailing allows for reducing tie spacing and increasing the strength of bearing connections.
4. Conduct a finite element modelling/analysis to widen the spectrum of parameters addressed in this experimental research. For instance, lower bar bend angles than 45-degree bends combined with reduced bar length might lead to larger stiffness and load-carrying capacity under parallel loading. Also, greater compressive strength in the grout cast in the connection might lead to greater lateral-load capacity.
5. Investigate the effect of gravity loads on the lateral load capacity of the connection bar.

6.4.2 Specimens supported on masonry beams under axial and shear loading

Based on the observations of the specimens supported on masonry beams and the literature review, the following suggestions could be considered in future work:

1. Investigate the effect of using cast concrete for masonry beam supports instead of grout. Accordingly, increasing the reinforcement ratio of the bond beam might result in a greater capacity and a more desirable mode of failure compared to the current connection detailing.
2. Examine the effect of implementing larger reinforcement ratios in HCS bearing connections (e.g., provide size 15M connection bars instead of size 10M).
3. Investigate the effect of incorporating gravity loads on the lateral-load capacity of the connections.
4. Investigate the effect of inverting the bar position of the connection bar where the bar side anchored to the masonry beam is, instead, grouted to the course of masonry blocks erected in the upper level. This connection detailing is common in Western Canada and has not been tested yet.

REFERENCES

ACI Committee 318. (2019). "Building Code Requirements for Structural Concrete (ACI 318-19) and commentary (ACI 318R-18)". *American Concrete Institute*: Farmington Hills, Detroit, MI, United States.

Angel, N. M., Correal, J. F., & Restrepo, J. I. (2019). "Cyclic Behavior of Hollow-Core Diaphragm Subassemblies." *PCI Journal*, 64(2), 80–96. DOI: 10.15554/pcij64.2-02

ASTM. (2019). "Standard Specification for Mortar for Unit Masonry." ASTM C270-19a. American Standards for Testing of Materials, International: West Conshohocken, Pennsylvania, United States.

ASTM. (2020a). "Standard Test Methods and Definitions for Mechanical Testing of Steel Products." ASTM A370-20. American Standards for Testing of Materials, International: West Conshohocken, Pennsylvania, United States.

ASTM. (2020b). "Standard Test Method for Compressive Strength of Hydraulic Cement Mortars (Using 2-in. or [50 mm] Cube Specimens). ASTM C109/C109M-20b. American Standards for Testing of Materials, International: West Conshohocken, Pennsylvania, United States.

Cleland, N. M., & Ghosh, S. K. (2002). "Un-topped Precast Concrete Diaphragms in High-Seismic Applications." *PCI Journal*, 47(6), 94–99.

Concrete Design Committee P 3101. (2006). "Concrete structures standard. Part 1- The Design of Concrete Structures." NZS 3101-1-2006. Standards New Zealand: Wellington, New Zealand.

Corney, S. R., Ingham, J. M., & Henry, R. S. (2018). "Seismic Testing of Support Connections in Deep Hollow-Core Floor Units." *ACI Structural Journal*, 115(3), 735–748. DOI: 10.14359/51702062

CPCI. (2017). "CPCI Design Manual 5th Edition. Precast and Prestressed Concrete." CPCI-17. Canadian Precast/Prestressed Concrete Institute: Ottawa, Ontario, Canada.

CPCI. (2019). "Technical: Drawings." Canadian Precast/Prestressed Concrete Institute: https://www.cpci.ca/en/resources/technical_drawings/

CSA. (2014). "Mortar and Grout for Unit Masonry." CSA A179-04. Canadian Standards Association: Mississauga, Ontario, Canada.

CSA. (2019). "Design of Concrete Structures." CSA A23.3-19. Canadian Standards Association: Toronto, Ontario, Canada.

Dhakal, R. P. and Maekawa, K. (2002). "Modeling for Post-yield Buckling of Reinforcement." *Journal of Structural Engineering*, 128 (9): 1139–47.

Darwin, D., & Zavaregh, S. S. (1996). "Bond strength of grouted reinforcing bars." *ACI Structural Journal*, 93(4), 486–495. DOI: 10.14359/9707

Henry, R. S., Ingham, J., & Corney, S. (2014). "Performance of precast concrete floor systems during the 2010/2011 Canterbury earthquake series." *Magazine of Concrete Research*, 66(11), 563–575. DOI: 10.1680/macr.13.00106

Herlihy, M. D. (1999). "Precast concrete floor support and diaphragm action." Ph.D. Thesis. Department of Civil Engineering. University of Canterbury, Christchurch, New Zealand.

Hilti Corporation-Canada. (2019). Hilti anchors for attachments to hollow core concrete panels.

Jensen, J. (2006). "The Seismic Behaviour of Existing Hollow-core Seating Connections Pre and Post Retrofit." M.Eng. Thesis. Department of Civil Engineering. University of Canterbury, Christchurch, New Zealand.

Jensen, J. P., & Bull, D. K. (2007). "Experimental Investigation of Existing Hollow-core Seating Connection Seismic Behaviour Pre and Post Retrofit Intervention." *2007 NZSEE*

Conference (pp. 1–10). Paper Number 12. March 30- April 1, 2007. Palmerston North, New Zealand.

Jensen, J. P., Bull, D. K., & Pampanin, S. (2006). Conceptual Retrofit Strategy for Existing Hollow-core Seating Connections. *2006 NZSEE Conference* (pp. 1–9). March 10-12, 2004. Napier, New Zealand.

Lam, D. (2002). "Composite steel beams with precast hollow core slabs: behaviour and design." *Progress in Structural Engineering and Materials*, 4(2), 179–185. DOI: 10.1002/pse.128

Lam, D. (2007). "Capacities of headed stud shear connectors in composite steel beams with precast hollow-core slabs." *Journal of Constructional Steel Research*, 63(9), 1160–1174. DOI: 10.1016/j.jcsr.2006.11.012

Lee, J. Y., & Watanabe, F. (2003). "Predicting the longitudinal axial strain in the plastic hinge regions of reinforced concrete beams subjected to reversed cyclic loading." *Engineering Structures*, 25(7), 927–939. DOI: 10.1016/S0141-0296(03)00026-9

Lindsay, R. A., Mander, J. B., & Bull, D. K. (2004). "Hollow-Core Floor Systems in Precast Concrete Buildings." *13th World Conference on Earthquake Engineering*. August 1-6, 2004. Vancouver, British Columbia, Canada.

MacPherson, C. (2005). "Seismic Performance and Forensic Analysis of a Precast Concrete Hollow-Core Floor Super-Assemblage." Ph.D. Thesis. University of Canterbury, Christchurch, New Zealand.

MacPherson, C. J., Mander, J. B., & Bull, D. K. (2005). "Reinforced Concrete Seating Details of Hollow-core Floor Systems." *2005 NZSEE Conference*. Paper Number 24. March 11-13, 2005. Taupo, New Zealand

Mander, J. B., Priestley, M. J. N., and Park, R. (1984). "Seismic design of bridge piers." Research Report. No 84-2, Department of Civil Engineering, University of Canterbury, New Zealand.

Matthews, J. (2004). "Hollow-core floor slab performance following a severe earthquake" Ph.D. Thesis. Department of Civil Engineering. University of Canterbury, Christchurch, New Zealand.

Matthews, J., Bull, D., & Mander, J. (2001). "Investigating the load paths of floor diaphragm forces during severe damaging earthquakes." *Combined Concrete Industry Conference*. 15-17 October 2020, Rotorua, New Zealand

McSaveney, E. (2017). "Historic earthquakes - The 2011 Christchurch earthquake." http://www.teara.govt.nz/en/historic-earthquakes/page-13

Mejia-McMaster, J. C., & Park, R. (1994). "Tests on Special Reinforcement for the End Support of Hollow-Core Slabs." *PCI Journal*, 39(5), 90–105. DOI: 10.15554/pcij.09011994.90.105

Minor, J. (1971). "A study of bent bar anchorages in concrete." Ph.D. Thesis. Department of Civil Engineering. Rice University, Houston, Texas, United States.

PCI. (2015). "PCI Manual for the Design of Hollow Core Slabs and Walls. Third Edition - Electronic Version." MNL-126-15E. PCI Hollow Core Slab Producers Committee. Chicago, Illinois, United States. DOI:10.1007/b137286

Personal contact. (2019). MSc. Karl Truderung. Associate: Tower Engineering Group.

Personal contact. (2021). MBA. Brian J Hall. Canadian Precast/Prestressed Concrete Institute. Contacted on April 12, 2021.

Technical Committee CEN/TC 250. (2008). "Eurocode 2: Design of concrete structures - Part 1-2: General rules - Structural Fire Design." EN 1992-1-2: 2004. European Committee for Standardization: Brussels, Belgium.

Technical Committee CEN/TC 229. (2010). "Precast Concrete Products-Hollow core slabs." DIN EN 1168:2008-10. European Committee for Standardization: Berlin, Germany.

Truderung, K. A. (2011). "Shear Capacity of Dry-Cast Extruded Precast / Prestressed Hollow-Core Slabs." Department of Civil Engineering, University of Manitoba, Winnipeg, Canada.